Electronic Supplementary Material (ESI) for Chemical Science.

SUPPORTING INFORMATION

Transient self-assembly of metal-organic complexes

Jean-François Ayme,[*a] Bernd Bruchmann,[a] Lydia Karmazin[b] and Nathalie Kyritsakas[b]

[a]BASF SE, Joint Research Network on Advanced Materials and Systems (JONAS), Carl-Bosch Str. 38, 67056 Ludwigshafen, Germany

[b]Service de Radiocristallographie, Fédération de chimie Le Bel FR2010, Université de Strasbourg, 1 rue Blaise Pascal, 67008 Strasbourg, France.

Email : jeff.ayme@gmail.com

Table of contents

1. General experimental section 4
   1.1 General material 4
   1.2 Characterization and analysis methods 4
2. Synthesis 4
   2.1 Synthesis of the ligands 4
      2.1.1 Synthesis of dialdehyde **6** 4
      2.1.2 Synthesis of imine (**3**,**1**) 4
      2.1.3 Synthesis of diamine **7** 5
   2.2 Synthesis of mononuclear metal complexes 7
      2.2.1 General synthetic procedure 7
      2.2.2 Synthesis of Cu^{I} complex $[Cu(\mathbf{3},\mathbf{1})_2](BF_4)$ 7
      2.2.3 Synthesis of Cu^{I} complex $[Cu(\mathbf{3},\mathbf{4})_2](BF_4)$ 7
      2.2.4 Synthesis of Ag^{I} complex $[Ag(\mathbf{3},\mathbf{1})_2](SbF_6)$ 8
      2.2.5 Synthesis of Cu^{I} complex $[Cu(\mathbf{3},\mathbf{5})_2](BF_4)$ 9
   2.3 Synthesis of mononuclear metal complexes with diamine 9
      2.3.1 General synthetic procedure 9
      2.3.2 Synthesis of Cu^{I} complex $[Cu(\mathbf{3}_2,\mathbf{2})](BF_4)$ 9
      2.3.3 Synthesis of Ag^{I} complex $[Ag(\mathbf{3}_2,\mathbf{2})](SbF_6)$ 10
   2.4 Synthesis of polynuclear metal complexes 11
      2.4.1 General synthetic procedure 11
      2.4.2 Synthesis of Ag^{I} complex $[Ag_2(\mathbf{6}_2,\mathbf{2}_2)](SbF_6)_2$ 11
      2.4.3 Synthesis of Ag^{I} complex $[Ag_2(\mathbf{6},\mathbf{7})_2](SbF_6)_2$ 12
3. Probing of the initial equilibrium state of the systems 14
   3.1 Mononuclear complexes 14
      3.1.1 Equilibrium composition of a mixture of $Cu(BF_4)$ and components **3**, **2** and **1** 14
      3.1.2 Equilibrium composition of a mixture of $Cu(BF_4)$ and components **4**, **3** and **1** 15
      3.1.3 Equilibrium composition of a mixture of $Ag(SbF_6)$ and components **3**, **2** and **1** 17
      3.1.4 Equilibrium from a mixture of $Cu(BF_4)$ and components **5**, **3** and **2** 21
   3.2 Equilibrium from a mixture of $Ag(SbF_6)$ and components **7**, **6** and **2** 23
4. Transient rearrangement 24
   4.1 Mononuclear complexes 24
      4.1.1 Transient self-assembly of $[Cu(\mathbf{3},\mathbf{1})_2](BF_4)$ from $[Cu(\mathbf{3}_2,\mathbf{2})](BF_4)$ and **1** 24
      4.1.2 Transient self-assembly of $[Cu(\mathbf{3},\mathbf{1})_2](BF_4)$ from a mixture of complexes 34
      4.1.3 Transient self-assembly of $[Ag(\mathbf{3},\mathbf{1})_2](SbF_6)$ from a mixture of complexes 41

4.1.4 Transient self-assembly of [Ag(**3**,**1**)$_2$](SbF$_6$) from a non-equilibrated mixture of [Ag(**3**$_2$,**2**)](SbF$_6$) and **1** 48
4.1.5 Transient self-assembly of [Cu(**3**,**5**)$_2$](BF$_4$) from [Cu(**3**$_2$,**2**)](BF$_4$) and **5** 56
4.2 Transient self-assembly of [Ag$_2$(**6**,**7**$_2$)](SbF$_6$)$_2$ from [Ag$_2$(**6**$_2$,**2**$_2$)](SbF$_6$)$_2$ and **7** 62
5. X-ray crystal structures 69
5.1 X-ray crystal structure of [Ag$_2$(**6**$_2$,**2**$_2$)](BPh$_4$)$_2$ 69
5.2 X-ray crystal structure of [Ag$_2$(**6**,**7**)$_2$](BPh$_4$)$_2$·xSolvent 69
6. References 70

1. General experimental section

1.1 General material

Unless stated otherwise, solvents and commercial reagents were used as received. Anhydrous DMF was bought for Sigma-Aldrich. All reactions requiring anhydrous conditions were carried-out in oven-dried glassware. All reactions not performed in a NMR tubes were agitated using magnetic stirrer bars. Room temperature is taken as 293 K. Flash column chromatography was carried out using silica gel (Geduran Si60, 40-63 μm, Merck) using eluents as specified. TLC was performed on precoated silica gel plates (Merck TLC silica gel 60 F254 aluminium plates) and product spots were visualized under UV light (λ_{max} = 280 nm or 365 nm) or by staining with $KMnO_4$. Celite® was obtained for Sigma-Aldrich and refers to diatomaceous earth.

1.2 Characterization and analysis methods

NMR spectra were recorded on a Bruker Avance III 400 MHz, Bruker Avance III HD 400 MHz spectrometer, Bruker Avance Neo 500 MHz spectrometer or Bruker Ascend Aeon 600 MHz NMR spectrometer. NMR spectra were digitally processed (phase and baseline corrections, integration, peak analysis) using MestReNova 10.0. Deuterated acetonitrile (CD_3CN) was obtained from Sigma-Aldrich and used without further purification. Deuterated chloroform ($CDCl_3$) was obtained from Sigma-Aldrich and was passed through a plug of sodium bicarbonate immediately before use to remove any acidic impurities. Chemical shifts are reported in parts per million (ppm) from low to high frequency using residual protonated solvent signals as reference (for ^1H NMR spectra $CDCl_3$ =7.26 ppm, CD_3CN = 1.94 ppm; for ^{13}C NMR spectra $CDCl_3$ =77.16 ppm, CD_3CN = 1.32 ppm). Coupling constants (*J*) are reported in hertz (Hz). The multiplicity of the 1H signals are indicated using the following standard abbreviations: s = singlet, d = doublet, t = triplet, dd = double doublet, q = quartet, p = pentet, m = multiplet, br = broad, ddd = doublet of double doublets. NMR signals are reported in terms of chemical shift (*δ*), multiplicity, coupling constants (*J*), relative integral, and assignment, in that order. All resonances are reported to the nearest 0.01 ppm. ^1H and ^{13}C NMR assignments were made using 2D-NMR methods (COSY, ROESY, TOCSY, HSQC, HMBC) and are unambiguous unless stated otherwise. High resolution ESI mass spectra were obtained by direct injection into a ThermoFisher Exactive Plus EMR Orbitrap mass spectrometer or a Bruker MaXis Impact quadrupole time-of-flight mass spectrometer.

2. Synthesis

2.1 Synthesis of the ligands

2.1.1 Synthesis of dialdehyde 6

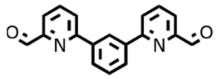

6

6 was synthesized as described in the literature. NMR and mass data were consistent with those previously reported.[S1]

2.1.2 Synthesis of imine (3,1)

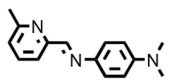

(**3**,**1**)

(**3**,**1**) was synthesized as described in the literature. NMR and mass data were consistent with those previously reported.[S2]

2.1.3 **Synthesis of diamine 7**

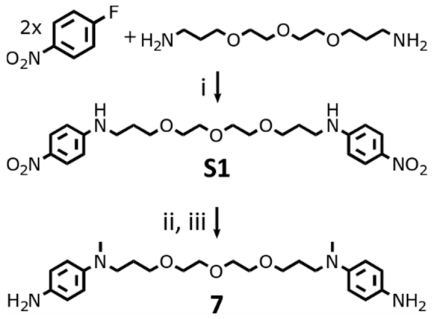

Scheme S1. Synthesis of diamine **7**. Reagents and conditions: (i) NEt_3, DMSO, 80 °C, overnight, 38 %; (ii) NaH, MeI, DMF, 0 °C to r.t, overnight; (iii) Pd/C, H_2, THF:EtOH, r.t., overnight (55 %, two steps).

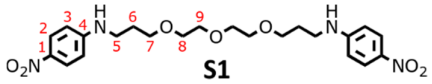

S1 was prepared by a modified literature procedure.[S3]

1-Fluoro-4-nitrobenzene (3.00 g, 21.2 mmol, 2.5 eq.) and triethylamine (3.55 mL, 2.58 g, 25.5 mmol, 3 eq.) were added to a solution of 4,7,10-trioxa-1,13-tridecanediamine (1.86 mL, 1.87 g, 8.5 mmol , 1 eq.) in DMSO (40 mL). The resulting mixture was stirred at 80 °C overnight. CH_2Cl_2 (250 mL) was added to the mixture. The organic phase was washed with H_2O (2 × 200 mL) before being dried over $MgSO_4$. Removal of the solvent under reduced pressure yielded **S1** (1.5 g, 3.24 mmol, 38 %) as a yellow crystalline product—pure by NMR spectroscopy.

Due to overlapping signals in the ^{1}H NMR spectrum, H^8 and H^9 could not be assigned with precision (similarly, C^8 and C^9 could not be assigned with precision).

^{1}H-NMR (500 MHz, $CDCl_3$): δ (ppm) 8.04 (d, J = 9.2 Hz, 4H, H^2), 6.50 (d, J = 9.2 Hz, 4H, H^3), 5.33 (br s, 2H, H^{NH}), 3.72 – 3.67 (m, 4H, $H^{8/9}$), 3.65 – 3.60 (m, 8H, $H^{8/9}$ + H^7), 3.31 (q, J = 6.0 Hz, 4H, H^5), 1.91 (p, J = 5.9 Hz, 4H, H^6).

^{13}C-NMR (125.8 MHz, $CDCl_3$): δ (ppm) 153.81 (C^4), 137.65 (C^1), 126.56 (C^2), 110.97 (C^3), 70.69 ($C^{8/9}$), 70.33 ($C^{8/9}$), 70.06 (C^7), 42.02 (C^5), 28.62 (C^6).

HRMS (ESI+): *m/z* calcd. for [**S1**+Na]$^+$ 485.2007 found 485.1997.

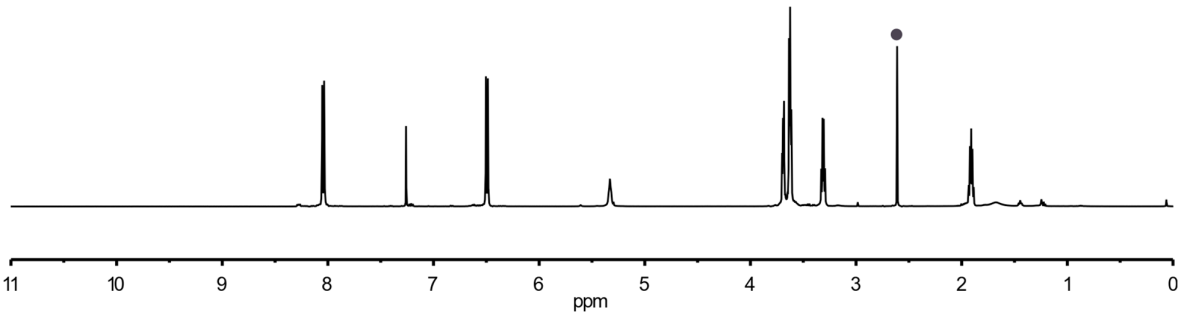

Figure S1. ^{1}H NMR spectra (500 MHz, 297 K, $CDCl_3$) of compound **S1**. The signal from residual traces of DMSO is highlighted by a grey circle.

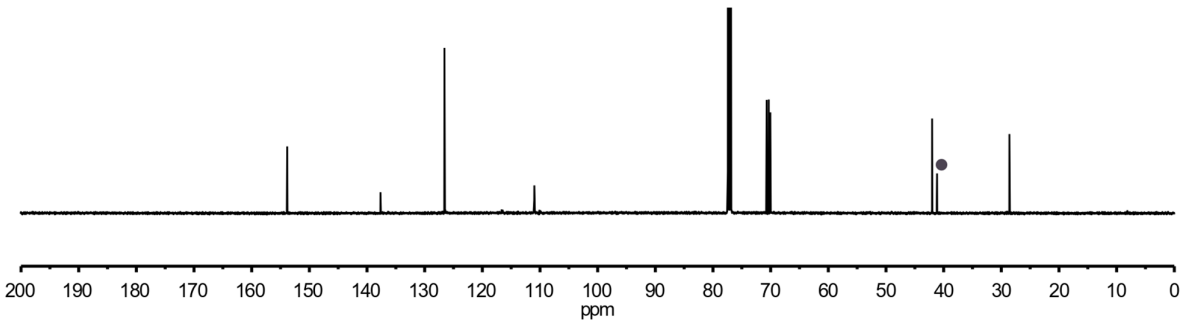

Figure S2. ^{13}C NMR spectra (125 MHz, 297 K, $CDCl_3$) of compound **S1**. The signal from residual traces of DMSO is highlighted by a grey circle.

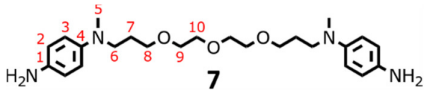

7 was prepared by a modified literature procedures.[S3, S4]

In an oven-dried flask, **S1** (1.5 g, 3.24 mmol, 1 eq.) was dissolved in dry DMF (40 mL). The resulting solution was cooled to 0 °C, before NaH (25% in mineral oil, 744 mg, 7.78 mmol , 2.4 eq.) was added portion-wise. After 15 min of stirring, MeI (444 µL, 1.01 g, 7.14 mmol, 2.2 eq.) was added. The stirring was continued overnight at room temperature. The reaction mixture was diluted with H_2O (100 mL) and the aqueous phase was extracted with EtOAc (2 x 100 mL). The combined organic phases were dried over $MgSO_4$, filtered, and the solvent removed under reduced pressure. The crude product was purified by flash chromatography (SiO_2, CH_2Cl_2 then CH_2Cl_2:EtOAc 1:1). The resulting methylated product was taken up in THF:EtOH 1:1 (100 mL) and Pd/C (10 mol%, 190 mg) was added. The reaction mixture was stirred overnight under an atmosphere of H_2 before being filtered through a pad of celite. Removal of the solvent under reduced pressure yielded **7** (768 mg, 1.78 mmol, 55 %) as a purple oil—pure by NMR spectroscopy.

^{1}H-NMR (500 MHz, $CDCl_3$): δ (ppm) 6.64 (s, 8H, H^2 + H^3), 3.66 (dd, J = 5.9, 3.8 Hz, 4H, H^{10}), 3.58 (dd, J = 5.9, 3.8 Hz, 4H, H^9), 3.49 (t, J = 6.2 Hz, 4H, H^8), 3.28 (t, J = 7.1 Hz, 4H, H^6), 2.80 (s, 6H, H^5), 1.80 (p, J = 6.4 Hz, 4H, H^7).

^{13}C-NMR (125.8 MHz, $CDCl_3$): δ (ppm) 143.77 (C^4), 137.39 (C^1), 116.89 (C^2), 115.30 (C^3), 70.79 (C^{10}), 70.37 (C^9), 69.11 (C^8), 51.05 (C^6), 39.18 (C^5), 27.12 (C^7).

HRMS (ESI+): *m/z* calcd. for [**7**+H]$^+$ 431.3017 found 431.3009.

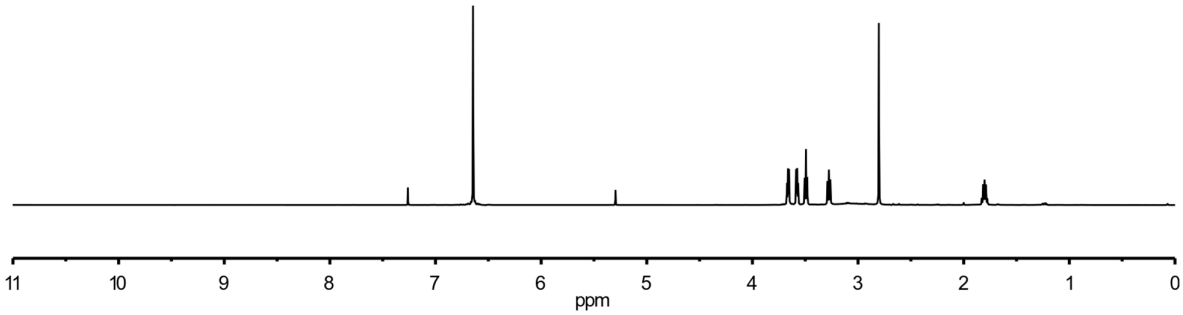

Figure S3. ^{1}H NMR spectra (500 MHz, 297 K, $CDCl_3$) of compound **7**.

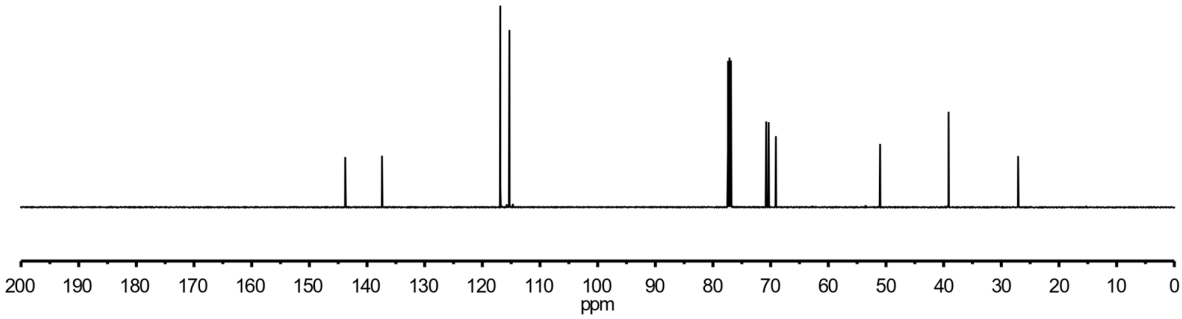

Figure S4. 13C NMR spectra (125 MHz, 297 K, CDCl3) of compound **7**.

2.2 Synthesis of mononuclear metal complexes

2.2.1 General synthetic procedure

The general procedure used to synthesize mononuclear metal complexes from 6-methyl-2-pyridinecarboxaldehyde **3** and monoamines is shown in Scheme S2.

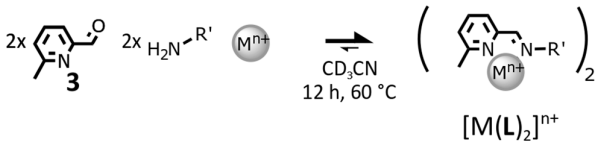

Scheme S2. Synthesis of mononuclear complexes $[M(\mathbf{L})_2]^{n+}$.

General synthetic procedure: CD_3CN solutions of 6-methyl-2-pyridinecarboxaldehyde **3** (200 µL of 128 mM, 25.6 µmol, 2 eq.) and of monoamine (200 µL of 128 mM, 25.6 µmol, 2 eq.) were combined in a NMR tube. The resulting mixture was treated with either a CD_3CN solution of $[Cu(CH_3CN)_4](BF_4)$ (200 µL of 64 mM, 12.8 µmol, 1 eq.) or a CD_3CN solution of $Ag(SbF_6)$ (200 µL of 64 mM, 12.8 µmol, 1 eq.). The mixture, which was left to react at 60 °C for 12 h. In all cases, the major product observed in solution by NMR spectroscopy was the desired complex.

2.2.2 Synthesis of Cu^{I} complex $[Cu(3,1)_2](BF_4)$

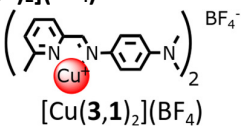

$[Cu(\mathbf{3},\mathbf{1})_2](BF_4)$ was synthesized as described in the literature. NMR and mass data were consistent with those previously reported.[S5]

2.2.3 Synthesis of Cu^{I} complex $[Cu(3,4)_2](BF_4)$

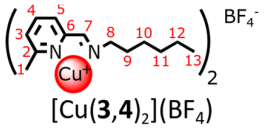

$[Cu(\mathbf{3},\mathbf{4})_2](BF_4)$ was synthesized using the general procedure described in section 2.2.1.

^{1}H-NMR (500 MHz, CD_3CN): δ (ppm) 8.60 (s, 2H, H^7), 7.98 (t, J = 7.6 Hz, 2H, H^4), 7.68 (d, J = 7.3 Hz, 2H, H^5), 7.56 (d, J = 7.6 Hz, 2H, H^3), 3.79 (t, J = 6.9 Hz, 4H, H^8), 2.24 (br s, 6H, H^1), 1.59 (p, J = 7.4 Hz, 4H, H^9), 1.25 (p, J = 7.5 Hz, 4H, H^{10}), 1.13 (br s, 8H, H^{11}+ H^{12}), 0.78 (t, J = 6.5 Hz, 6H, H^{13}).

^{13}C-NMR (125.8 MHz, CD_3CN): δ (ppm) 162.14 (C^7), 158.89 (C^2), 150.92 (C^6), 139.15 (C^4), 128.46 (C^3), 124.97 (C^5), 60.55 (C^8), 31.92 (C^{11}), 31.38 (C^9), 27.12 (C^{10}), 24.72 (C^1), 22.98 (C^{12}), 14.03 (C^{13}).

HRMS (ESI+): *m/z* calcd. for $[Cu(\mathbf{3},\mathbf{4})_2]^+$ 471.2543 found 471.2547.

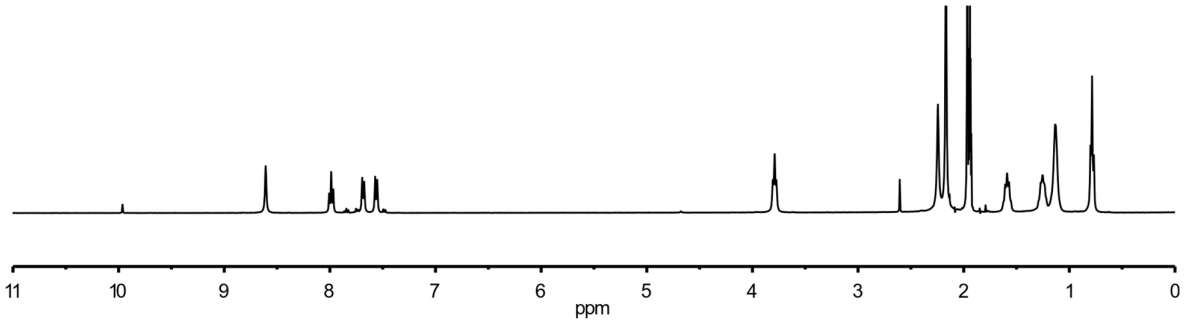

Figure S5. ^{1}H NMR spectra (500 MHz, 297 K, CD_3CN) of Cu^{I} complex $[Cu(\mathbf{3},\mathbf{4})_2](BF_4)$.

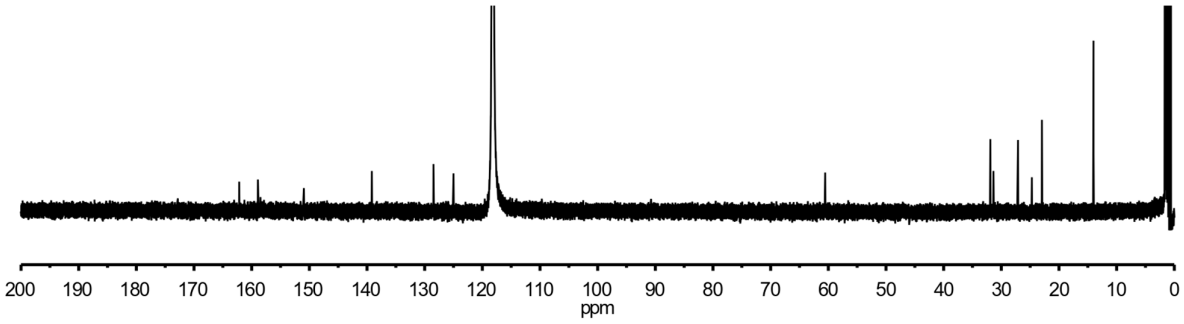

Figure S6. ^{13}C NMR spectra (125 MHz, 297 K, CD_3CN) of Cu^{I} complex $[Cu(\mathbf{3},\mathbf{4})_2](BF_4)$.

2.2.4 Synthesis of Ag^{I} complex $[Ag(3,1)_2](SbF_6)$

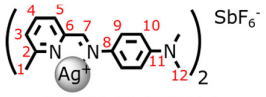

$[Ag(\mathbf{3},\mathbf{1})_2](SbF_6)$

$[Ag(\mathbf{3},\mathbf{1})_2](SbF_6)$ was synthesized using the general procedure described in section 2.2.1.

^{1}H-NMR (500 MHz, CD_3CN): δ (ppm) 8.94 (s, 2H, H^7), 8.02 (t, J = 7.7 Hz, 2H, H^4), 7.76 (d, J = 7.6 Hz, 2H, H^5), 7.54 (d, J = 7.7 Hz, 2H, H^3), 7.49 (d, J = 9.1 Hz, 4H, H^9), 6.70 (d, J = 9.1 Hz, 4H, H^{10}), 2.96 (s, 12H, H^{12}), 2.52 (s, 6H, H^1).

^{13}C-NMR (125.8 MHz, CD_3CN): δ (ppm) 160.01(C^2), 152.68(C^6), 152.23 (C^{11}), 151.23 (C^7), 140.35 (C^4), 136.34 (C^8), 127.66 (C^3), 126.06 (C^5), 125.16 (C^9), 113.12 (C^{10}), 40.45 (C^{12}), 26.38 (C^1).

HRMS (ESI+): *m/z* calcd. for $[Ag(\mathbf{3},\mathbf{1})_2]^+$ 585.1890 found 585.1880.

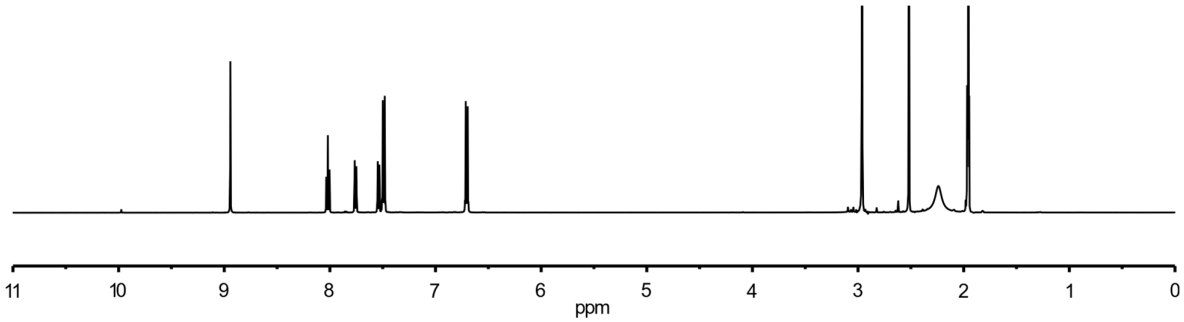

Figure S7. ^{1}H NMR spectra (500 MHz, 297 K, CD_3CN) of Ag^{I} complex $[Ag(\mathbf{3},\mathbf{1})_2](SbF_6)$.

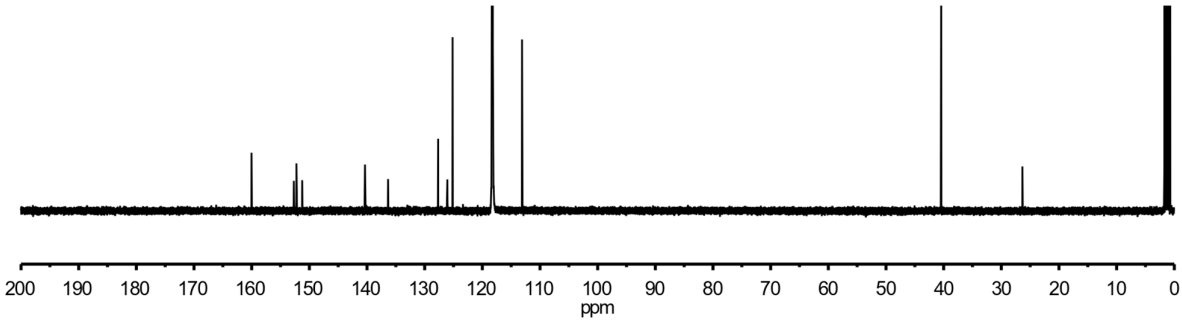

Figure S8. ^{13}C NMR spectra (125 MHz, 297 K, CD_3CN) of Ag^{I} complex [Ag(**3**,**1**)$_2$](SbF_6).

2.2.5 Synthesis of Cu^{I} complex [Cu(3,5)$_2$](BF_4)

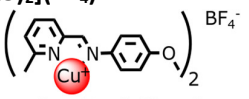

[Cu(**3**,**5**)$_2$](BF_4)

[Cu(**3**,**5**)$_2$](BF_4) was synthesized as described in the literature. NMR and mass data were consistent with those previously reported.[S5]

2.3 Synthesis of mononuclear metal complexes with diamine

2.3.1 General synthetic procedure

The general procedure used to synthesize mononuclear metal complexes from 6-methyl-2-pyridinecarboxaldehyde **3** and 2,2′-(ethylenedioxy)bis(ethylamine) **2** is shown in Scheme S2.

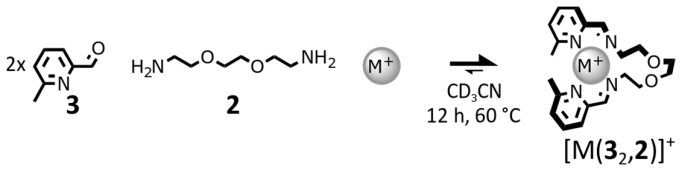

Scheme S3. Synthesis of mononuclear complexes [M(**3**$_2$,**2**)]$^+$.

General synthetic procedure: CD_3CN solutions of 6-methyl-2-pyridinecarboxaldehyde **3** (200 µL of 128 mM, 25.6 µmol, 2 eq.) and 1,2-bis(2-aminoethoxy)ethane **2** (200 µL of 64 mM, 12.8 µmol, 1 eq.) were combined in a NMR tube. The resulting mixture was treated with either a CD_3CN solution of [Cu(CH_3CN)$_4$](BF_4) (200 µL of 64 mM, 12.8 µmol, 1 eq.) or a CD_3CN solution of Ag(SbF_6) (200 µL of 64 mM, 12.8 µmol, 1 eq.). The mixture, which was left to react at 60 °C for 12 h. In all cases, the major product observed in solution by NMR spectroscopy was the desired complex.

2.3.2 Synthesis of Cu^{I} complex [Cu(3$_2$,2)](BF_4)

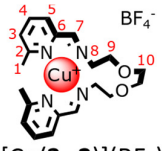

[Cu(**3**$_2$,**2**)](BF_4)

[Cu(**3**$_2$,**2**)](BF_4) was synthesized using the general procedure described in section 2.3.1.

Due to overlapping signals, C^9 and C^{10} could not be assigned with precision.

^{1}H-NMR (500 MHz, CD_3CN): δ (ppm) 8.65 (s, 2H, H^{7}), 8.01 (t, J = 7.5 Hz, 2H, H^{4}), 7.72 (d, J = 7.6 Hz, 2H, H^{5}), 7.60 (d, J = 7.8 Hz, 2H, H^{3}), 3.87 (br m, 4H, H^{8}), 3.81 (br m, 2H, H^{9a}), 3.68 (br s, 2H, H^{9b}), 3.59 (br m, 2H, H^{10a}), 3.33 (br m, 2H, H^{10b}), 2.33 (s, 6H, H^{1}).

^{13}C-NMR (125.8 MHz, CD_3CN): δ (ppm) 163.23 (C^{7}), 159.14 (C^{2}), 150.98 (C^{6}), 139.16 (C^{4}), 128.66 (C^{3}), 125.05 (C^{5}), 71.54 ($C^{9/10}$), 71.51 ($C^{9/10}$), 60.34 (C^{8}), 24.85 (C^{1}).

HRMS (ESI+): *m/z* calcd. for $[Cu(\mathbf{3}_2,\mathbf{2})]^+$ 417.1346 found 417.1344.

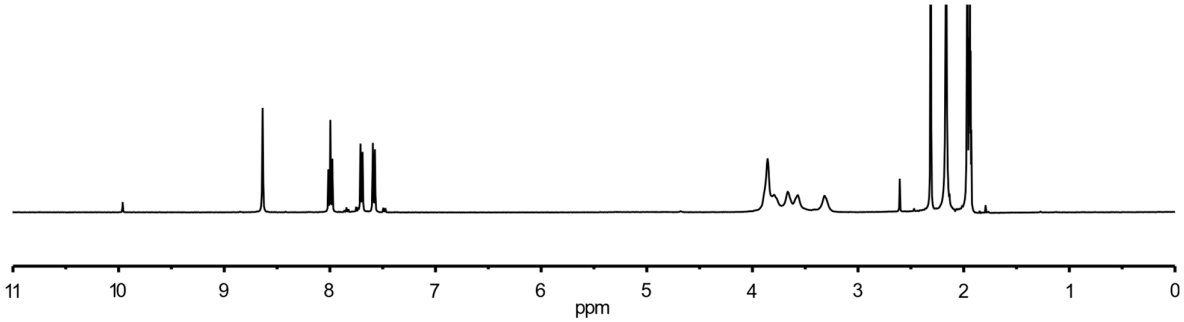

Figure S9. ^{1}H NMR spectra (500 MHz, 297 K, CD_3CN) of Cu^{I} complex $[Cu(\mathbf{3}_2,\mathbf{2})](BF_4)$.

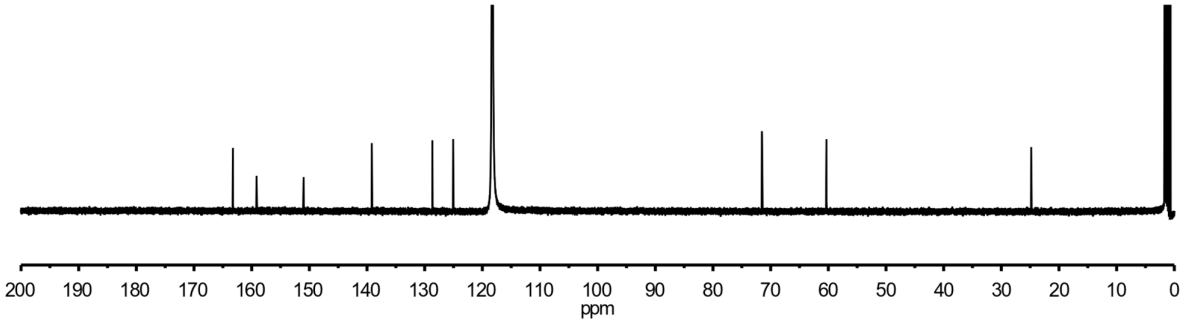

Figure S10. ^{13}C NMR spectra (125 MHz, 297 K, CD_3CN) of Cu^{I} complex $[Cu(\mathbf{3}_2,\mathbf{2})](BF_4)$.

2.3.3 Synthesis of Ag^{I} complex $[Ag(\mathbf{3}_2,\mathbf{2})](SbF_6)$

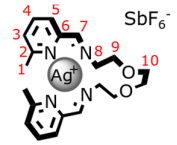

$[Ag(\mathbf{3}_2,\mathbf{2})](SbF_6)$

$[Ag(\mathbf{3}_2,\mathbf{2})](SbF_6)$ was synthesized using the general procedure described in section 2.3.1.

^{1}H-NMR (500 MHz, CD_3CN): δ (ppm) 8.60 (br s, 2H, H^{7}), 7.98 (t, J = 7.7 Hz, 2H, H^{4}), 7.61 (d, J = 7.6 Hz, 2H, H^{5}), 7.54 (d, J = 7.8 Hz, 2H, H^{3}), 3.97 – 3.91 (br m, 4H, H^{8}), 3.89 – 3.81 (br m, 4H, H^{9}), 3.57 (s, 4H, H^{10}), 2.36 (s, 6H, H^{1}).

^{13}C-NMR (125.8 MHz, CD_3CN): δ (ppm) 163.93 (C^{7}), 160.36 (C^{2}), 149.49 (C^{6}), 140.23 (C^{4}), 128.66 (C^{3}), 126.20 (C^{5}), 71.52 (C^{9}), 71.03 (C^{10}), 60.82 (C^{8}), 25.62 (C^{1}).

HRMS (ESI+): *m/z* calcd. for $[Ag(\mathbf{3}_2,\mathbf{2})]^+$ 483.1101 found 461.1097.

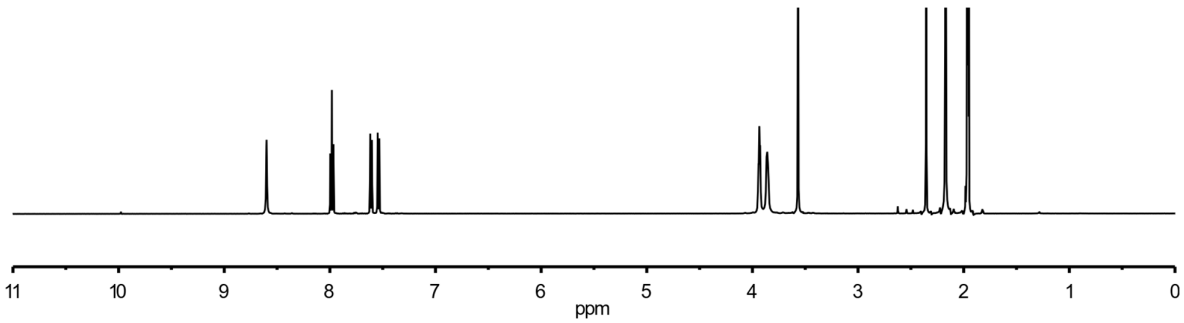

Figure S11. ^{1}H NMR spectra (500 MHz, 297 K, CD_3CN) of Ag^{I} complex [Ag(**3**$_2$,**2**)](SbF_6).

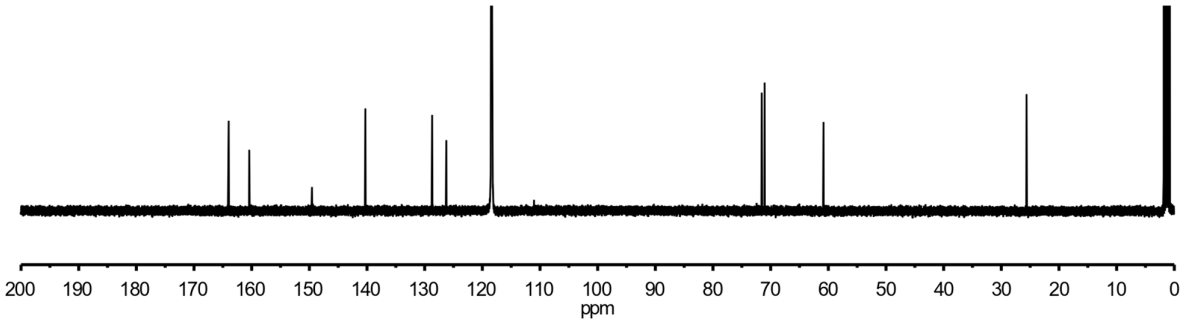

Figure S12. ^{13}C NMR spectra (125 MHz, 297 K, CD_3CN) of Ag^{I} complex [Ag(**3**$_2$,**2**)](SbF_6).

2.4 Synthesis of polynuclear metal complexes

2.4.1 General synthetic procedure

General synthetic procedure: $CDCl_3$:CD_3CN 3:1 solution of dialdehyde **6** (200 µL of 64 mM, 12.8 µmol, 1 eq.) and a CD_3CN solution of 1,2-bis(2-aminoethoxy)ethane **2** or of diamine **7** (200 µL of 64 mM, 12.8 µmol, 1 eq.) were combined in a NMR tube. The resulting mixture was treated with a CD_3CN solution of Ag(SbF_6) (200 µL of 64 mM, 12.8 µmol, 1 eq.). The mixture was left to react at 60 °C for 12 h. In all cases, the major product observed in solution by NMR spectroscopy was the desired complex.

2.4.2 Synthesis of Ag^{I} complex [Ag_2(**6**$_2$,**2**$_2$)](SbF_6)$_2$

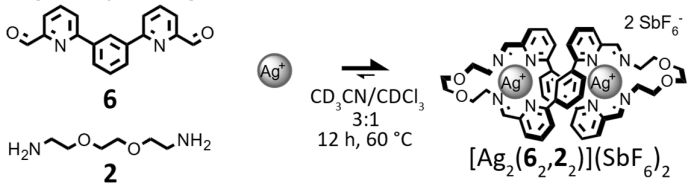

Scheme S4. Synthesis of the Ag^{I} complex [Ag_2(**6**$_2$,**2**$_2$)](SbF_6)$_2$.

[Ag_2(**6**$_2$,**2**$_2$)](SbF_6)$_2$ was synthesized using the general procedure described in section 2.4.1.·

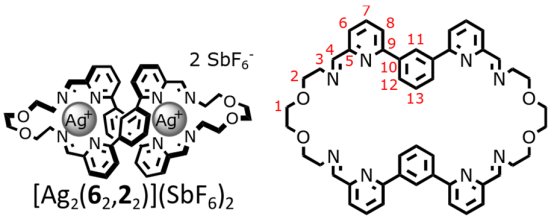

^{1}H-NMR (400 MHz, CD_3CN:$CDCl_3$ 3:1): δ (ppm) 9.40 (s, 2H, H^{11}), 8.04 – 7.97 (m, 8H, H^4 + H^7), 7.91 (dd, J = 8.0, 1.1 Hz, 4H, H^8), 7.86 (dd, J = 7.7, 1.9 Hz, 4H, H^{12}), 7.66 (t, J = 7.7 Hz, 2H, H^{13}), 7.29 (d, J = 7.5 Hz, 4H, H^6), 3.39 – 3.28 (m, 4H, H^{2a}), 3.31 – 3.16 (m, 12H, H^1 + H^{3a}), 3.07 (d, J = 10.4 Hz, 4H, H^{2b}), 2.79 – 2.66 (br m, 4H, H^{3b}).

^{13}C-NMR (125.8 MHz, CD_3CN:$CDCl_3$ 3:1): δ (ppm) 162.52 (C^4), 157.87 (C^9), 149.35 (C^5), 141.18 (C^7), 140.45 (C^{10}), 130.57 (C^{13}), 130.01 (C^{12}), 128.26 (C^6), 126.68 (C^8), 126.31 (C^{11}), 71.61 (C^2), 71.33 (C^1), 60.02 (C^3).

HRMS (ESI+): *m/z* calcd. for $[Ag_2(\mathbf{6}_2,\mathbf{2}_2)]^{2+}$ 507.0945 found 507.0951.

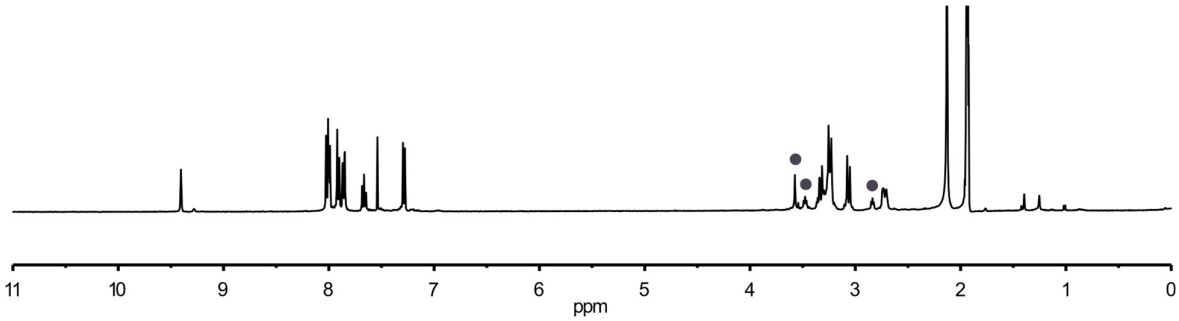

Figure S13. ^{1}H NMR spectra (400 MHz, 297 K, CD_3CN:$CDCl_3$ 3:1) of Ag^{I} complex $[Ag_2(\mathbf{6}_2,\mathbf{2}_2)](SbF_6)_2$. Signals from residual traces of diamine **2** are highlighted by grey circles.

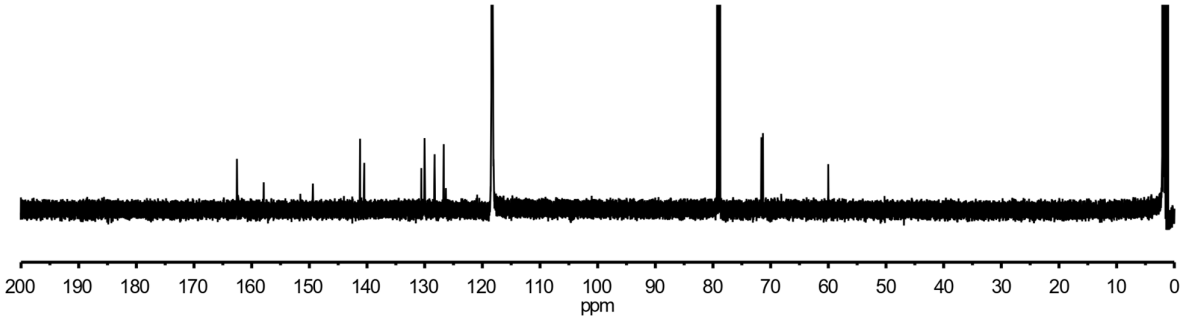

Figure S14. ^{13}C NMR spectra (125 MHz, 297 K, CD_3CN:$CDCl_3$ 3:1) of Ag^{I} complex $[Ag_2(\mathbf{6}_2,\mathbf{2}_2)](SbF_6)_2$.

2.4.3 Synthesis of Ag^{I} complex $[Ag_2(6,7)_2](SbF_6)_2$

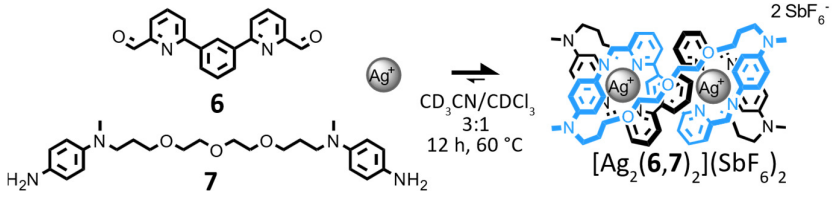

Scheme S5. Synthesis of the Ag^{I} complex $[Ag_2(\mathbf{6},\mathbf{7})_2](SbF_6)_2$.

$[Ag_2(\mathbf{6},\mathbf{7})_2](SbF_6)_2$ was synthesized using the general procedure described in section 2.4.1.

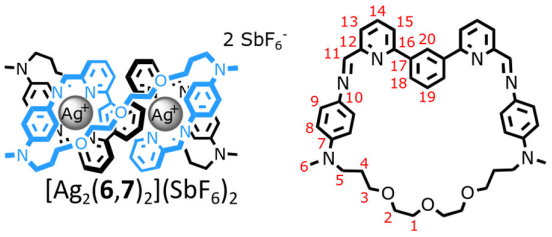

Due to overlapping signals, C^{7}, C^{11} and C^{12}could not be assigned with precision.

^{1}H-NMR (500 MHz, CD_3CN:$CDCl_3$ 3:1): δ (ppm) 9.19 (t, J = 1.9 Hz, 2H, H^{20}), 8.03 (s, 2H, H^{11a}), 8.01 (s, 2H, H^{11b}), 7.91 (t, J = 7.7 Hz, 4H, H^{14}), 7.70 (d, J = 7.7 Hz, 4H, H^{15}), 7.21 (dd, J = 7.8, 1.9 Hz, 4H, H^{18}), 7.12 (d, J = 7.5 Hz, 4H, H^{13}), 6.81 (t, J = 7.7 Hz, 2H, H^{19}), 6.67 (d, J = 9.0 Hz, 8H, H^{9}), 6.16 (d, J = 9.1 Hz, 8H, H^{8}), 3.70 – 3.67 (m, 8H, H^{1}), 3.59 (t, J = 4.8 Hz, 8H, H^{2}), 3.47 (dt, J = 9.6, 6.6 Hz, 4H, H^{3a}), 3.43 – 3.34 (m, 8H, H^{3b} + H^{5a}), 3.25 (dt, J = 15.0, 6.7 Hz, 4H, H^{5b}), 2.79 (s, 12H, H^{6}), 1.76 (p, J = 6.8 Hz, 8H, H^{4}).

^{13}C-NMR (125.8 MHz, CD_3CN:$CDCl_3$ 3:1): δ (ppm) 157.19 (C^{16}), 150.70 ($C^{7/11/12}$), 150.56 ($C^{7/11/12}$), 140.44 (C^{14}), 139.00 (C^{17}), 134.45 (C^{10}), 129.76 (C^{19}), 128.98 (C^{18}), 127.99 (C^{13}), 125.89 (C^{20}), 125.24 (C^{15}), 125.02 (C^{9}), 112.25 (C^{8}), 71.36 (C^{1}), 70.95 (C^{2}), 69.15 (C^{3}), 49.29 (C^{5}), 38.69 (C^{6}), 27.73 (C^{4}).

HRMS (ESI+): *m/z* calcd. for $[Ag_2(\mathbf{6},\mathbf{7})_2]^{2+}$ 790.2682 found 790.2661.

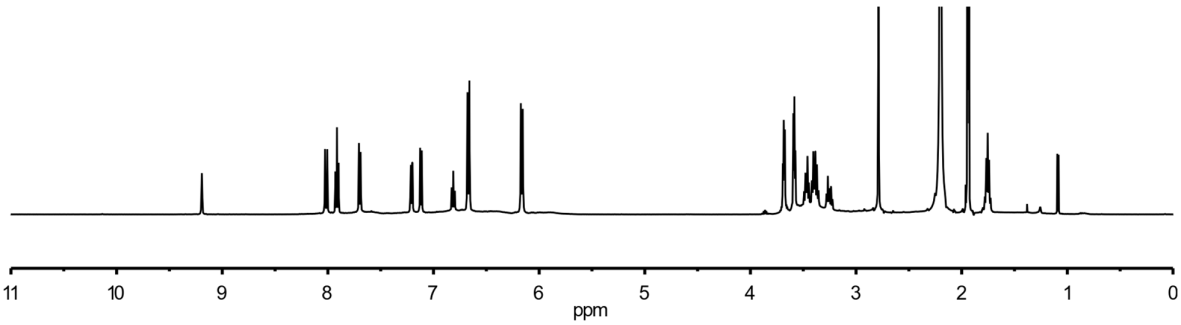

Figure S15. ^{1}H NMR spectra (500 MHz, 297 K, CD_3CN:$CDCl_3$ 3:1) of Ag^{I} complex $[Ag_2(\mathbf{6},\mathbf{7})_2](SbF_6)_2$.

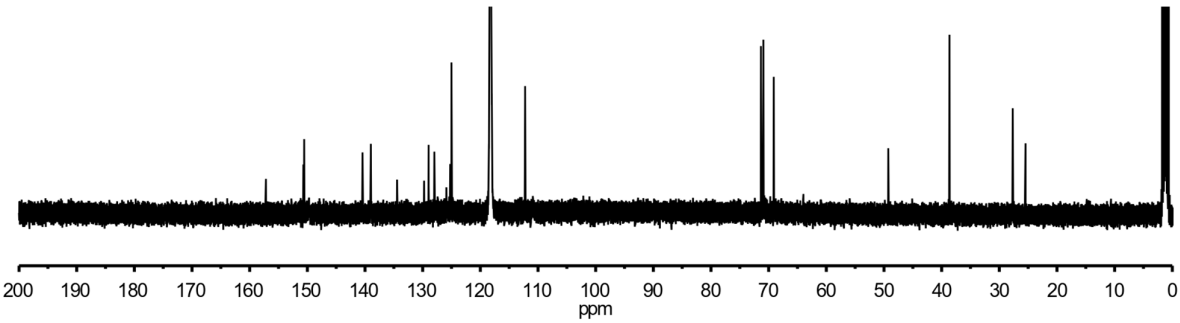

Figure S16. ^{13}C NMR spectra (125 MHz, 297 K, CD_3CN:$CDCl_3$ 3:1) of Ag^{I} complex $[Ag_2(\mathbf{6},\mathbf{7})_2](SbF_6)_2$.

3. Probing of the initial equilibrium composition of the systems

3.1 Mononuclear complexes

3.1.1 Equilibrium composition of a mixture of Cu(BF$_4$) and components 3, 2 and 1

3.1.1.1 Synthetic procedure

The distribution of products obtained at equilibrium from a mixture of Cu(BF$_4$) and components **3**, **2** and **1** was determined using a three-pronged approach. Mixtures of Cu(BF$_4$) and components **3**, **2** and **1** were equilibrated from three different starting points:

- by adding diamine **2** to preformed [Cu(**3**,**1**)$_2$](BF$_4$) (Procedure A)
- by adding arylamine **1** to preformed [Cu(**3**$_2$,**2**)](BF$_4$) (Procedure B)
- and, by mixing all four free components together (Procedure C).

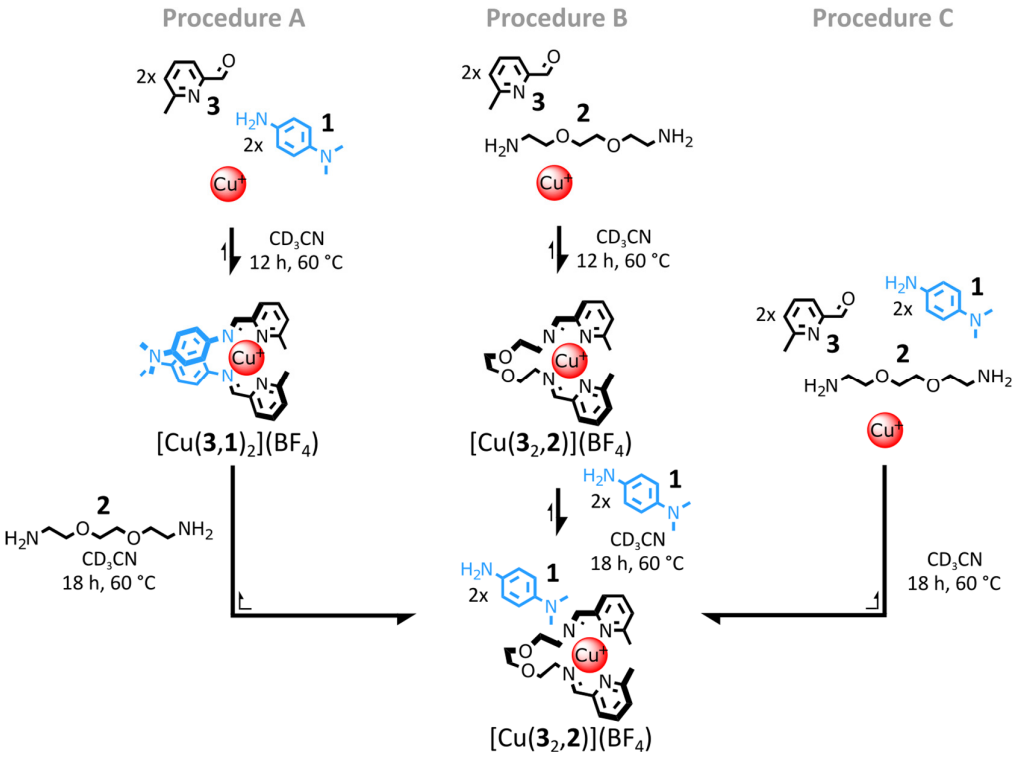

Scheme S6. Probing of the equilibrium composition of a mixture of Cu(BF$_4$), **3**, **2** and **1**.

Procedure A: Complex [Cu(**3**,**1**)$_2$](BF$_4$) was prepared by heating at 60 °C for 12 h a mixture of CD_3CN solutions of 6-methyl-2-pyridinecarboxaldehyde **3** (100 µL of 64 mM, 6.4 µmol, 2 eq.), 4-(dimethylamino)aniline **1** (100 µL of 64 mM, 6.4 µmol, 2 eq.) and [Cu(CH_3CN)$_4$](BF$_4$) (100 µL of 32 mM, 3.2 µmol, 1 eq.). The resulting CD_3CN solution of [Cu(**3**,**1**)$_2$](BF$_4$) was diluted with 100 µL of CD_3CN before being treated with a CD_3CN solution of 1,2-bis(2-aminoethoxy)ethane **2** (100 µL of 33.6 mM, 3.36 µmol, 1.05 eq.) and left to react at 60 °C for 18 h. The evolution of the reaction mixture was monitored by ^{1}H NMR spectroscopy. The complexes were never isolated, all the present experiments and analysis were performed on the crude reaction mixture.

Procedure B: Complex [Cu(**3**$_2$,**2**)](BF$_4$) was prepared by heating at 60 °C for 12 h a mixture of CD_3CN solutions of 6-methyl-2-pyridinecarboxaldehyde **3** (100 µL of 64 mM, 6.4 µmol, 2 eq.), 1,2-bis(2-aminoethoxy)ethane **2** (100 µL of 33.6 mM, 3.36 µmol, 1.05 eq.) and [Cu(CH_3CN)$_4$](BF$_4$) (100 µL of 32 mM, 3.2 µmol, 1 eq.). The resulting CD_3CN solution of [Cu(**3**$_2$,**2**)](BF$_4$) was diluted with 100 µL of CD_3CN before being treated with a CD_3CN solution of 4-(dimethylamino)aniline **1** (100 µL of 64 mM,

6.4 µmol, 2 eq.) and left to react at 60 °C for 18 h. The evolution of the reaction mixture was monitored by ^{1}H NMR spectroscopy. The complexes were never isolated, all the present experiments and analysis were performed on the crude reaction mixture.

Procedure C: A mixture of CD_3CN solutions of 6-methyl-2-pyridinecarboxaldehyde **3** (100 µL of 64 mM, 6.4 µmol, 2 eq.), 1,2-bis(2-aminoethoxy)ethane **2** (100 µL of 33.6 mM, 3.36 µmol, 1.05 eq.), (dimethylamino)aniline **1** (100 µL of 64 mM, 6.4 µmol, 2 eq.) and $[Cu(CH_3CN)_4](BF_4)$ (100 µL of 32 mM, 3.2 µmol, 1 eq.) was heated at 60 °C for 18 h. The evolution of the reaction mixture was monitored by ^{1}H NMR spectroscopy. The complexes were never isolated, all the present experiments and analysis were performed on the crude reaction mixture.

3.1.1.2 Composition of the reaction mixtures after 18 h at 60 °C

All three procedures yielded a similar equilibrium mixture containing (almost) exclusively $[Cu(\mathbf{3}_2,\mathbf{2})](BF_4)$ and free arylamine **1**, confirming that $[Cu(\mathbf{3}_2,\mathbf{2})](BF_4)$ is the most thermodynamically stable complex in these conditions. The composition of the equilibrated mixture was confirmed by mass spectrometry (see SI, section 4.1.1.2). $[Cu(\mathbf{3}_2,\mathbf{2})]+$ was the only complex visible by ESI-MS.

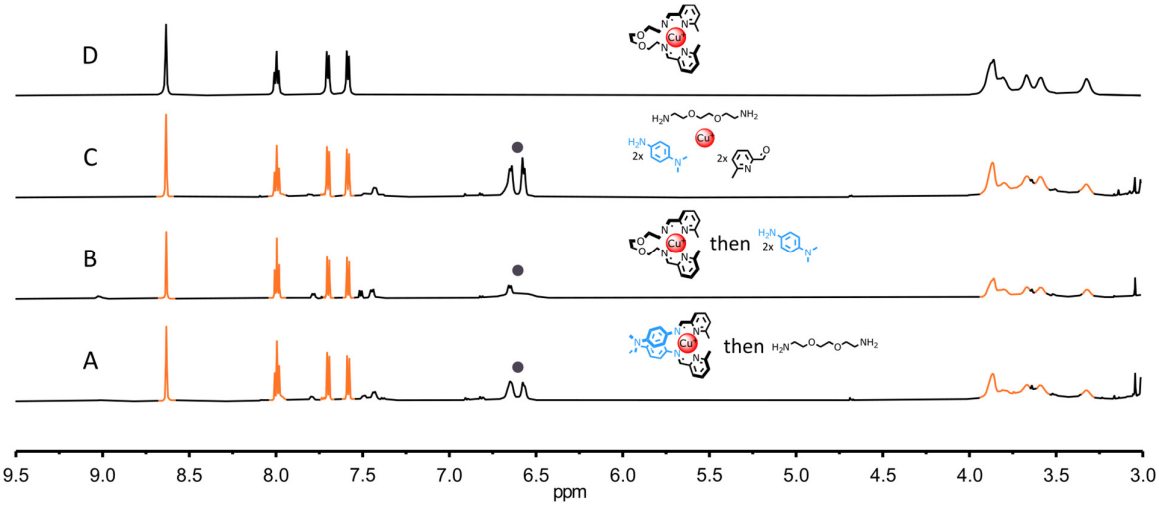

Figure S17. Partial ^{1}H NMR spectra (600 MHz, 297 K, CD_3CN) of: (A) a mixture of $[Cu(\mathbf{3},\mathbf{1})_2](BF_4)$ and **2** in a 1:1 molar ratio after 18 h at 60 °C (B) a mixture of $[Cu(\mathbf{3}_2,\mathbf{2})](BF_4)$ and **1** in a 1:2 molar ratio after 18 h at 60 °C (C) a mixture of $Cu(BF_4)$ and **3**, **2**, **1** in a 1:2:2:1 molar ratio after 18 h at 60 °C (D) complex $[Cu(\mathbf{3}_2,\mathbf{2})](BF_4)$. Diagnostic signals of $[Cu(\mathbf{3}_2,\mathbf{2})](BF_4)$ and $[Cu(\mathbf{3},\mathbf{1})_2](BF_4)$ are highlighted in orange. Diagnostic signals of **1** are highlighted by a grey circle.

3.1.2 Equilibrium composition of a mixture of $Cu(BF_4)$ and components 4, 3 and 1

3.1.2.1 Synthetic procedure

The distribution of products obtained at equilibrium from a mixture of $Cu(BF_4)$ and components **4**, **3** and **1** was determined using a two-pronged approach. Mixtures of $Cu(BF_4)$ and components **4**, **3** and **1** were equilibrated from two different starting points:

- by adding arylamine **1** to preformed $[Cu(\mathbf{3},\mathbf{4})_2](BF_4)$ (Procedure B)
- and, by mixing all four free components together (Procedure C).

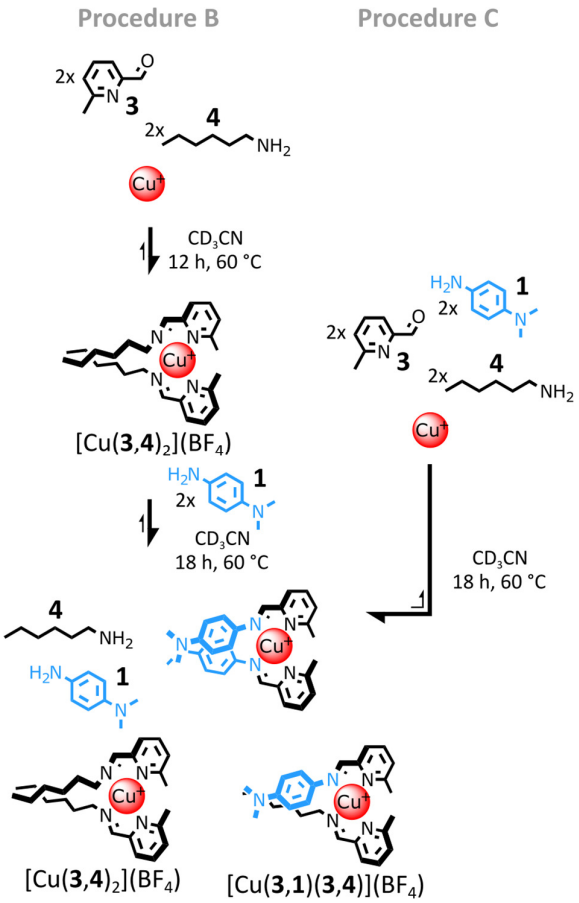

Scheme S7. Probing of the equilibrium composition of a mixture of $Cu(BF_4)$, **4**, **3** and **1**.

Procedure B: Complex $[Cu(\mathbf{3},\mathbf{4})_2](BF_4)$ was prepared by heating at 60 °C for 12 h a mixture of CD_3CN solutions of 6-methyl-2-pyridinecarboxaldehyde **3** (100 µL of 64 mM, 6.4 µmol, 2 eq.), hexylamine **4** (100 µL of 64 mM, 6.4 µmol, 2 eq.) and $[Cu(CH_3CN)_4](BF_4)$ (100 µL of 32 mM, 3.2 µmol, 1 eq.). The resulting CD_3CN solution of $[Cu(\mathbf{3},\mathbf{4})_2](BF_4)$ was diluted with 100 µL of CD_3CN before being treated with a CD_3CN solution of 4-(dimethylamino)aniline **1** (100 µL of 64 mM, 6.4 µmol, 2 eq.) and left to react at 60 °C for 18 h. The evolution of the reaction mixture was monitored by ^1H NMR spectroscopy. The complexes were never isolated, all the present experiments and analysis were performed on the crude reaction mixture.

Procedure C: A mixture of CD_3CN solutions of 6-methyl-2-pyridinecarboxaldehyde **3** (100 µL of 64 mM, 6.4 µmol, 2 eq.), hexylamine **4** (100 µL of 64 mM, 6.4 µmol, 2 eq.), (dimethylamino)aniline **1** (100 µL of 64 mM, 6.4 µmol, 2 eq.) and $[Cu(CH_3CN)_4](BF_4)$ (100 µL of 32 mM, 3.2 µmol, 1 eq.) was heated at 60 °C for 18 h. The evolution of the reaction mixture was monitored by ^1H NMR spectroscopy. The complexes were never isolated, all the present experiments and analysis were performed on the crude reaction mixture.

3.1.2.2 Composition of the reaction mixtures after 18 h at 60 °C

The two procedures yielded a similar equilibrium mixture containing the three complexes: $[Cu(\mathbf{3},\mathbf{1})_2]^+$, $[Cu(\mathbf{3},\mathbf{4})_2]^+$ and $[Cu(\mathbf{3},\mathbf{1})(\mathbf{3},\mathbf{4})]^+$. The formation of the two homoleptic complexes $[Cu(\mathbf{3},\mathbf{1})_2]^+$ and $[Cu(\mathbf{3},\mathbf{4})_2]^+$ was confirmed by ^{1}H NMR spectroscopy (Fig. S18) and by mass spectrometry (see SI, section 4.1.2.2). The formation of $[Cu(\mathbf{3},\mathbf{1})(\mathbf{3},\mathbf{4})]^+$ was confirmed by mass spectrometry (see SI, section 4.1.2.2); the ^{1}H NMR signals of $[Cu(\mathbf{3},\mathbf{1})(\mathbf{3},\mathbf{4})]^+$ overlapped with those of the two homoleptic complexes. All three complexes are formed under thermodynamic control.

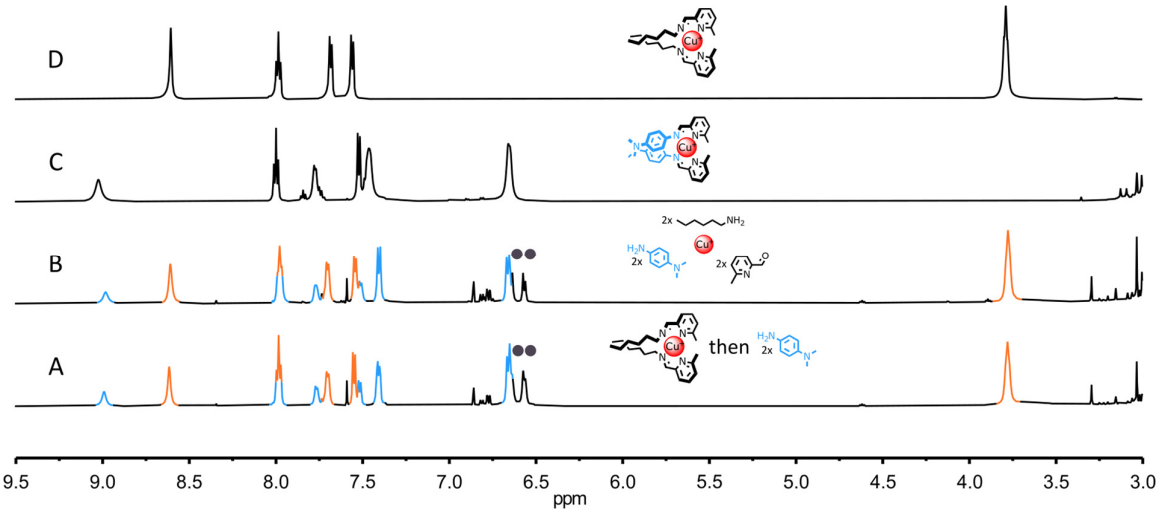

Figure S18. Partial ^{1}H NMR spectra (600 MHz, 297 K, CD_3CN) of: (A) a mixture of $[Cu(\mathbf{3},\mathbf{4})_2](BF_4)$ and **1** in a 1:2 molar ratio after 18 h at 60 °C (B) a mixture of $Cu(BF_4)$ and **4**, **3**, **1** in a 1:2:2:2 molar ratio after 18 h at 60 °C (C) complex $[Cu(\mathbf{3},\mathbf{1})_2](BF_4)$ (D) complex $[Cu(\mathbf{3},\mathbf{4})_2](BF_4)$. Diagnostic signals of $[Cu(\mathbf{3},\mathbf{1})_2](BF_4)$ and $[Cu(\mathbf{3},\mathbf{4})_2](BF_4)$ are highlighted in blue and orange, respectively. Diagnostic signals of **1** highlighted by grey circles.

3.1.3 Equilibrium composition of a mixture of $Ag(SbF_6)$ and components 3, 2 and 1

3.1.3.1 Synthetic procedure

The distribution of products obtained at equilibrium from a mixture of $Ag(SbF_6)$ and components **3**, **2** and **1** was determined using a two-pronged approach, investigating if the products obtained are formed under thermodynamic control. Mixtures of $Ag(SbF_6)$ and components **3**, **2** and **1** were equilibrated from two different starting points:

- by adding arylamine **1** to preformed $[Ag(\mathbf{3}_2,\mathbf{2})](SbF_6)$ (Procedure B)
- and, by mixing all four free components together (Procedure C).

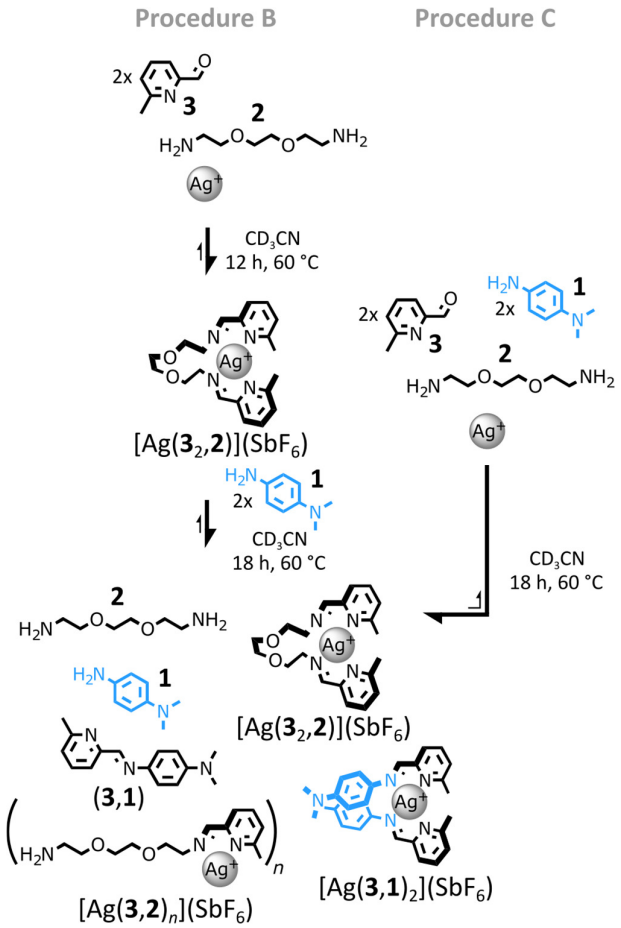

Scheme S8. Probing of the equilibrium composition of a mixture of $Ag(SbF_6)$, **3**, **2** and **1**.

Procedure B: Complex $[Ag(\mathbf{3}_2,\mathbf{2})](SbF_6)$ was prepared by heating at 60 °C for 12 h a mixture of CD_3CN solutions of 6-methyl-2-pyridinecarboxaldehyde **3** (100 µL of 64 mM, 6.4 µmol, 2 eq.), 1,2-bis(2-aminoethoxy)ethane **2** (100 µL of 33.6 mM, 3.36 µmol, 1.05 eq.) and $Ag(SbF_6)$ (100 µL of 32 mM, 3.2 µmol, 1 eq.). The resulting CD_3CN solution of $[Ag(\mathbf{3}_2,\mathbf{2})](SbF_6)$ was diluted with 100 µL of CD_3CN before being treated with a CD_3CN solution of 4-(dimethylamino)aniline **1** (100 µL of 64 mM, 6.4 µmol, 2 eq.) and left to react at 60 °C for 18 h. The evolution of the reaction mixture was monitored by ^1H NMR spectroscopy. The complexes were never isolated, all the present experiments and analysis were performed on the crude reaction mixture.

Procedure C: A mixture of CD_3CN solutions of 6-methyl-2-pyridinecarboxaldehyde **3** (100 µL of 64 mM, 6.4 µmol, 2 eq.), 1,2-bis(2-aminoethoxy)ethane **2** (100 µL of 33.6 mM, 3.36 µmol, 1.05 eq.), (dimethylamino)aniline **1** (100 µL of 64 mM, 6.4 µmol, 2 eq.) and $Ag(SbF_6)$ (100 µL of 32 mM, 3.2 µmol, 1 eq.) was heated at 60 °C for 18 h. The evolution of the reaction mixture was monitored by ^1H NMR spectroscopy. The complexes were never isolated, all the present experiments and analysis were performed on the crude reaction mixture.

3.1.3.2 Composition of the reaction mixtures after 18 h at 60 °C

The two procedures yielded a similar equilibrium mixture containing four different species: $[Ag(\mathbf{3}_2,\mathbf{2})]^+$, $[Ag(\mathbf{3},\mathbf{1})_2]^+$, $[Ag(\mathbf{3},\mathbf{2})_n]^+$, and (**3**,**1**). In both cases (i) the diagnostic signals of $[Ag(\mathbf{3}_2,\mathbf{2})]^+$ and (**3**,**1**) dominated the ^{1}H NMR spectra of the reaction, (ii) the formation of some $[Ag(\mathbf{3},\mathbf{1})_2]^+$ was indicated by a slight shift of the signals of (**3**,**1**) compared to the spectra of the free imine (see section 3.1.3.3) and (iii) the signals of a fourth species—likely, corresponding to a $[Ag(\mathbf{3},\mathbf{2})_n]^+$ type complex (see section 3.1.3.4)—could be observed. The formation of $[Ag(\mathbf{3}_2,\mathbf{2})]^+$, $[Ag(\mathbf{3},\mathbf{1})_2]^+$ and (**3**,**1**) were confirmed by mass spectrometry (see SI, section 4.1.3.2). All four species formed under thermodynamic control.

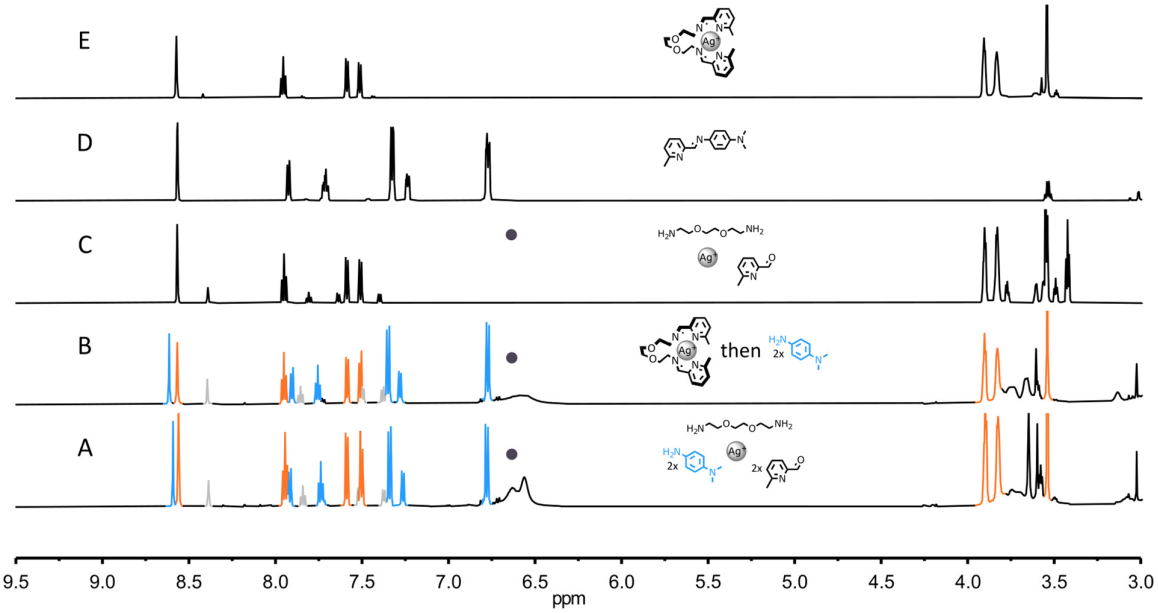

Figure S19. Partial ^{1}H NMR spectra (600 MHz, 297 K, CD_3CN) of: (A) a mixture of $Ag(SbF_6)$ and **3**, **2**, **1** in a 1:2:1:2 molar ratio after 18 h at 60 °C (B) a mixture of $[Ag(\mathbf{3}_2,\mathbf{2})](SbF_6)$ and **1** in a 1:2 molar ratio after 18 h at 60 °C (C) a mixture of $Ag(SbF_6)$, **3** and **2** in a 0.6:1:1 molar ratio (D) imine (**3**,**1**) (D) complex $[Ag(\mathbf{3}_2,\mathbf{2})](SbF_6)$. Diagnostic signals $[Ag(\mathbf{3}_2,\mathbf{2})](SbF_6)$ are highlighted in orange. Diagnostic signals of imine (**3**,**1**) and $[Ag(\mathbf{3},\mathbf{1})_2](SbF_6)$ are highlighted in blue. Diagnostic signals of imine (**3**,**2**) and $[Ag(\mathbf{3},\mathbf{2})_n](SbF_6)$ are highlighted in grey. Diagnostic signals of **1** are highlighted by grey circles.

*3.1.3.3 Titration of free imine (**3**,**1**) with Ag(SbF$_6$)*

A 12.8 mM solution of (**3**,**1**) in CD_3CN was titrated with a 32 mM solution of Ag(SbF_6) in CD_3CN. Upon the addition of each aliquot of Ag(SbF_6), the evolution of the reaction mixture was followed by ^{1}H NMR spectroscopy. A single set of signals was observed in the ^{1}H NMR spectra of the mixture, indicating that [Ag(**3**,**1**)$_2$]$^+$ and free imine (**3**,**1**) are in fast exchange on the NMR timescale (see Fig. S20).

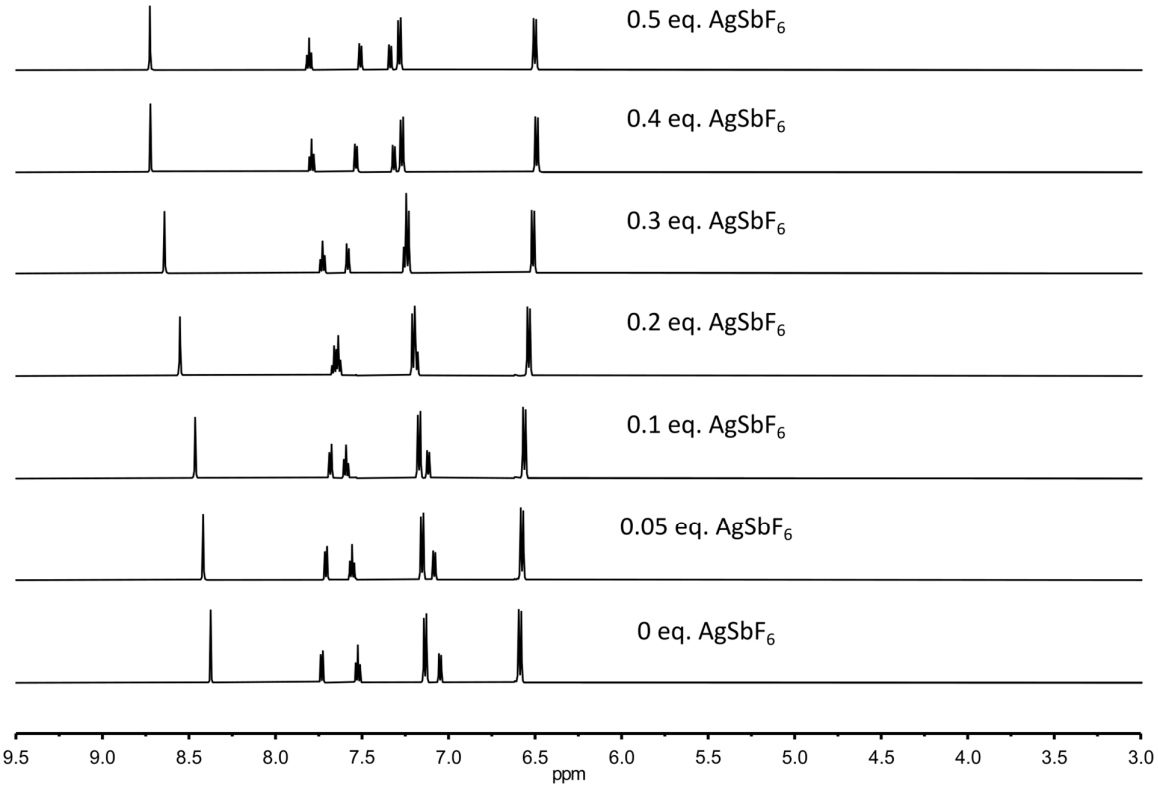

Figure S20. Partial ^{1}H NMR spectra (600 MHz, 297 K, CD_3CN) of 12.8 mM solution of imine (**3**,**1**) in the presence of an increasing amount of Ag(SbF_6).

*3.1.3.4 Titration of an equimolar mixture of **3** and **2** with Ag(SbF$_6$)*

Procedure: CD_3CN solutions of 6-methyl-2-pyridinecarboxaldehyde **3** (100 µL of 32 mM, 3.2 µmol, 1 eq.) and 1,2-bis(2-aminoethoxy)ethane **2** (100 µL of 32 mM, 3.2 µmol, 1 eq.) were mixed together in 300 µL of CD_3CN. The resulting mixture was heated at 60 °C for 18 h before being titrated with a 32 mM solution of Ag(SbF$_6$) in CD_3CN.

Before the addition of Ag(SbF$_6$), two sets of signals were observable in the ^{1}H NMR spectrum of the mixture, corresponding to di-imine (**3**$_2$,**2**) and mono-imine (**3**,**2**). Upon addition of Ag(SbF$_6$), the gradual shifting of both sets of signals indicated the formation of complexes [Ag(**3**$_2$,**2**)]$^+$ and [Ag(**3**,**2**)$_n$]$^+$—the exact nature of [Ag(**3**,**2**)$_n$]$^+$ could not be determined as only [Ag(**3**$_2$,**2**)]$^+$ could be observed via ESI-MS.

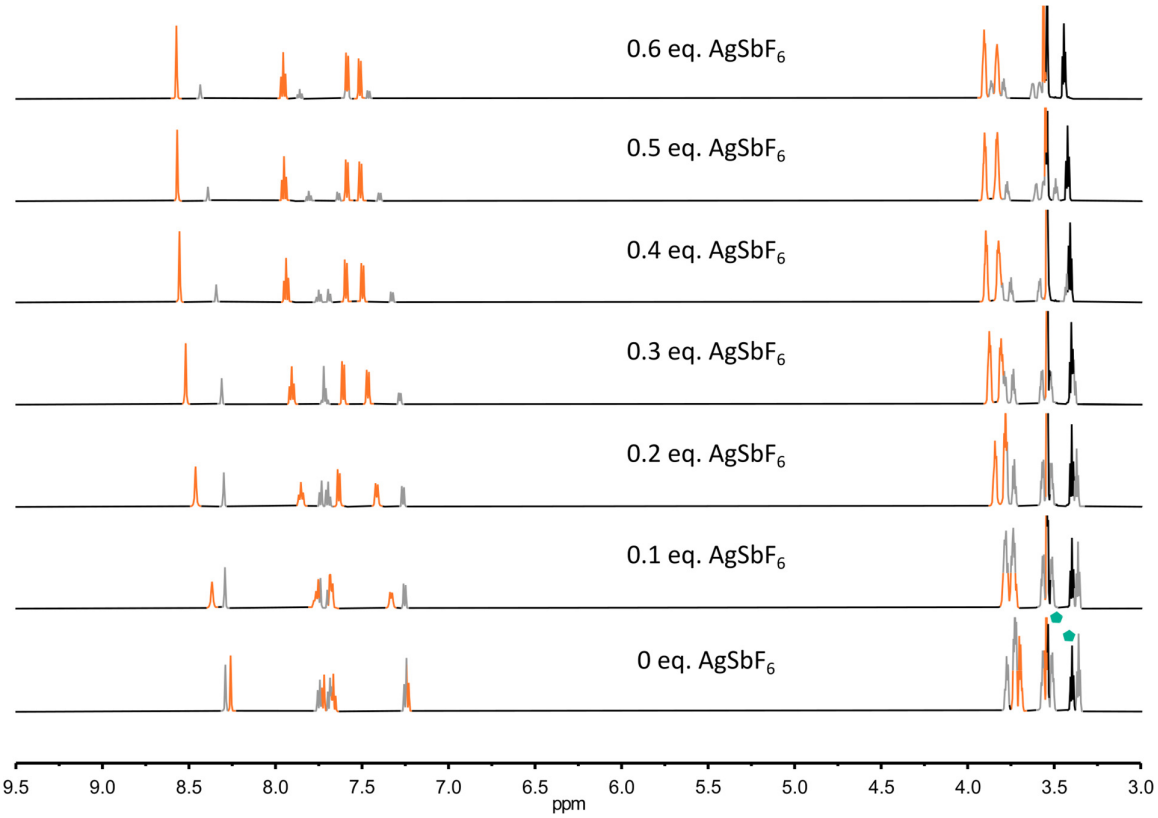

Figure S21. Partial ^{1}H NMR spectra (600 MHz, 297 K, CD_3CN) of a pre-equilibrated mixture of **3** and **2** (i a 1 :1 molar ratio) in the presence of an increasing amount of Ag(SbF$_6$).Diagnostic signals of imine (**3**$_2$,**2**) and [Ag(**3**$_2$,**2**)](BF$_4$) are highlighted in orange. Diagnostic signals of imine (**3**,**2**) and [Ag(**3**,**2**)$_n$](BF$_4$) are highlighted in grey. Diagnostic signals of **2** are highlighted by green pentagons.

3.1.4 Equilibrium from a mixture of Cu(BF$_4$) and components 5, 3 and 2

3.1.4.1 Synthetic procedure

The distribution of products obtained at equilibrium from a mixture of Cu(BF$_4$) and components **5**, **3** and **2** was determined using a two-pronged approach. Mixtures of Cu(BF$_4$) and components **5**, **3** and **2** were equilibrated from two different starting points:

- by adding arylamine **5** to preformed [Cu(**3**$_2$,**2**)](BF$_4$) (Procedure B)
- and, by mixing all four free components together (Procedure C).

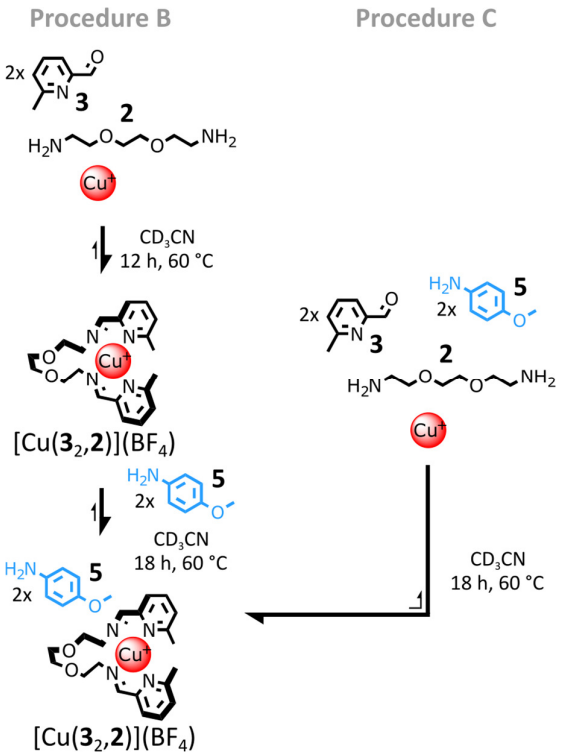

Scheme S9. Probing of the equilibrium composition of a mixture of $Cu(BF_4)$, **5**, **3** and **2**.

Procedure B: Complex $[Cu(\mathbf{3}_2,\mathbf{2})](BF_4)$ was prepared by heating at 60 °C for 12 h a mixture of CD_3CN solutions of 6-methyl-2-pyridinecarboxaldehyde **3** (100 µL of 64 mM, 6.4 µmol, 2 eq.), 1,2-bis(2-aminoethoxy)ethane **2** (100 µL of 33.6 mM, 3.36 µmol, 1.05 eq.) and $[Cu(CH_3CN)_4](BF_4)$ (100 µL of 32 mM, 3.2 µmol, 1 eq.). The resulting CD_3CN solution of $[Cu(\mathbf{3}_2,\mathbf{2})](BF_4)$ was diluted with 100 µL of CD_3CN before being treated with a CD_3CN solution of p-anisidine **5** (100 µL of 64 mM, 6.4 µmol, 2 eq.) and left to react at 60 °C for 18 h. The evolution of the reaction mixture was monitored by ^1H NMR spectroscopy. The complexes were never isolated, all the present experiments and analysis were performed on the crude reaction mixture.

Procedure C: A mixture of CD_3CN solutions of 6-methyl-2-pyridinecarboxaldehyde **3** (100 µL of 64 mM, 6.4 µmol, 2 eq.), 1,2-bis(2-aminoethoxy)ethane **2** (100 µL of 33.6 mM, 3.36 µmol, 1.05 eq.), p-anisidine **5** (100 µL of 64 mM, 6.4 µmol, 2 eq.) and $[Cu(CH_3CN)_4](BF_4)$ (100 µL of 32 mM, 3.2 µmol, 1 eq.) was heated at 60 °C for 18 h. The evolution of the reaction mixture was monitored by ^1H NMR spectroscopy. The complexes were never isolated, all the present experiments and analysis were performed on the crude reaction mixture.

3.1.4.2 Composition of the reaction mixtures after 18 h at 60 °C

Both procedures yielded an equilibrium mixture containing (almost) exclusively $[Cu(\mathbf{3}_2,\mathbf{2})](BF_4)$ and free arylamine **5**, confirming that $[Cu(\mathbf{3}_2,\mathbf{2})](BF_4)$ is the most thermodynamically stable complex in these conditions. The composition of the mixture at equilibrium was confirmed by mass spectrometry (see SI, section 4.1.5.2). $[Cu(\mathbf{3}_2,\mathbf{2})]+$ was the only complex visible by ESI-MS.

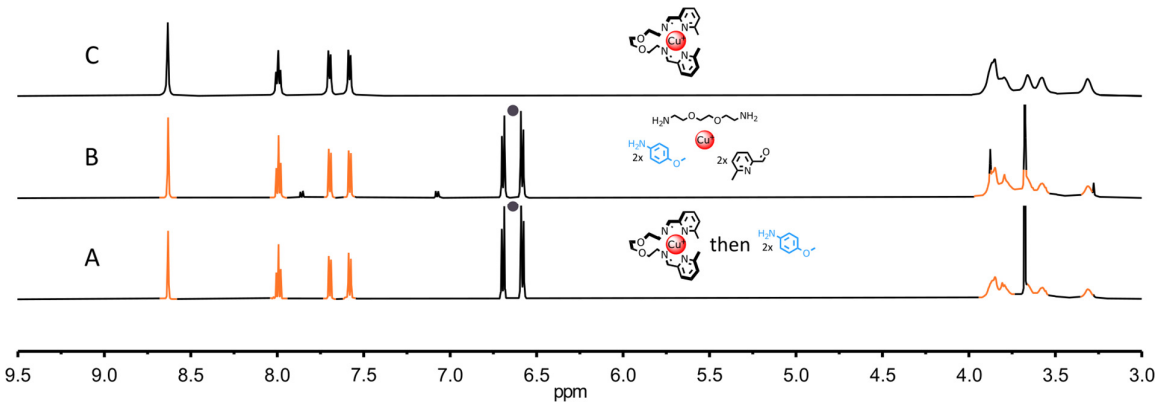

Figure S22. Partial ^{1}H NMR spectra (600 MHz, 297 K, CD_3CN) of: (A) a mixture of [Cu(**3**$_2$,**2**)$_2$](BF$_4$) and **5** in a 1:1 molar ratio after 18 h at 60 °C (B) a mixture of Cu(BF$_4$) and **5**, **3**, **2** in a 1:2:2:1 molar ratio after 18 h at 60 °C (D) complex [Cu(**3**$_2$,**2**)](BF$_4$). Diagnostic signals of [Cu(**3**$_2$,**2**)](BF$_4$) are highlighted in orange. Diagnostic signals of **5** are highlighted by a grey circle.

3.2 Equilibrium composition of a mixture of Ag(SbF$_6$) and components 7, 6 and 2

3.2.1.1 Synthetic procedure

The distribution of products obtained at equilibrium from a mixture of Ag(SbF$_6$) and components **7**, **6** and **2** was determined letting a mixture of all four free components equilibrate at 60 °C for 18 h.

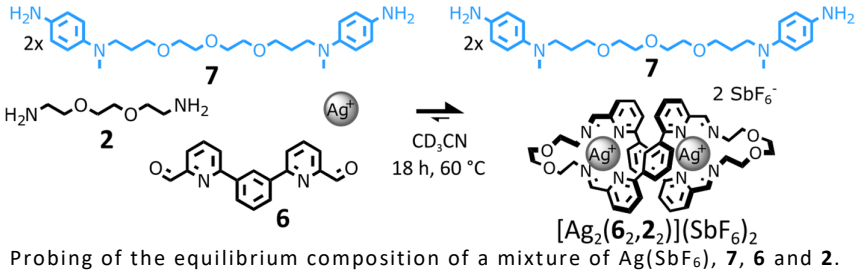

Scheme S10. Probing of the equilibrium composition of a mixture of Ag(SbF$_6$), **7**, **6** and **2**.

A mixture of CD_3CN solutions of dialdehyde **6** (100 µL of 32 mM, 3.2 µmol, 1 eq.), 1,2-bis(2-aminoethoxy)ethane **2** (100 µL of 35.2 mM, 3.52 µmol, 1.1 eq.), diamine **7** (100 µL of 32 mM, 3.2 µmol, 1 eq.) and Ag(SbF$_6$) (100 µL of 32 mM, 12.8 µmol, 1 eq.) was heated at 60 °C for 18 h. The evolution of the reaction mixture was monitored by ^{1}H NMR spectroscopy. The complexes were never isolated, all the present experiments and analysis were performed on the crude reaction mixture.

3.2.1.2 Composition of the reaction mixtures after 18 h at 60 °C

After 18 h at 60 °C, the diagnostic signals of $[Ag_2(\mathbf{6}_2,\mathbf{2}_2)](SbF_6)_2$ were the only ones visible in the spectrum of the crude reaction mixture (alongside free diamine **7**), indicating that $[Ag_2(\mathbf{6}_2,\mathbf{2}_2)](SbF_6)_2$ is the most thermodynamically stable complex in these conditions.

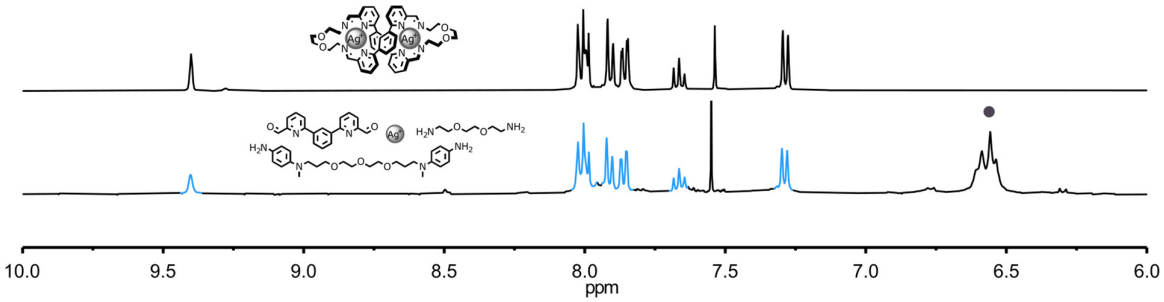

Figure S23. Partial ^{1}H NMR spectra (400 MHz, 297 K, CD_3CN) of: (Bottom) a mixture of $Ag(SbF_6)$ and **7**, **6**, **2** in a 1:1:1:1 molar ratio after 18 h at 60 °C (Top) complex $[Ag_2(\mathbf{6}_2,\mathbf{2}_2)](SbF_6)_2$. Diagnostic signals of $[Ag_2(\mathbf{6}_2,\mathbf{2}_2)](SbF_6)_2$ are highlighted in blue. Diagnostic signals of **7** are highlighted by grey circles.

4. Transient rearrangement

4.1 Mononuclear complexes

4.1.1 Transient self-assembly of $[Cu(3,1)_2](BF_4)$ from $[Cu(3_2,2)](BF_4)$ and 1

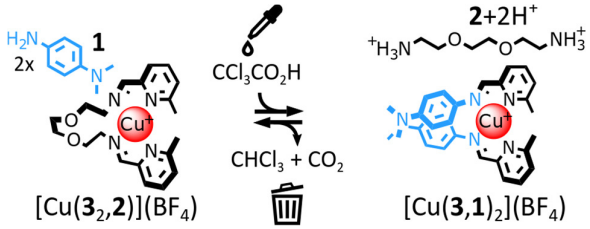

Scheme S11. Transient self-assembly of $[Cu(\mathbf{3},\mathbf{1})_2](BF_4)$ from $[Cu(\mathbf{3}_2,\mathbf{2})](BF_4)$ and **1** in the presence of trichloroacetic acid. Reagents and conditions: 2.5 eq. CCl_3CO_2H, CD_3CN, r.t.

Complex $[Cu(\mathbf{3}_2,\mathbf{2})](BF_4)$ was prepared by heating at 60 °C for 12 h a mixture of CD_3CN solutions of 6-methyl-2-pyridinecarboxaldehyde **3** (100 µL of 64 mM, 6.4 µmol, 2 eq.), 1,2-bis(2-aminoethoxy)ethane **2** (100 µL of 33.6 mM, 3.36 µmol, 1.05 eq.) and $[Cu(CH_3CN)_4](BF_4)$ (100 µL of 32 mM, 3.2 µmol, 1 eq.). After cooling to room temperature, the resulting CD_3CN solution of $[Cu(\mathbf{3}_2,\mathbf{2})](BF_4)$ was diluted with 100 µL of CD_3CN before being treated sequentially with CD_3CN solutions of 4-(dimethylamino)aniline **1** (100 µL of 64 mM, 6.4 µmol, 2 eq.) and trichloroacetic acid (10 µL of 0.8 M, 8.0 µmol, 2.5 eq.). The evolution of the reaction mixture was monitored over time by ^{1}H NMR spectroscopy. The complexes were never isolated, all the present experiments and analysis were performed on the crude reaction mixture.

4.1.1.1 Monitoring of the transient process by ^{1}H NMR spectroscopy

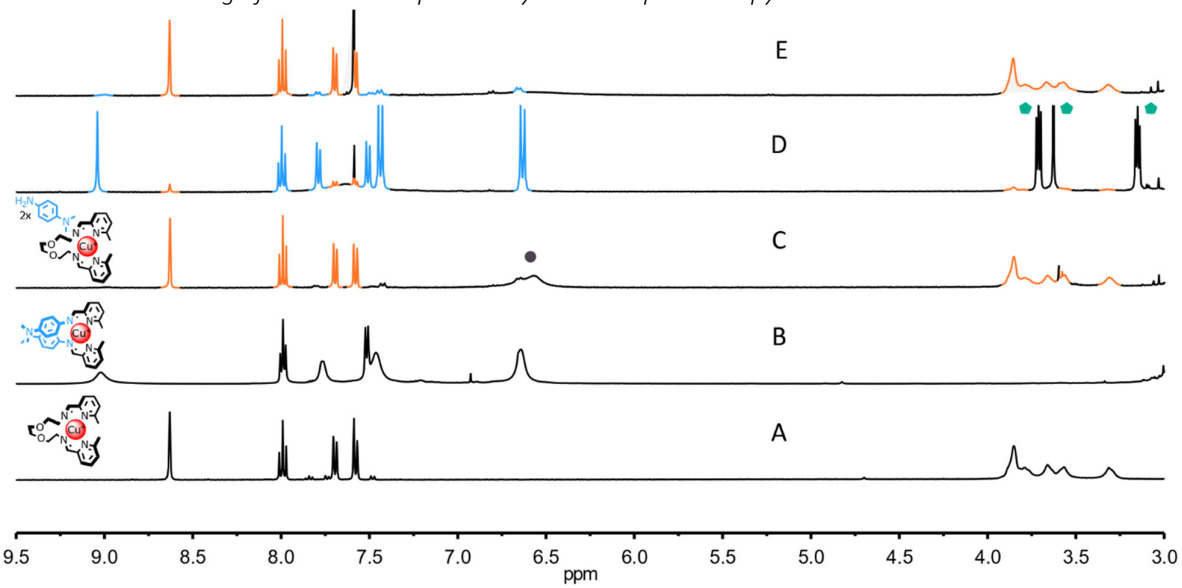

Figure S24. Partial ^{1}H NMR spectra (400 MHz, 297 K, CD_3CN) of: (A) complex [Cu(**3**$_2$,**2**)](BF$_4$), (B) complex [Cu(**3**,**1**)$_2$](BF$_4$), (C) a mixture of [Cu(**3**$_2$,**2**)](BF$_4$) and **1** in a 1:2 molar ratio, the evolution of this mixture 1.5 min (D) and 42 min (E) after the addition of 2.5 eq. CCl_3CO_2H. Diagnostic signals of [Cu(**3**$_2$,**2**)](BF$_4$) and [Cu(**3**,**1**)$_2$](BF$_4$) are highlighted respectively in orange and blue. Diagnostic signals of **1** and **2**+2H$^+$ are highlighted by grey circles and green pentagons, respectively.

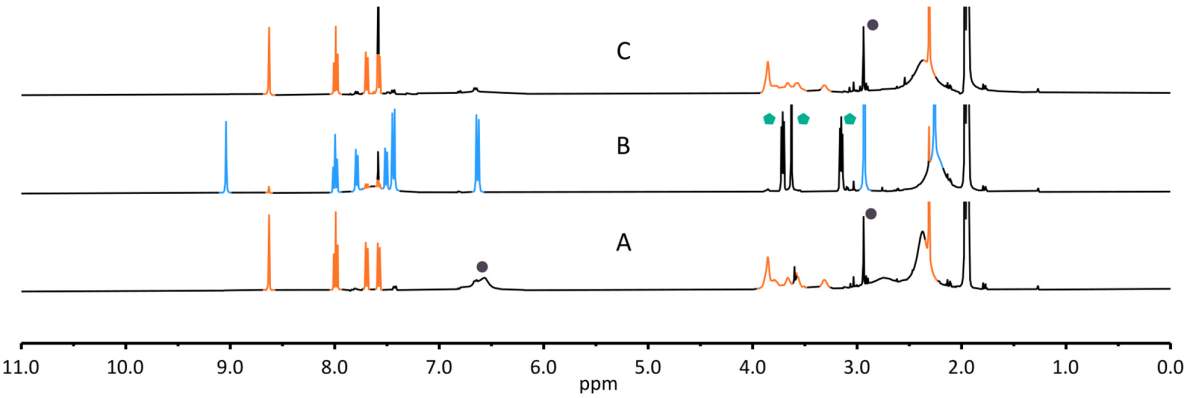

Figure S25. ^{1}H NMR spectra (400 MHz, 297 K, CD_3CN) of: (A) complex [Cu(**3**$_2$,**2**)](BF$_4$), (B) complex [Cu(**3**,**1**)$_2$](BF$_4$), (C) a mixture of [Cu(**3**$_2$,**2**)](BF$_4$) and **1** in a 1:2 molar ratio, the evolution of this mixture 1.5 min (D) and 42 min (E) after the addition of 2.5 eq. CCl_3CO_2H. Diagnostic signals of [Cu(**3**$_2$,**2**)](BF$_4$) and [Cu(**3**,**1**)$_2$](BF$_4$) are highlighted respectively in orange and blue. Diagnostic signals of **1** and **2**+2H$^+$ are highlighted by grey circles and green pentagons, respectively.

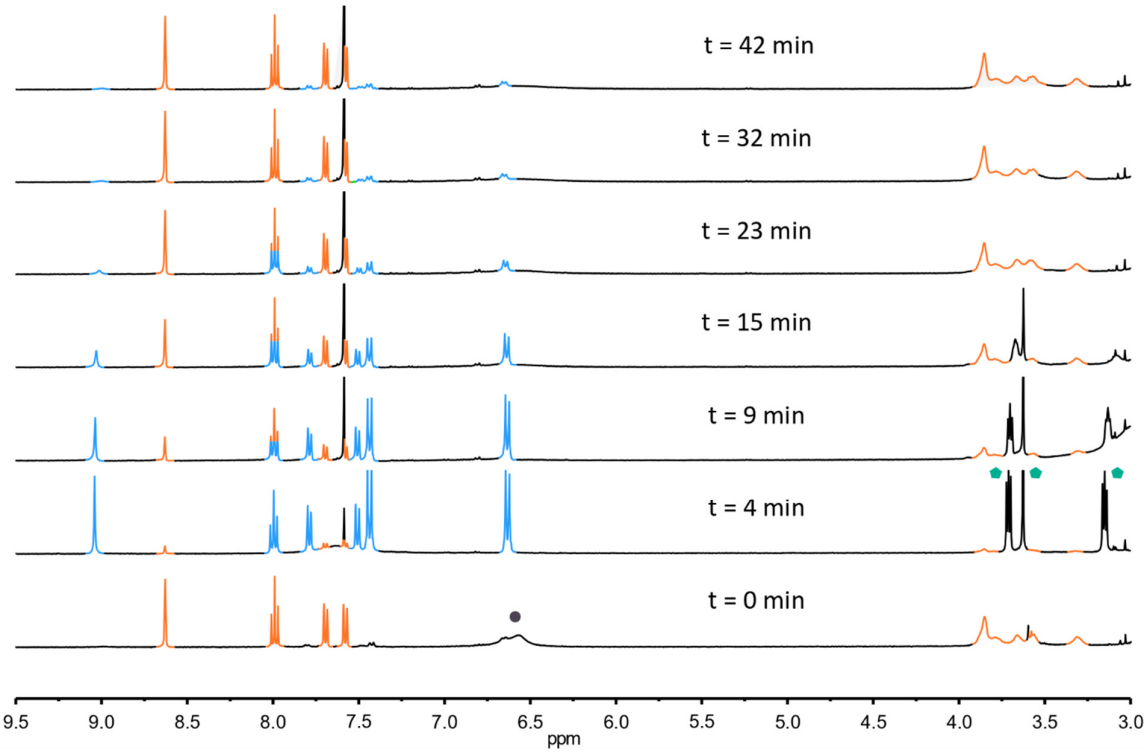

Figure S26. Monitoring by ^{1}H NMR spectroscopy (400 MHz, CD_3CN) of the transient self-assembly of [Cu(**3**,**1**)$_2$](BF$_4$) from [Cu(**3**$_2$,**2**)](BF$_4$) and **1** upon addition of an initial aliquot of trichloroacetic acid. Reagents and conditions: 2.5 eq. CCl_3CO_2H, CD_3CN, r.t. Spectra of the crude reaction mixture were recorded at increasing time increments (up to a final total time of 42 min), aromatic region and part of the aliphatic region of the spectra shown. Diagnostic signals of [Cu(**3**$_2$,**2**)](BF$_4$) and [Cu(**3**,**1**)$_2$](BF$_4$) are highlighted respectively in orange and blue. Diagnostic signals of **1** and **2**+2H$^+$ are highlighted by grey circles and green pentagons, respectively.

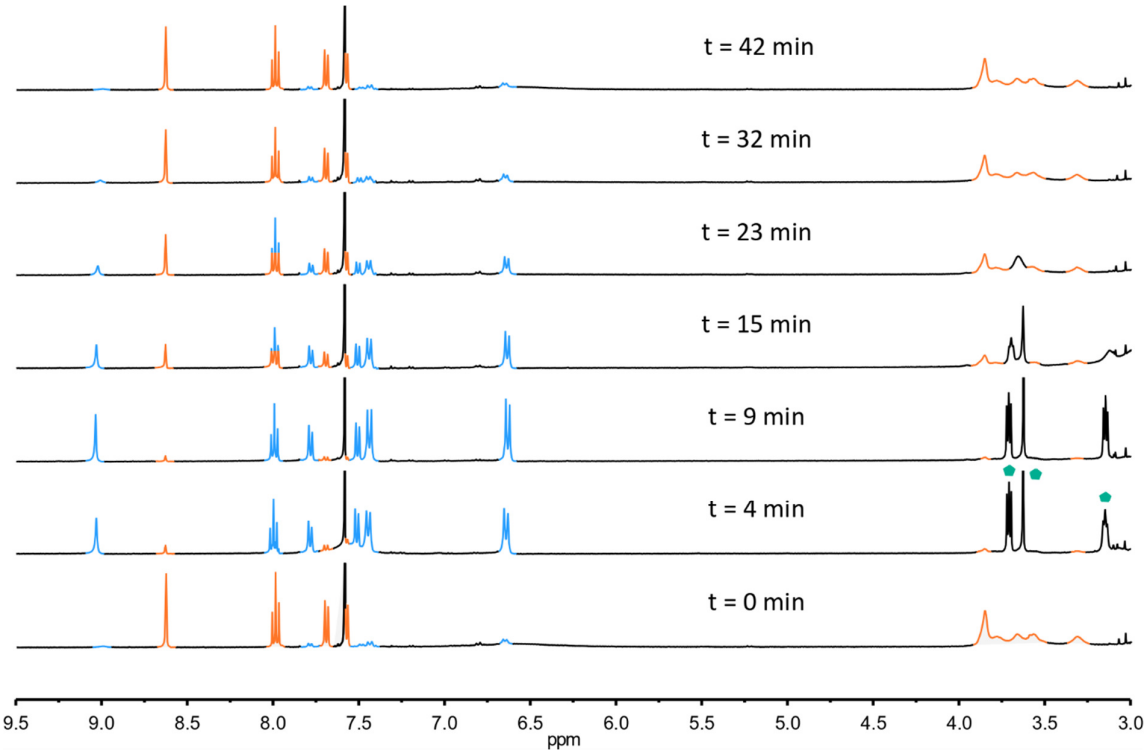

Figure S27. Monitoring by ^{1}H NMR spectroscopy (400 MHz, CD_3CN) of the transient self-assembly of [Cu(**3**,**1**)$_2$](BF$_4$) from [Cu(**3**$_2$,**2**)](BF$_4$) and **1** upon addition of a second aliquot of trichloroacetic acid. Reagents and conditions: 2.5 eq. CCl_3CO_2H, CD_3CN, r.t. Spectra of the crude reaction mixture were recorded at increasing time increments (up to a final total time of 42 min), aromatic region and part of the aliphatic region of the spectra shown. Diagnostic signals of [Cu(**3**$_2$,**2**)](BF$_4$) and [Cu(**3**,**1**)$_2$](BF$_4$) are highlighted respectively in orange and blue. Diagnostic signals of **1** and **2**+2H$^+$ are highlighted by grey circles and green pentagons, respectively.

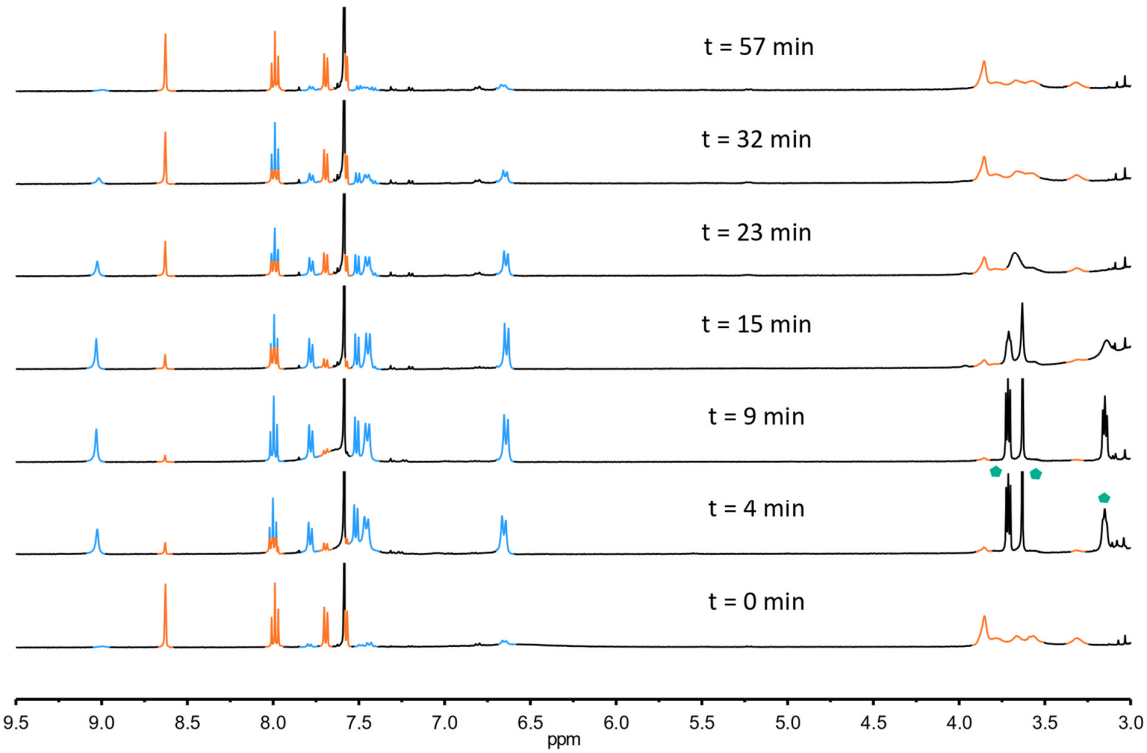

Figure S28. Monitoring by ^{1}H NMR spectroscopy (400 MHz, CD_3CN) of the transient self-assembly of [Cu(**3**,**1**)$_2$](BF$_4$) from [Cu(**3**$_2$,**2**)](BF$_4$) and **1** upon addition of a third aliquot of trichloroacetic acid. Reagents and conditions: 2.5 eq. CCl_3CO_2H, CD_3CN, r.t. Spectra of the crude reaction mixture were recorded at increasing time increments (up to a final total time of 42 min), aromatic region and part of the aliphatic region of the spectra shown. Diagnostic signals of [Cu(**3**$_2$,**2**)](BF$_4$) and [Cu(**3**,**1**)$_2$](BF$_4$) are highlighted respectively in orange and blue. Diagnostic signals of **1** and **2**+2H$^+$ are highlighted by grey circles and green pentagons, respectively.

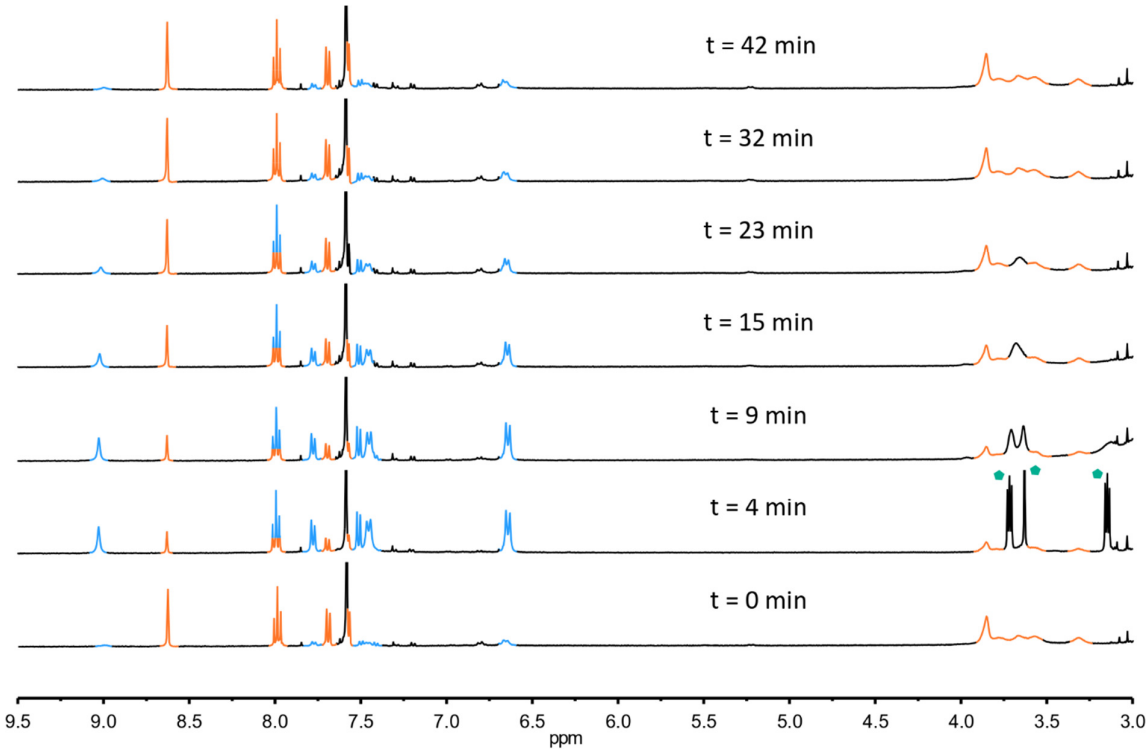

Figure S29. Monitoring by ^{1}H NMR spectroscopy (400 MHz, CD_3CN) of the transient self-assembly of [Cu(**3**,**1**)$_2$](BF$_4$) from [Cu(**3**$_2$,**2**)](BF$_4$) and **1** upon addition of a fourth aliquot of trichloroacetic acid. Reagents and conditions: 2.5 eq. CCl_3CO_2H, CD_3CN, r.t. Spectra of the crude reaction mixture were recorded at increasing time increments (up to a final total time of 42 min), aromatic region and part of the aliphatic region of the spectra shown. Diagnostic signals of [Cu(**3**$_2$,**2**)](BF$_4$) and [Cu(**3**,**1**)$_2$](BF$_4$) are highlighted respectively in orange and blue. Diagnostic signals of **1** and **2**+2H$^+$ are highlighted by grey circles and green pentagons, respectively.

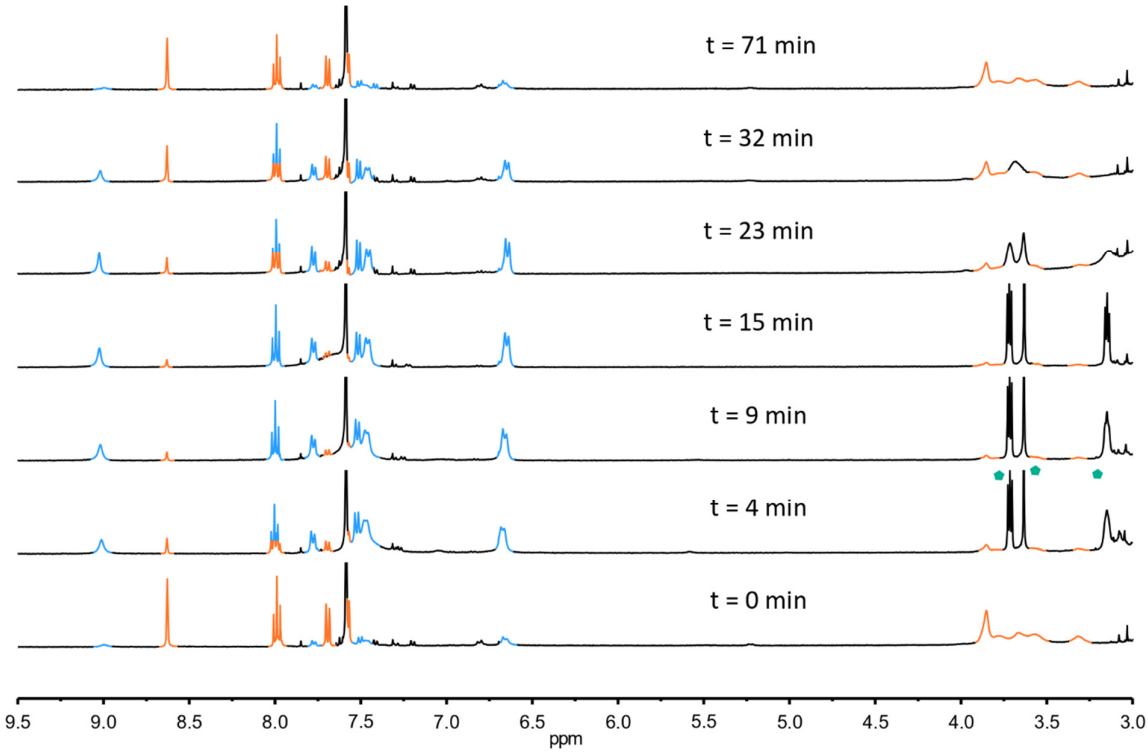

Figure S30. Monitoring by ^{1}H NMR spectroscopy (400 MHz, CD_3CN) of the transient self-assembly of [Cu(**3**,**1**)$_2$](BF$_4$) from [Cu(**3**$_2$,**2**)](BF$_4$) and **1** upon addition of a fifth aliquot of trichloroacetic acid. Reagents and conditions: 2.5 eq. CCl_3CO_2H, CD_3CN, r.t. Spectra of the crude reaction mixture were recorded at increasing time increments (up to a final total time of 42 min), aromatic region and part of the aliphatic region of the spectra shown. Diagnostic signals of [Cu(**3**$_2$,**2**)](BF$_4$) and [Cu(**3**,**1**)$_2$](BF$_4$) are highlighted respectively in orange and blue. Diagnostic signals of **1** and **2**+2H$^+$ are highlighted by grey circles and green pentagons, respectively.

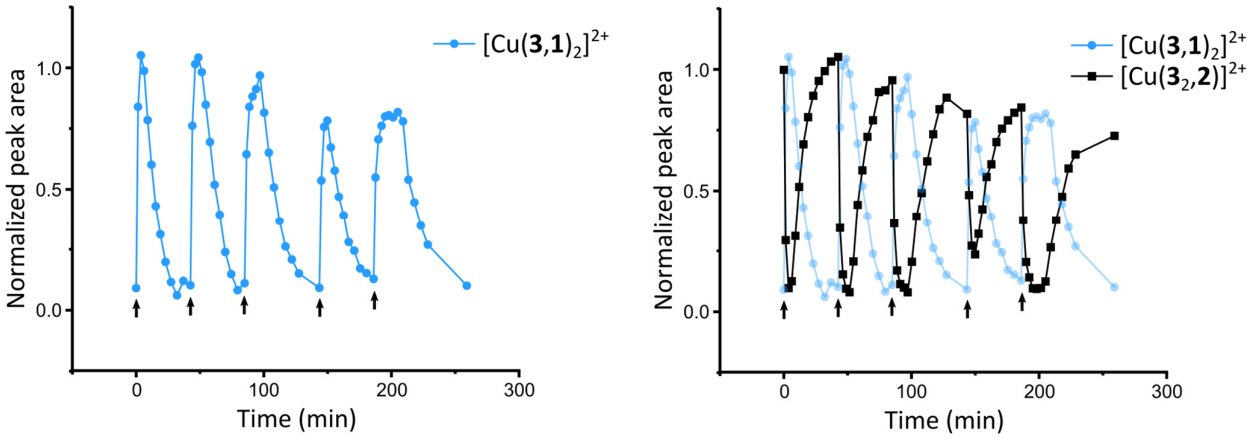

Figure S31. (Left) Assembly/disassembly as a function of time of $[Cu(\mathbf{3},\mathbf{1})_2](BF_4)$ upon addition of aliquots of trichloroacetic acid, monitored by ^1H NMR. (Right) Diassembly/assembly as a function of time of $[Cu(\mathbf{3}_2,\mathbf{2})](BF_4)$ upon addition of aliquots of trichloroacetic acid, monitored by ^1H NMR. Graph plotting of the imine peak areas for $[Cu(\mathbf{3},\mathbf{1})_2](BF_4)$ and $[Cu(\mathbf{3}_2,\mathbf{2})](BF_4)$ both normalized to the imine peak area for $[Cu(\mathbf{3}_2,\mathbf{2})](BF_4)$ prior to the first addition of trichloroacetic acid. Each arrow indicates the addition of an aliquot of trichloroacetic acid. Reagents and conditions: 2.5 eq. CCl_3CO_2H, CD_3CN, r.t.

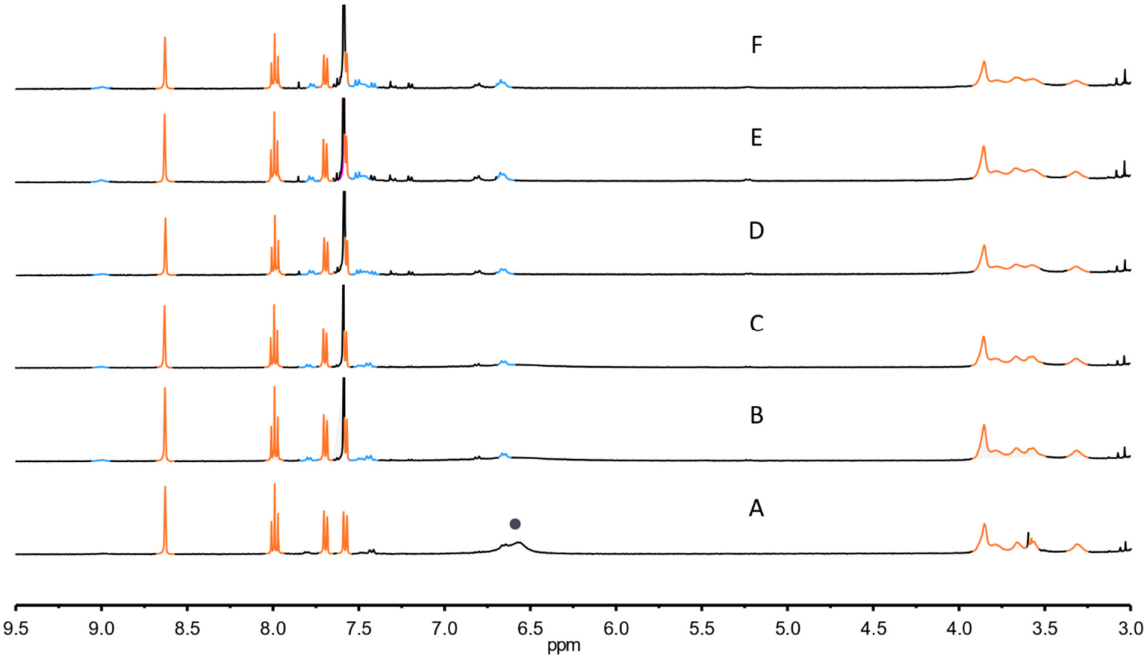

Figure S32. Evaluation of the stability of the system after several rearrangement cycles. Partial ^{1}H NMR spectra (400 MHz, CD_3CN) of: (A) a 1:2 mixture of [Cu(**3**$_2$,**2**)](BF_4) and **1** before the addition of trichloroacetic acid, (B) this mixture following the re-assembly of [Cu(**3**$_2$,**2**)](BF_4) upon consumption of the initial aliquot of trichloroacetic acid, (C) – (F) this mixture following two – five disassembly/re-assembly cycles. Reagents and conditions: 2.5 eq. CCl_3CO_2H, CD_3CN, r.t. Diagnostic signals of [Cu(**3**$_2$,**2**)](BF_4) and [Cu(**3**,**1**)$_2$](BF_4) are highlighted respectively in orange and blue. Diagnostic signals of **1** are highlighted by grey circles.

4.1.1.2 Monitoring of the transient process by ESI-MS

Complex [Cu(**3**$_2$,**2**)](BF_4) was prepared by heating at 60 °C for 12 h a mixture of CD_3CN solutions of 6-methyl-2-pyridinecarboxaldehyde **3** (100 µL of 64 mM, 6.4 µmol, 2 eq.), 1,2-bis(2-aminoethoxy)ethane **2** (100 µL of 33.6 mM, 3.36 µmol, 1.05 eq.) and [Cu(CH_3CN)$_4$](BF_4) (100 µL of 32 mM, 3.2 µmol, 1 eq.). The resulting CD_3CN solution of [Cu(**3**$_2$,**2**)](BF_4) was diluted with 100 µL of CD_3CN before being treated with a CD_3CN solution of 4-(dimethylamino)aniline **1** (100 µL of 64 mM, 6.4 µmol, 2 eq.) and left to react at 60 °C for 18 h. After cooling to room temperature, the resulting mixture was treated with trichloroacetic acid (10 µL of 0.8 M, 8.0 µmol, 2.5 eq.). The composition of the reaction mixture was monitored prior and after the addition of trichloroacetic acid via electrospray ionization mass spectrometry (ESI–MS). Samples for ESI–MS were prepared by diluting 5 µL of the reaction mixture into 1 mL of CH_3CN.

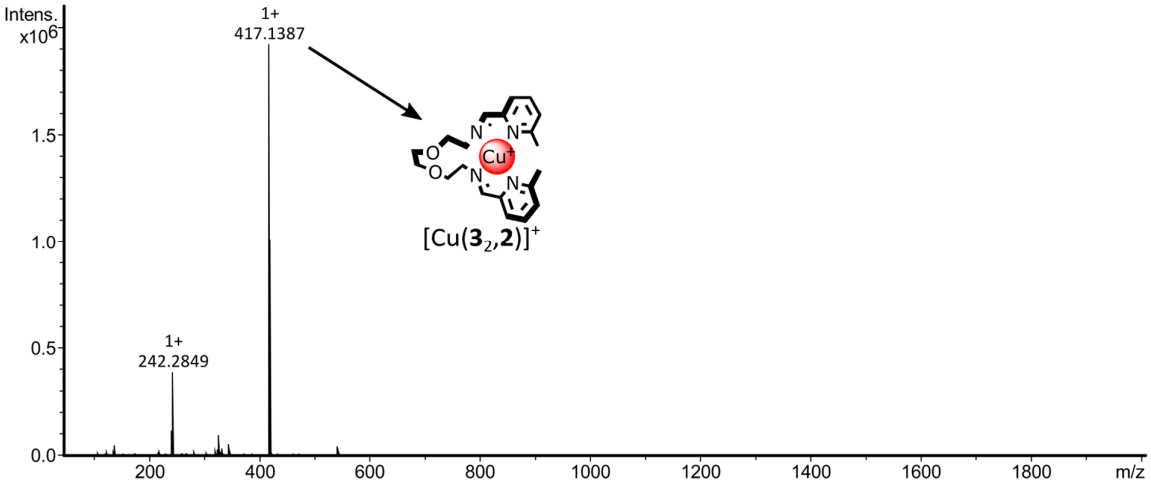

Figure S33. Electrospray ionization mass spectrometry (ESI–MS) analysis of a 1:2 mixture of [Cu(**3**$_2$,**2**)](BF$_4$) and **1** before the addition of trichloroacetic acid.

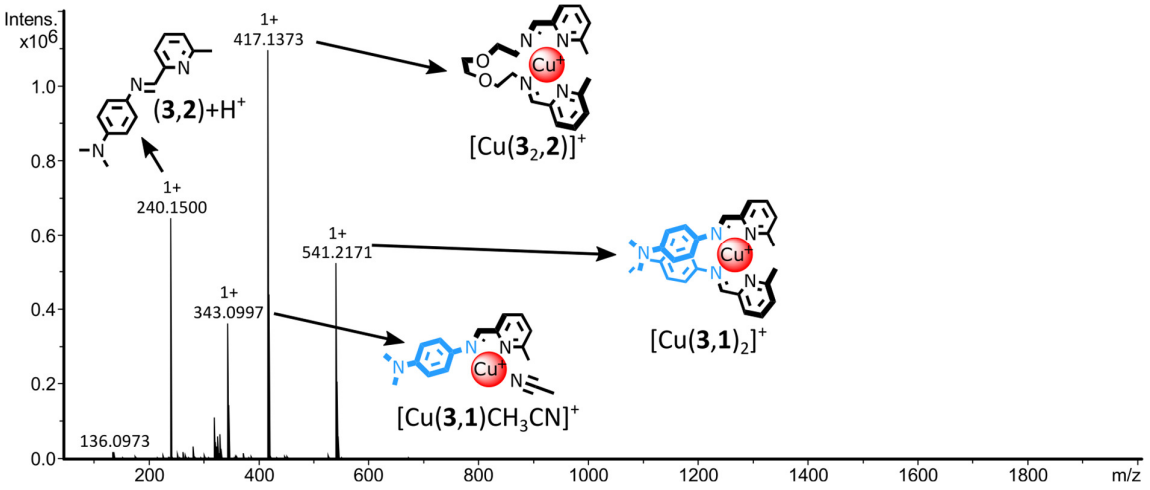

Figure S34. Electrospray ionization mass spectrometry (ESI–MS) analysis of a 1:2 mixture of [Cu(**3**$_2$,**2**)](BF$_4$) and **1** approximately 2 min following the addition of trichloroacetic acid.

4.1.2 **Transient self-assembly of [Cu(3,1)$_2$](BF$_4$) from a mixture of complexes**

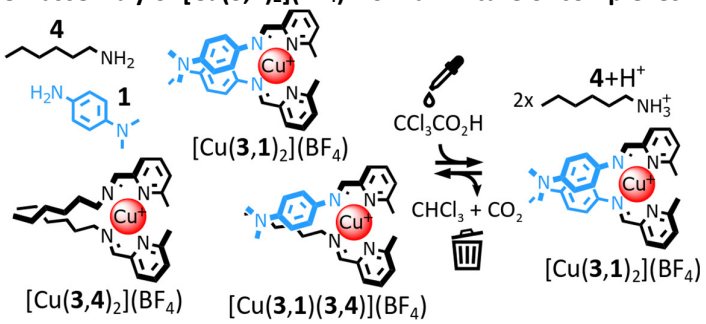

Scheme S12. Transient self-assembly of [Cu(**3**,**1**)$_2$](BF$_4$) from a mixture of [Cu(**3**,**4**)$_2$](BF$_4$), [Cu(**3**,**1**)(**3**,**4**)](BF$_4$), [Cu(**3**,**1**)$_2$](BF$_4$), **1** and **4** in the presence of trichloroacetic acid. Reagents and conditions: 2.5 eq. CCl_3CO_2H, CD_3CN, r.t.

Complex [Cu(**3**,**4**)$_2$](BF$_4$) was prepared by heating at 60 °C for 12 h a mixture of CD_3CN solutions of 6-methyl-2-pyridinecarboxaldehyde **3** (100 µL of 64 mM, 6.4 µmol, 2 eq.), hexylamine **4** (100 µL of 67.2 mM, 6.72 µmol, 2.1 eq.) and [Cu(CH_3CN)$_4$](BF$_4$) (100 µL of 32 mM, 3.2 µmol, 1 eq.). After cooling to room temperature, the resulting CD_3CN solution of [Cu(**3**,**4**)$_2$](BF$_4$) was diluted with 100 µL of CD_3CN before being treated sequentially with CD_3CN solutions of 4-(dimethylamino)aniline **1** (100 µL of 64 mM, 6.4 µmol, 2 eq.) and trichloroacetic acid (10 µL of 0.8 M, 8.0 µmol, 2.5 eq.). The evolution of the reaction mixture was monitored over time by ^{1}H NMR spectroscopy. The complexes were never isolated, all the present experiments and analysis were performed on the crude reaction mixture.

4.1.2.1 Monitoring of the transient process by ^{1}H NMR spectroscopy

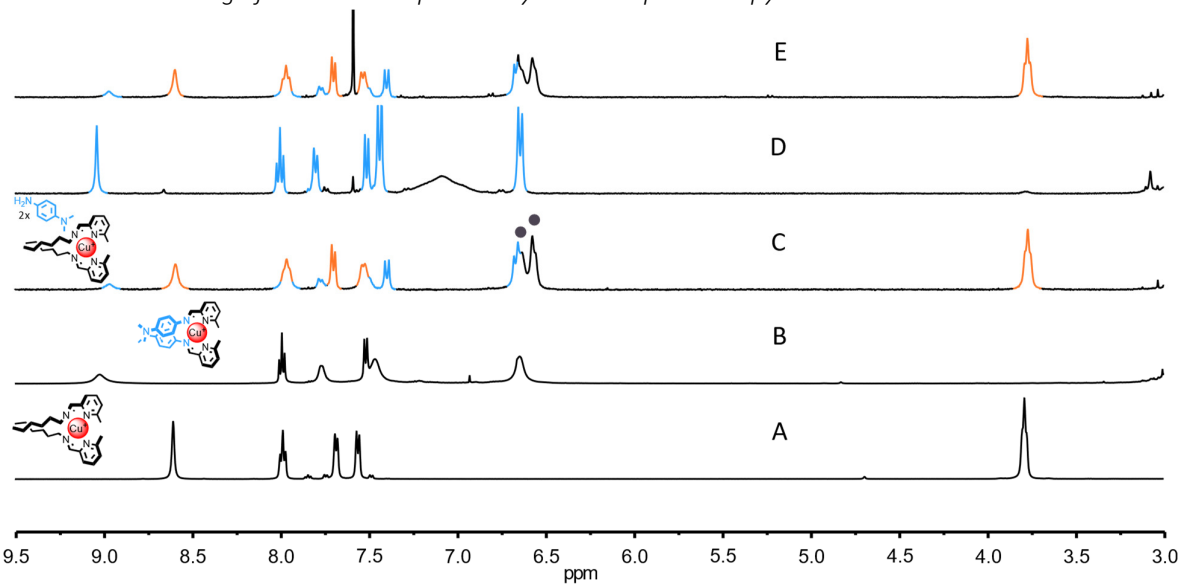

Figure S35. Partial ^{1}H NMR spectra (400 MHz, 297 K, CD_3CN) of: (A) complex [Cu(**3**,**4**)$_2$](BF$_4$), (B) complex [Cu(**3**,**1**)$_2$](BF$_4$), (C) a mixture of [Cu(**3**,**4**)$_2$](BF$_4$) and **1** in a 1:2 molar ratio, the evolution of this mixture 1.5 min (D) and 42 min (E) after the addition of 2.5 eq. CCl_3CO_2H. Diagnostic signals of [Cu(**3**,**4**)$_2$](BF$_4$) and [Cu(**3**,**1**)$_2$](BF$_4$) are highlighted respectively in orange and blue. The diagnostic signals of [Cu(**3**,**1**)(**3**,**4**)]$^+$ overlap with those of [Cu(**3**,**1**)$_2$]$^+$ and [Cu(**3**,**4**)$_2$]$^+$. Diagnostic signals of **1** are highlighted by grey circles.

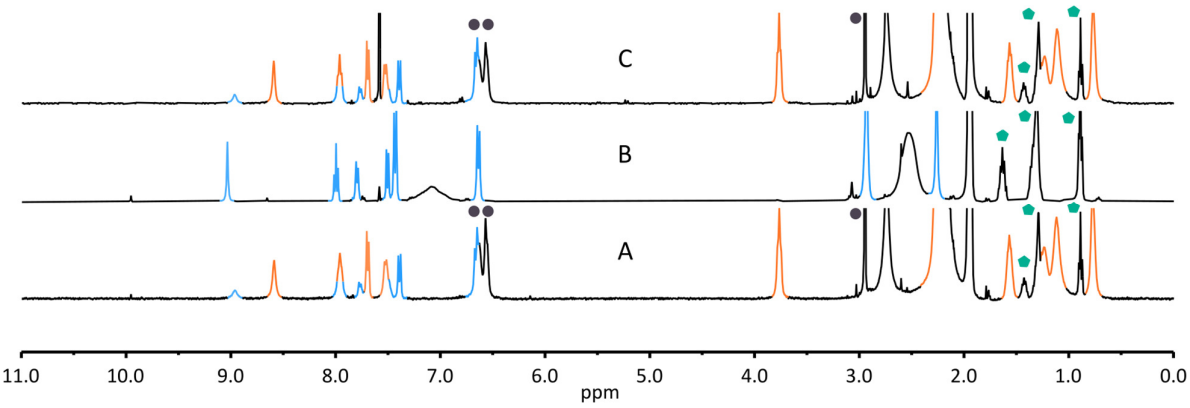

Figure S36. ^{1}H NMR spectra (400 MHz, 297 K, CD_3CN) of: (A) complex [Cu(**3**,**4**)$_2$](BF$_4$), (B) complex [Cu(**3**,**1**)$_2$](BF$_4$), (C) a mixture of [Cu(**3**,**4**)$_2$](BF$_4$) and **1** in a 1:2 molar ratio, the evolution of this mixture 1.5 min (D) and 42 min (E) after the addition of 2.5 eq. CCl_3CO_2H. Diagnostic signals of [Cu(**3**,**4**)$_2$](BF$_4$) and [Cu(**3**,**1**)$_2$](BF$_4$) are highlighted respectively in orange and blue. The diagnostic signals of [Cu(**3**,**1**)(**3**,**4**)]$^+$ overlap with those of [Cu(**3**,**1**)$_2$]$^+$ and [Cu(**3**,**4**)$_2$]$^+$. Diagnostic signals of **1** are highlighted by grey circles.

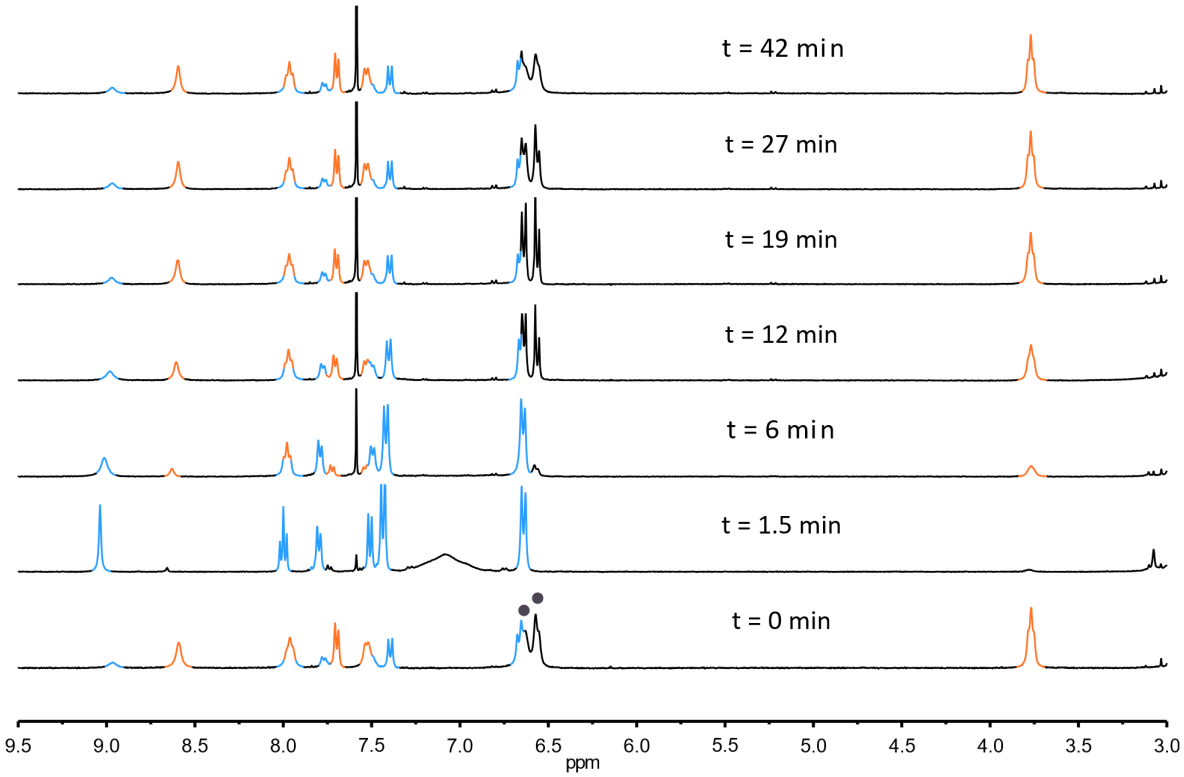

Figure S37. Monitoring by ^{1}H NMR spectroscopy (400 MHz, CD_3CN) of the transient self-assembly of [Cu(**3**,**1**)$_2$](BF$_4$) from a mixture of [Cu(**3**,**4**)$_2$](BF$_4$), [Cu(**3**,**1**)(**3**,**4**)](BF$_4$), [Cu(**3**,**1**)$_2$](BF$_4$), **1** and **4** upon addition of an initial aliquot of trichloroacetic acid. Reagents and conditions: 2.5 eq. CCl_3CO_2H, CD_3CN, r.t. Spectra of the crude reaction mixture were recorded at increasing time increments (up to a final total time of 42 min), aromatic region and part of the aliphatic region of the spectra shown. Diagnostic signals of [Cu(**3**,**4**)$_2$](BF$_4$) and [Cu(**3**,**1**)$_2$](BF$_4$) are highlighted respectively in orange and blue. The diagnostic signals of [Cu(**3**,**1**)(**3**,**4**)]$^+$ overlap with those of [Cu(**3**,**1**)$_2$]$^+$ and [Cu(**3**,**4**)$_2$]$^+$. Diagnostic signals of **1** are highlighted by grey circles.

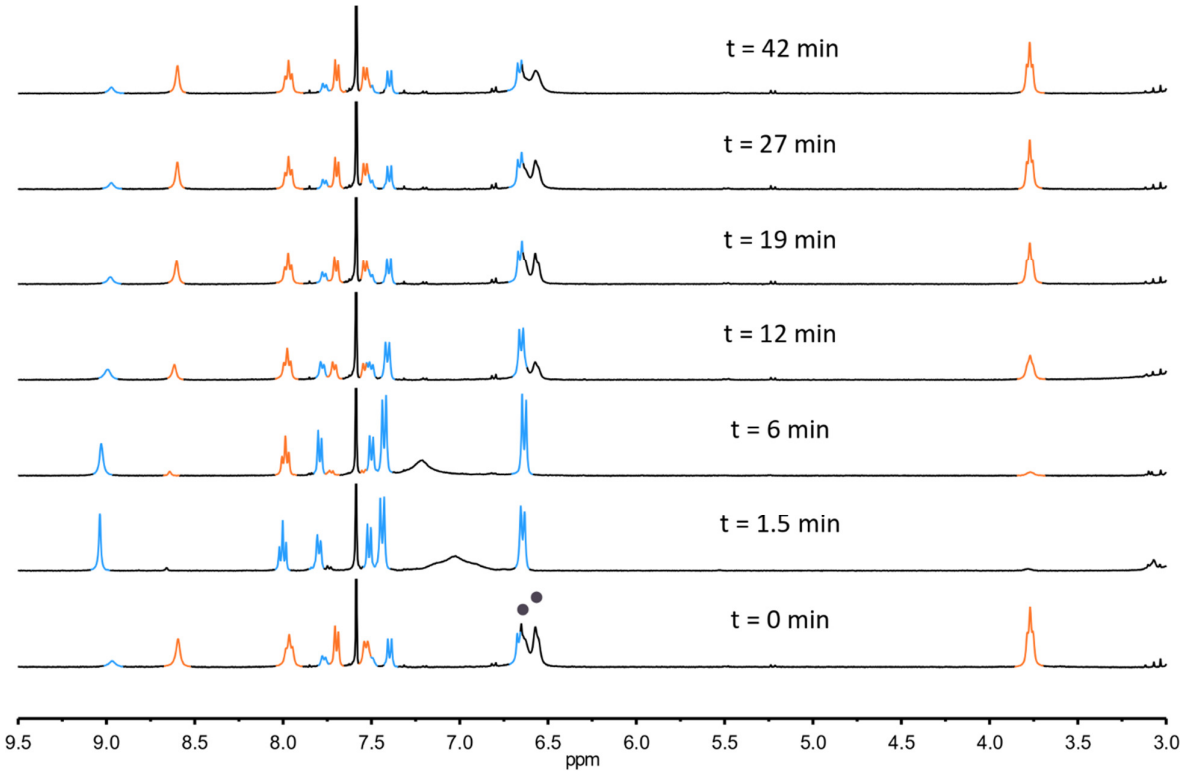

Figure S38. Monitoring by ^{1}H NMR spectroscopy (400 MHz, CD_3CN) of the transient self-assembly of $[Cu(\mathbf{3},\mathbf{1})_2](BF_4)$ from a mixture of $[Cu(\mathbf{3},\mathbf{4})_2](BF_4)$, $[Cu(\mathbf{3},\mathbf{1})(\mathbf{3},\mathbf{4})](BF_4)$, $[Cu(\mathbf{3},\mathbf{1})_2](BF_4)$, **1** and **4** upon addition of a second aliquot of trichloroacetic acid. Reagents and conditions: 2.5 eq. CCl_3CO_2H, CD_3CN, r.t. Spectra of the crude reaction mixture were recorded at increasing time increments (up to a final total time of 42 min), aromatic region and part of the aliphatic region of the spectra shown. Diagnostic signals of $[Cu(\mathbf{3},\mathbf{4})_2](BF_4)$ and $[Cu(\mathbf{3},\mathbf{1})_2](BF_4)$ are highlighted respectively in orange and blue. The diagnostic signals of $[Cu(\mathbf{3},\mathbf{1})(\mathbf{3},\mathbf{4})]^+$ overlap with those of $[Cu(\mathbf{3},\mathbf{1})_2]^+$ and $[Cu(\mathbf{3},\mathbf{4})_2]^+$. Diagnostic signals of **1** are highlighted by grey circles.

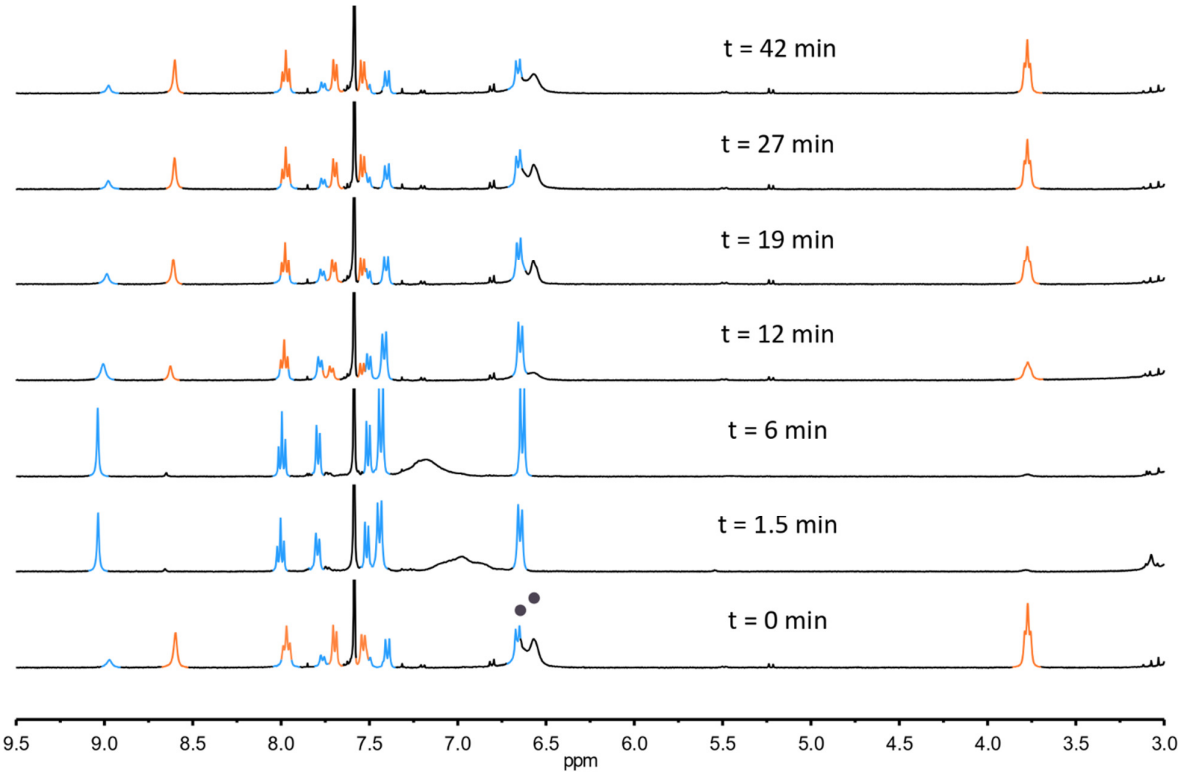

Figure S39. Monitoring by ^{1}H NMR spectroscopy (400 MHz, CD_3CN) of the transient self-assembly of $[Cu(\mathbf{3},\mathbf{1})_2](BF_4)$ from a mixture of $[Cu(\mathbf{3},\mathbf{4})_2](BF_4)$, $[Cu(\mathbf{3},\mathbf{1})(\mathbf{3},\mathbf{4})](BF_4)$, $[Cu(\mathbf{3},\mathbf{1})_2](BF_4)$, **1** and **4** upon addition of a third aliquot of trichloroacetic acid. Reagents and conditions: 2.5 eq. CCl_3CO_2H, CD_3CN, r.t. Spectra of the crude reaction mixture were recorded at increasing time increments (up to a final total time of 42 min), aromatic region and part of the aliphatic region of the spectra shown. Diagnostic signals of $[Cu(\mathbf{3},\mathbf{4})_2](BF_4)$ and $[Cu(\mathbf{3},\mathbf{1})_2](BF_4)$ are highlighted respectively in orange and blue. The diagnostic signals of $[Cu(\mathbf{3},\mathbf{1})(\mathbf{3},\mathbf{4})]^+$ overlap with those of $[Cu(\mathbf{3},\mathbf{1})_2]^+$ and $[Cu(\mathbf{3},\mathbf{4})_2]^+$. Diagnostic signals of **1** are highlighted by grey circles.

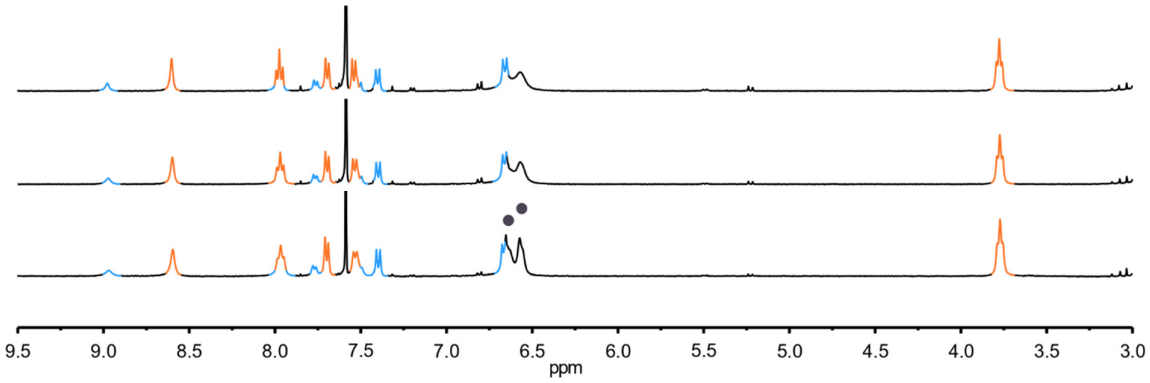

Figure S40. Evaluation of the stability of the system after several rearrangement cycles. Partial ^{1}H NMR spectra (400 MHz, CD_3CN) of: (bottom) non-self-sorted mixture of [Cu(**3**,**4**)$_2$](BF$_4$), [Cu(**3**,**1**)(**3**,**4**)](BF$_4$), [Cu(**3**,**1**)$_2$](BF$_4$), **1** and **4** before addition of acid, (middle) this mixture following the return to the non-self-sorted state upon consumption of the initial aliquot of trichloroacetic acid, (top) this mixture following a second disassembly/re-assembly cycle. Reagents and conditions for each cycle: 2.5 eq. CCl_3CO_2H, CD_3CN, r.t. Diagnostic signals of [Cu(**3**,**4**)$_2$](BF$_4$) and [Cu(**3**,**1**)$_2$](BF$_4$) are highlighted respectively in orange and blue. The diagnostic signals of [Cu(**3**,**1**)(**3**,**4**)]$^+$ overlap with those of [Cu(**3**,**1**)$_2$]$^+$ and [Cu(**3**,**4**)$_2$]$^+$. Diagnostic signals of **1** are highlighted by grey circles.

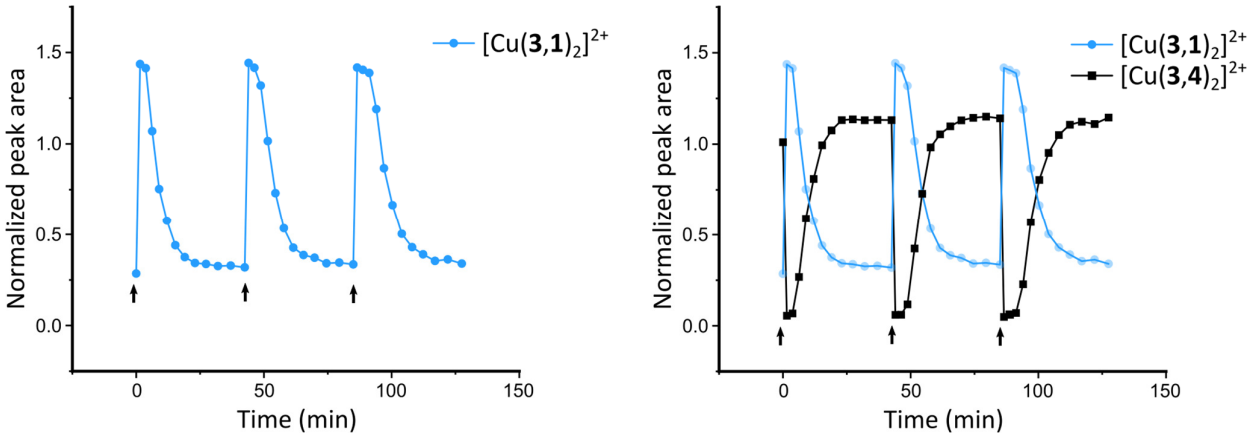

Figure S41. (Left) Assembly/disassembly as a function of time of [Cu(**3**,**1**)$_2$](BF$_4$) upon addition of aliquots of trichloroacetic acid, monitored by ^{1}H NMR spectroscopy. (Right) Diassembly/assembly as a function of time of [Cu(**3**,**4**)$_2$](BF$_4$) upon addition of aliquots of trichloroacetic acid, monitored by ^{1}H NMR. Graph plotting of the imine peak area for [Cu(**3**,**1**)$_2$](BF$_4$) and of the N-CH_2 peak area for [Cu(**3**,**4**)$_2$](BF$_4$) both normalized to the N-CH_2 peak area for [Cu(**3**,**4**)$_2$](BF$_4$) prior to the first addition of acid. Each arrow indicates the addition of an aliquot of trichloroacetic acid. Reagents and conditions for each cycle: 2.5 eq. CCl_3CO_2H, CD_3CN, r.t.

4.1.2.2 Monitoring of the transient process by ESI-MS

Complex [Cu(**3**,**4**)$_2$](BF$_4$) was prepared by heating at 60 °C for 12 h a mixture of CD$_3$CN solutions of 6-methyl-2-pyridinecarboxaldehyde **3** (100 µL of 64 mM, 6.4 µmol, 2 eq.), hexylamine **4** (100 µL of 64 mM, 6.4 µmol, 2 eq.) and [Cu(CH$_3$CN)$_4$](BF$_4$) (100 µL of 32 mM, 3.2 µmol, 1 eq.). The resulting CD$_3$CN solution of [Cu(**3**,**4**)$_2$](BF$_4$) was diluted with 100 µL of CD$_3$CN before being treated with a CD$_3$CN solution of 4-(dimethylamino)aniline **1** (100 µL of 64 mM, 6.4 µmol, 2 eq.) and left to react at 60 °C for 18 h. After cooling to room temperature, the resulting mixture was treated with trichloroacetic acid (10 µL of 0.8 M, 8.0 µmol, 2.5 eq.). The composition of the reaction mixture was monitored prior and after the addition of trichloroacetic acid via electrospray ionization mass spectrometry (ESI–MS). Samples for ESI–MS were prepared by diluting 5 µL of the reaction mixture into 1 mL of CH$_3$CN.

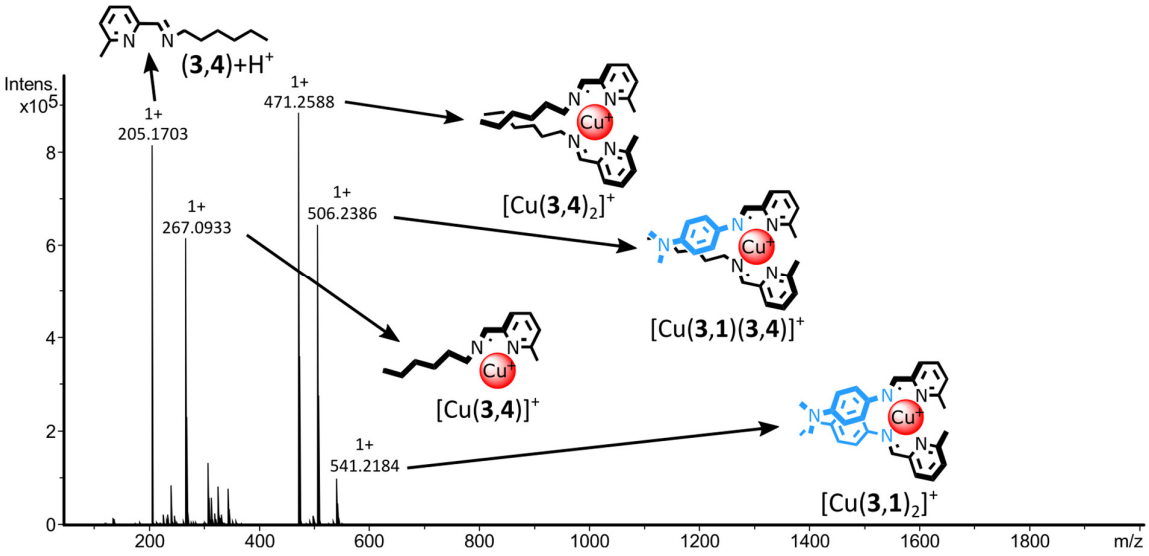

Figure S42. Electrospray ionization mass spectrometry (ESI–MS) analysis of a 1:2 mixture of [Cu(**3**,**4**)$_2$](BF$_4$) and **1** before the addition of trichloroacetic acid.

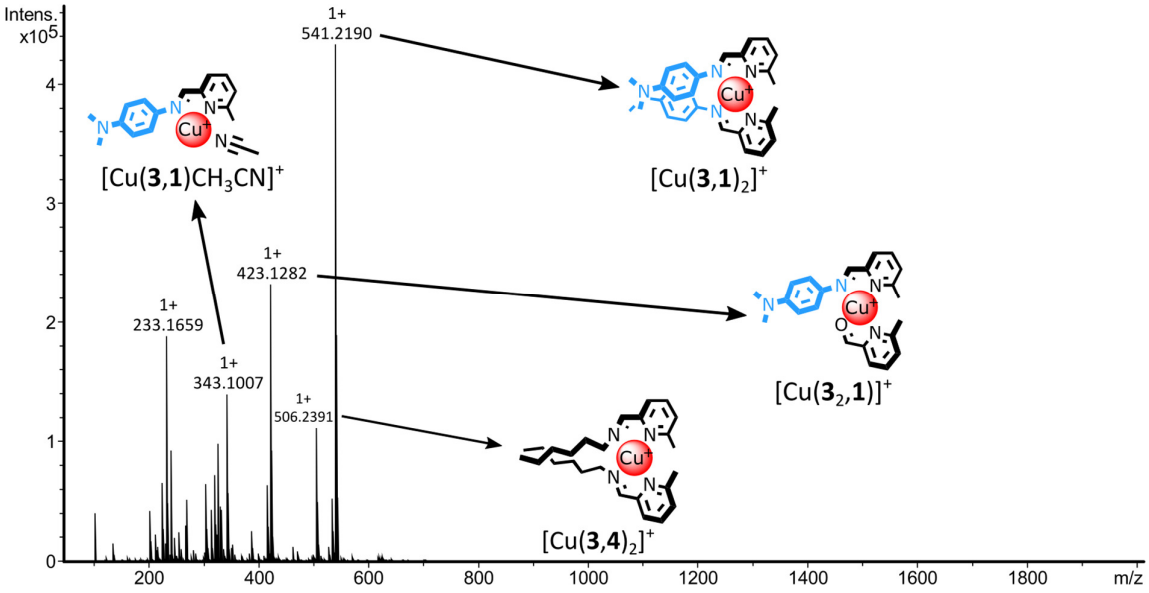

Figure S43. Electrospray ionization mass spectrometry (ESI–MS) analysis of a 1:2 mixture of [Cu(**3**,**4**)$_2$](BF$_4$) and **1** approximately 2 min following the addition of trichloroacetic acid.

4.1.3 Transient self-assembly of [Ag(3,1)$_2$](SbF$_6$) from a mixture of complexes

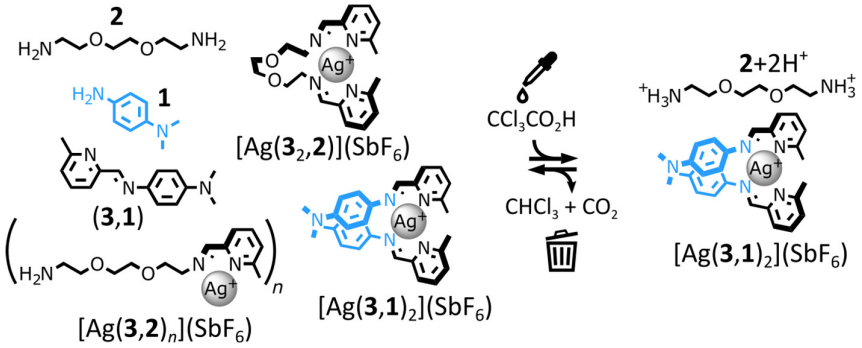

Scheme S13. Transient self-assembly of [Ag(**3**,**1**)$_2$](SbF$_6$) from a mixture of [Ag(**3**$_2$,**2**)](SbF$_6$), (**3**,**1**), [Ag(**3**,**1**)$_2$](SbF$_6$), [Ag(**3**,**2**)$_n$](SbF$_6$), **1** and **2** in the presence of trichloroacetic acid. Reagents and conditions: 2.5 eq. CCl_3CO_2H, CD_3CN, r.t.

Complex [Ag(**3**$_2$,**2**)](SbF$_6$) was prepared by heating at 60 °C for 12 h a mixture of CD_3CN solutions of 6-methyl-2-pyridinecarboxaldehyde **3** (100 µL of 64 mM, 6.4 µmol, 2 eq.), 1,2-bis(2-aminoethoxy)ethane **2** (100 µL of 33.6 mM, 3.36 µmol, 1.05 eq.) and Ag(SbF$_6$) (100 µL of 32 mM, 3.2 µmol, 1 eq.). The resulting CD_3CN solution of [Ag(**3**$_2$,**2**)](SbF$_6$) was diluted with 100 µL of CD_3CN before being treated with a CD_3CN solutions of 4-(dimethylamino)aniline **1** (100 µL of 64 mM, 6.4 µmol, 2 eq.) and left to react at 60 °C for 18 h. After cooling to room temperature, the resulting mixture was treated with trichloroacetic acid (10 µL of 0.8 M, 8.0 µmol, 2.5 eq.). The evolution of the reaction mixture was monitored over time by ^{1}H NMR spectroscopy. The complexes were never isolated, all the present experiments and analysis were performed on the crude reaction mixture.

4.1.3.1 Monitoring of the transient process by ^{1}H NMR spectroscopy

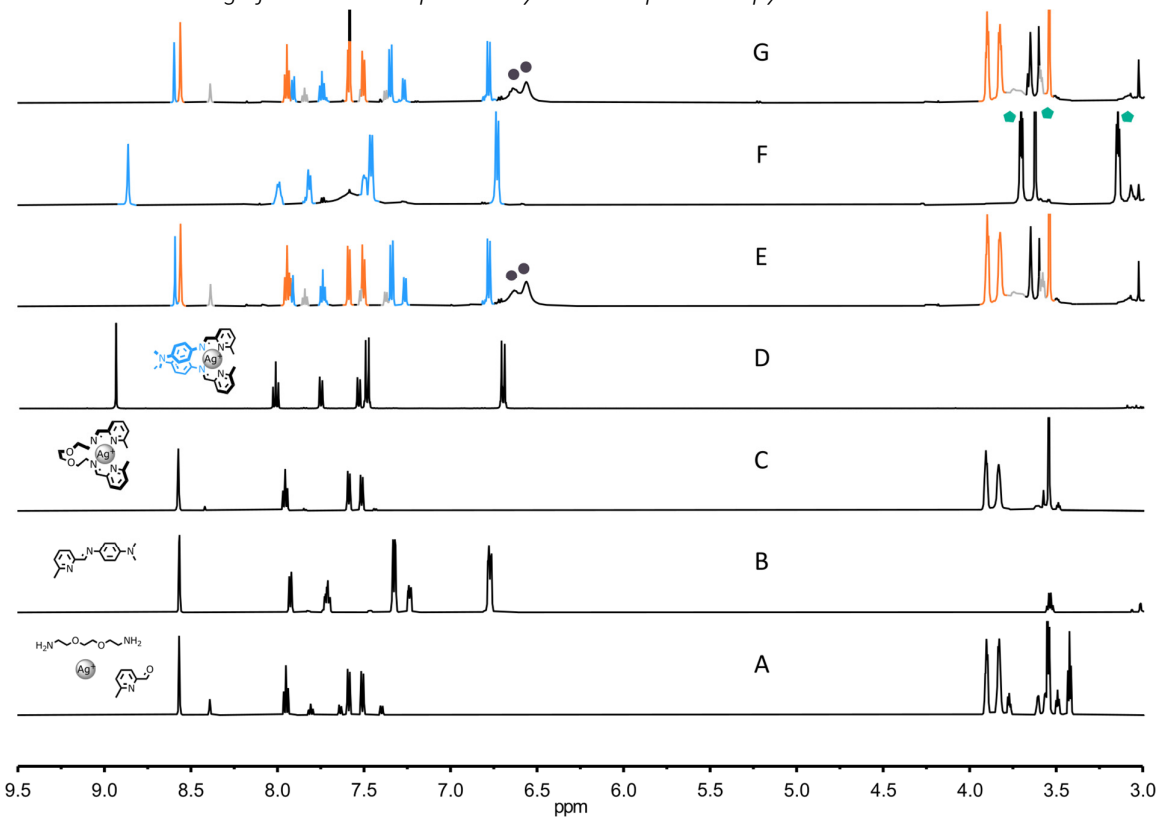

Figure S44. Partial ^{1}H NMR spectra (600 MHz, 297 K, CD_3CN) of: (A) a mixture of $Ag(SbF_6)$, **3** and **2** in a 0.6:1:1 molar ratio (B) imine (**3**,**1**) (C) complex [Ag(**3**$_2$,**2**)](SbF_6) (D) complex [Ag(**3**,**1**)$_2$](SbF_6) (E) a mixture of [Ag(**3**$_2$,**2**)](SbF_6), (**3**,**1**), [Ag(**3**,**1**)$_2$](SbF_6), [Ag(**3**,**2**)$_n$](SbF_6), **1** and **2**, the evolution of this mixture 1 min (F) and 43 min (G) following the addition of 2.5 eq. CCl_3CO_2H. Diagnostic signals of [Ag(**3**$_2$,**2**)](SbF_6), and [Ag(**3**,**2**)$_n$](SbF_6) are highlighted respectively in orange and grey. Diagnostic signals of imine (**3**,**1**) and [Ag(**3**,**1**)$_2$](SbF_6) are highlighted in blue. Diagnostic signals of **1** and **2**+2H$^+$ are highlighted by grey circles and green pentagons, respectively.

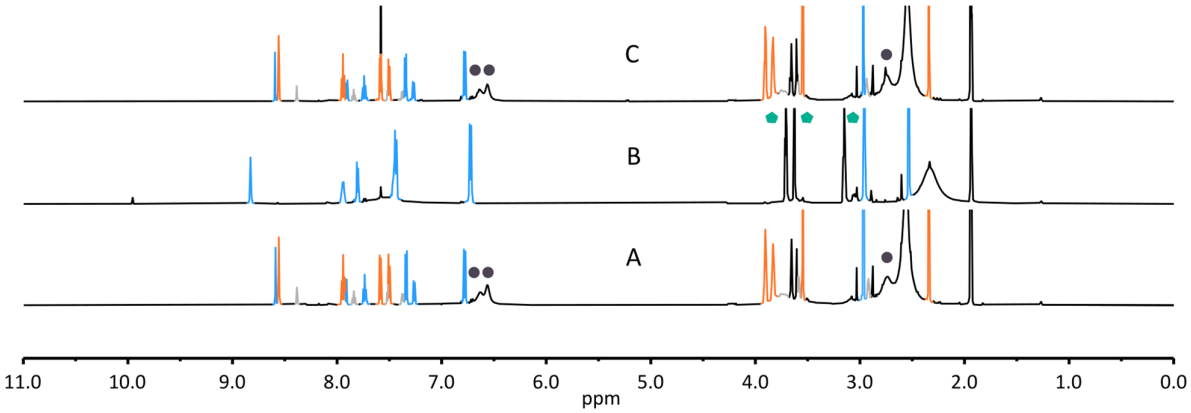

Figure S45. ^{1}H NMR spectra (600 MHz, 297 K, CD_3CN) of: (A) a mixture of [Ag(**3**,**1**)$_2$](SbF$_6$) from a mixture of [Ag(**3**$_2$,**2**)](SbF$_6$), (**3**,**1**), [Ag(**3**,**1**)$_2$](SbF$_6$), [Ag(**3**,**2**)$_n$](SbF$_6$), **1** and **2**, the evolution of this mixture 1 min (B) and 43 min (C) following the addition of 2.5 eq. CCl_3CO_2H. Diagnostic signals of [Ag(**3**$_2$,**2**)](SbF$_6$), and [Ag(**3**,**2**)$_n$](SbF$_6$) are highlighted respectively in orange and grey. Diagnostic signals of imine (**3**,**1**) and [Ag(**3**,**1**)$_2$](SbF$_6$) are highlighted in blue. Diagnostic signals of **1** and **2**+2H$^+$ are highlighted by grey circles and green pentagons, respectively.

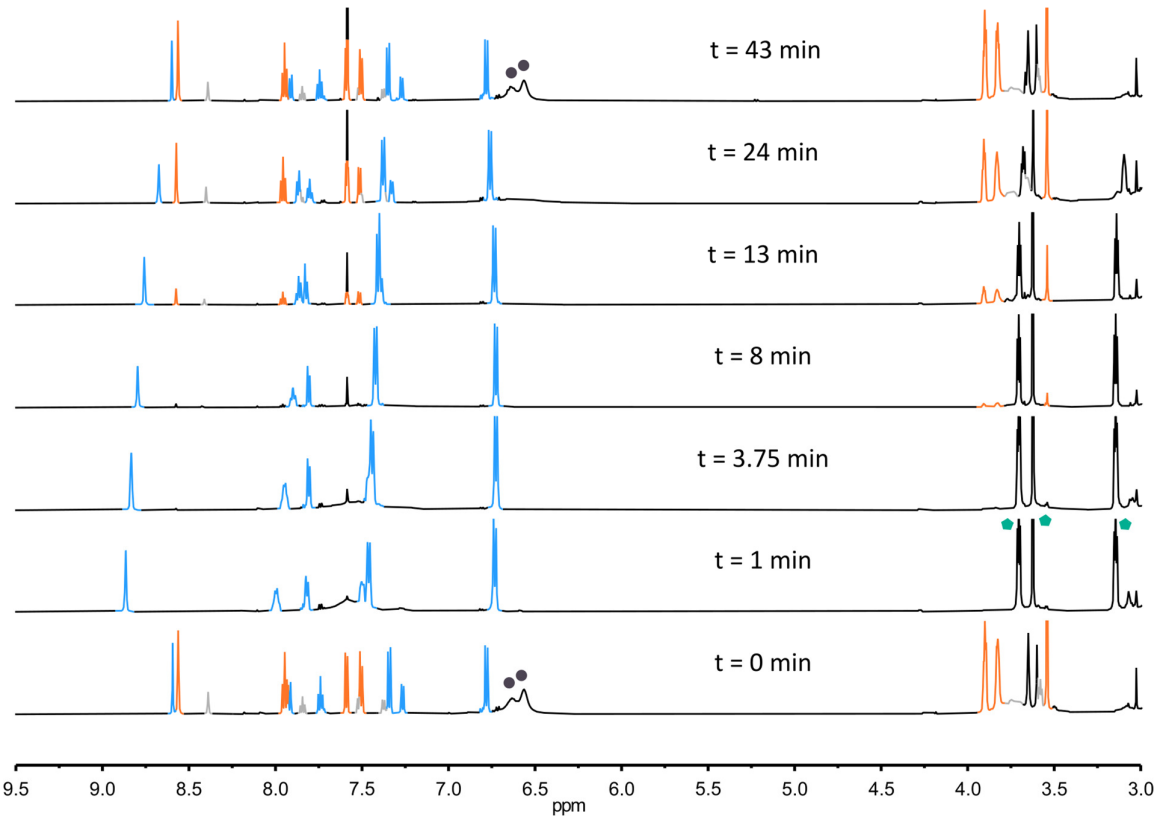

Figure S46. Monitoring by ^{1}H NMR spectroscopy (600 MHz, CD_3CN) of the transient self-assembly of [Ag(**3**,**1**)$_2$](SbF$_6$) from a mixture of [Ag(**3**$_2$,**2**)](SbF$_6$), (**3**,**1**), [Ag(**3**,**1**)$_2$](SbF$_6$), [Ag(**3**,**2**)$_n$](SbF$_6$), **1** and **2** upon addition of an initial aliquot of trichloroacetic acid. Reagents and conditions: 2.5 eq. CCl_3CO_2H, CD_3CN, r.t. Spectra of the crude reaction mixture were recorded at increasing time increments (up to a final total time of 43 min), aromatic region and part of the aliphatic region of the spectra shown. Diagnostic signals of [Ag(**3**$_2$,**2**)](SbF$_6$), and [Ag(**3**,**2**)$_n$](SbF$_6$) are highlighted respectively in orange and grey. Diagnostic signals of imine (**3**,**1**) and [Ag(**3**,**1**)$_2$](SbF$_6$) are highlighted in blue. Diagnostic signals of **1** and **2**+2H$^+$ are highlighted by grey circles and green pentagons, respectively.

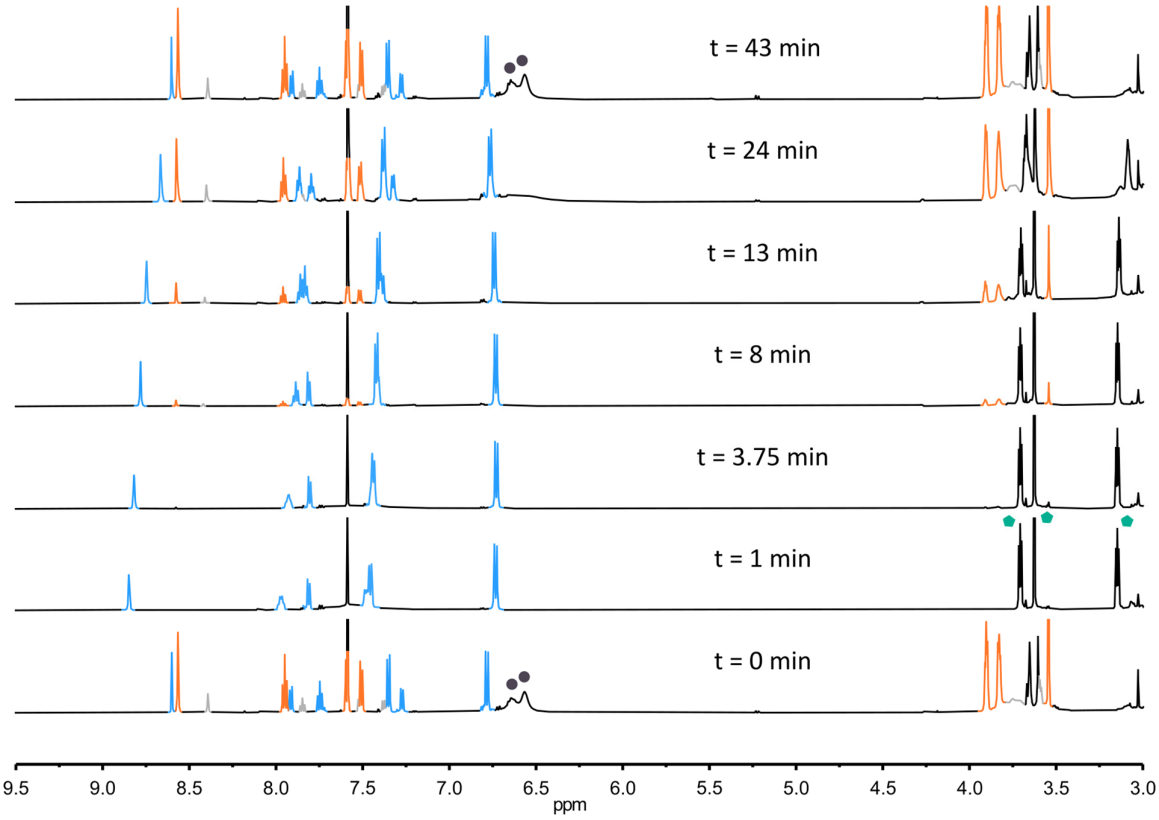

Figure S47. Monitoring by ^{1}H NMR spectroscopy (600 MHz, CD_3CN) of the transient self-assembly of [Ag(**3**,**1**)$_2$](SbF$_6$) from a mixture of [Ag(**3**$_2$,**2**)](SbF$_6$), (**3**,**1**), [Ag(**3**,**1**)$_2$](SbF$_6$), [Ag(**3**,**2**)$_n$](SbF$_6$), **1** and **2** upon addition of a second aliquot of trichloroacetic acid. Reagents and conditions: 2.5 eq. CCl_3CO_2H, CD_3CN, r.t. Spectra of the crude reaction mixture were recorded at increasing time increments (up to a final total time of 43 min), aromatic region and part of the aliphatic region of the spectra shown. Diagnostic signals of [Ag(**3**$_2$,**2**)](SbF$_6$), and [Ag(**3**,**2**)$_n$](SbF$_6$) are highlighted respectively in orange and grey. Diagnostic signals of imine (**3**,**1**) and [Ag(**3**,**1**)$_2$](SbF$_6$) are highlighted in blue. Diagnostic signals of **1** and **2**+2H$^+$ are highlighted by grey circles and green pentagons, respectively.

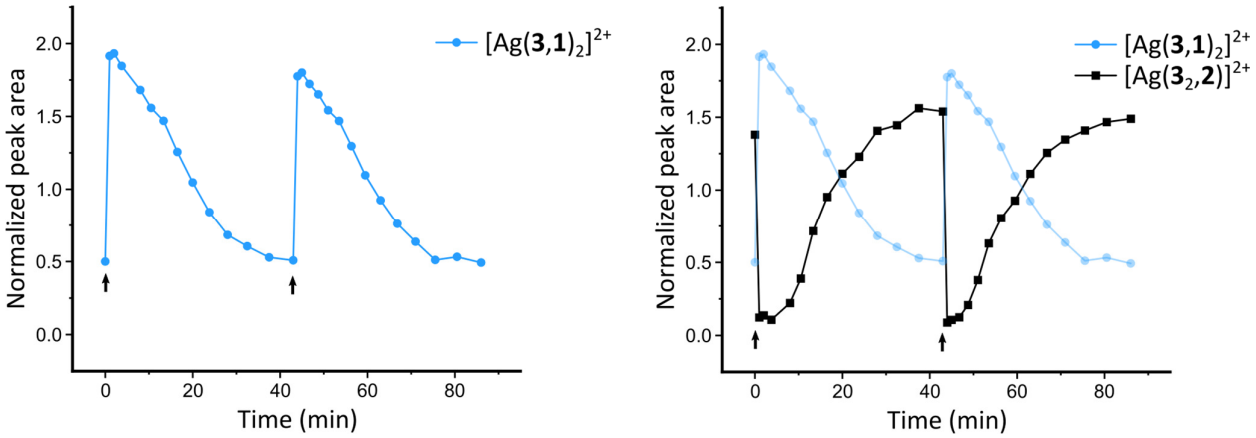

Figure S48. (Left) Assembly/disassembly as a function of time of [Ag(**3**,**1**)$_2$](SbF$_6$) upon addition of aliquots of trichloroacetic acid, monitored by ^{1}H NMR spectroscopy. (Right) Diassembly/assembly as a function of time of [Ag(**3**$_2$,**2**)](SbF$_6$) upon addition of aliquots of trichloroacetic acid, monitored by ^{1}H NMR. Graph plotting of the imine peak area for [Ag(**3**,**1**)$_2$](SbF$_6$) and [Ag(**3**$_2$,**2**)](SbF$_6$) both normalized to the imine peak area for [Ag(**3**$_2$,**2**)](SbF$_6$) prior to the first addition of trichloroacetic acid. Each arrow indicates the addition of an aliquot of trichloroacetic acid. Reagents and conditions for each cycle: 2.5 eq. CCl_3CO_2H, CD_3CN, r.t.

4.1.3.2 Monitoring of the transient process by ESI-MS

Complex [Ag(**3**$_2$,**2**)](SbF$_6$) was prepared by heating at 60 °C for 12 h a mixture of CD_3CN solutions of 6-methyl-2-pyridinecarboxaldehyde **3** (100 µL of 64 mM, 6.4 µmol, 2 eq.), 1,2-bis(2-aminoethoxy)ethane **2** (100 µL of 33.6 mM, 3.36 µmol, 1.05 eq.) and Ag(SbF$_6$) (100 µL of 32 mM, 3.2 µmol, 1 eq.). The resulting CD_3CN solution of [Ag(**3**$_2$,**2**)](SbF$_6$) was diluted with 100 µL of CD_3CN before being treated with a CD_3CN solutions of 4-(dimethylamino)aniline **1** (100 µL of 64 mM, 6.4 µmol, 2 eq.) and left to react at 60 °C for 18 h. After cooling to room temperature, the resulting mixture was treated with trichloroacetic acid (10 µL of 0.8 M, 8.0 µmol, 2.5 eq.). The composition of the reaction mixture was monitored prior and after the addition of trichloroacetic acid via electrospray ionization mass spectrometry (ESI–MS). Samples for ESI–MS were prepared by diluting 5 µL of the reaction mixture into 1 mL of CH_3CN.

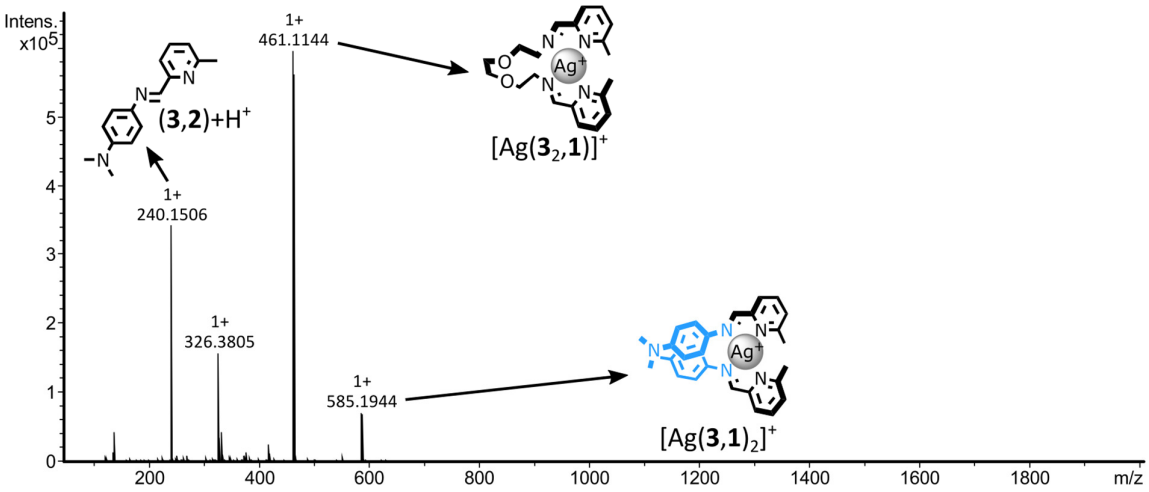

Figure S49. Electrospray ionization mass spectrometry (ESI–MS) analysis of a 1:2 mixture of [Ag(**3**$_2$,**2**)](SbF$_6$) and **1** before the addition of trichloroacetic acid.

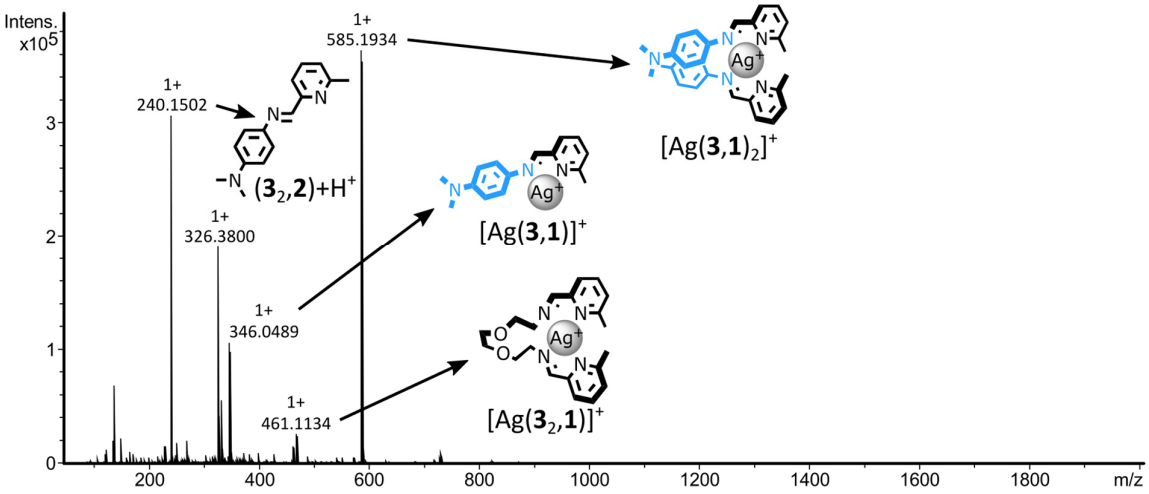

Figure S50. Electrospray ionization mass spectrometry (ESI–MS) analysis of a 1:2 mixture of [Ag(**3**$_2$,**2**)](SbF$_6$) and **1** approximately 2 min following the addition of trichloroacetic acid.

4.1.4 Transient self-assembly of [Ag(3,1)$_2$](SbF$_6$) from a non-equilibrated mixture of [Ag(3$_2$,2)](SbF$_6$) and 1

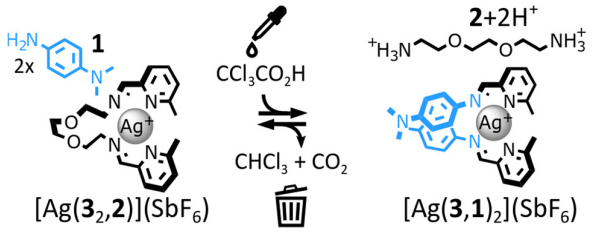

Scheme S14. Transient self-assembly of [Ag(**3**,**1**)$_2$](SbF$_6$) from a non-equilibrated mixture of [Ag(**3**$_2$,**2**)](SbF$_6$) and **1** in the presence of trichloroacetic acid. Reagents and conditions: 2.5 eq. CCl_3CO_2H, CD_3CN, r.t.

Complex [Ag(**3**$_2$,**2**)](SbF$_6$) was prepared by heating at 60 °C for 12 h a mixture of CD_3CN solutions of 6-methyl-2-pyridinecarboxaldehyde **3** (100 µL of 64 mM, 6.4 µmol, 2 eq.), 1,2-bis(2-aminoethoxy)ethane **2** (100 µL of 33.6 mM, 3.36 µmol, 1.05 eq.) and Ag(SbF$_6$) (100 µL of 32 mM, 3.2 µmol, 1 eq.). After cooling to room temperature, the resulting CD_3CN solution of [Ag(**3**$_2$,**2**)](SbF$_6$) was diluted with 100 µL of CD_3CN before being treated sequentially with CD_3CN solutions of 4-(dimethylamino)aniline **1** (100 µL of 64 mM, 6.4 µmol, 2 eq.) and trichloroacetic acid (10 µL of 0.8 M, 8.0 µmol, 2.5 eq.). The evolution of the reaction mixture was monitored over time by ^{1}H NMR spectroscopy. The complexes were never isolated, all the present experiments and analysis were performed on the crude reaction mixture.

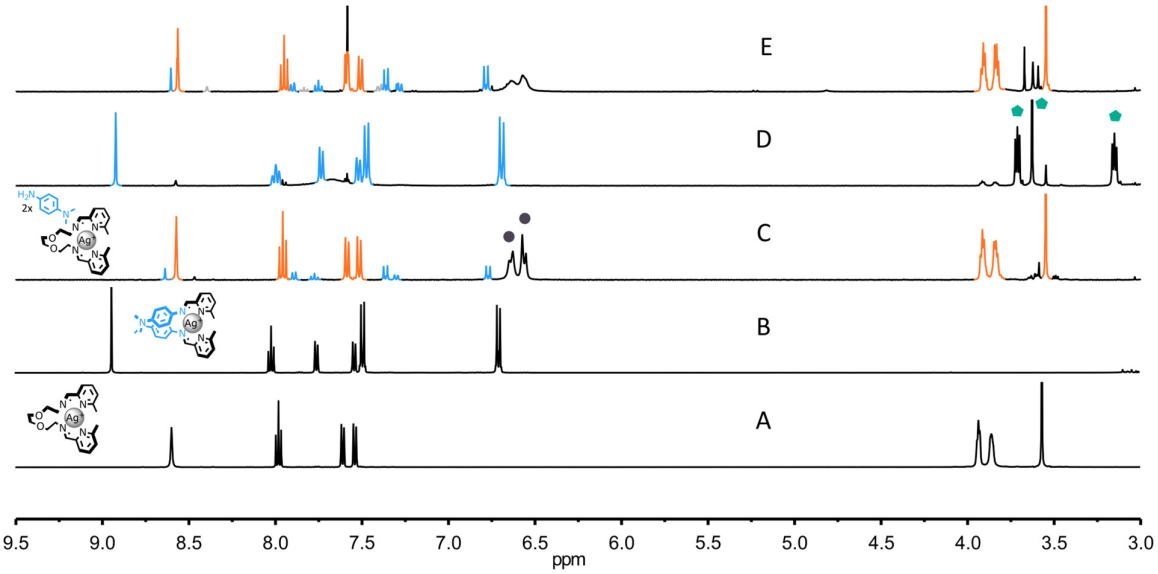

Figure S51. Partial ^{1}H NMR spectra (400 MHz, 297 K, CD_3CN) of: (A) complex [Ag(**3**$_2$,**2**)](SbF$_6$), (B) complex [Ag(**3**,**1**)$_2$](SbF$_6$), (C) a mixture of [Ag(**3**$_2$,**2**)](SbF$_6$) and **1** in a 1:2 molar ratio, the evolution of this mixture 1.5 min (D) and 42 min (E) following the addition of 2.5 eq. CCl_3CO_2H. Diagnostic signals of [Ag(**3**$_2$,**2**)](SbF$_6$), and [Ag(**3**,**2**)$_n$](SbF$_6$) are highlighted respectively in orange and grey. Diagnostic signals of imine (**3**,**1**) and [Ag(**3**,**1**)$_2$](SbF$_6$) are highlighted in blue. Diagnostic signals of **1** and **2**+2H$^+$ are highlighted by grey circles and green pentagons, respectively.

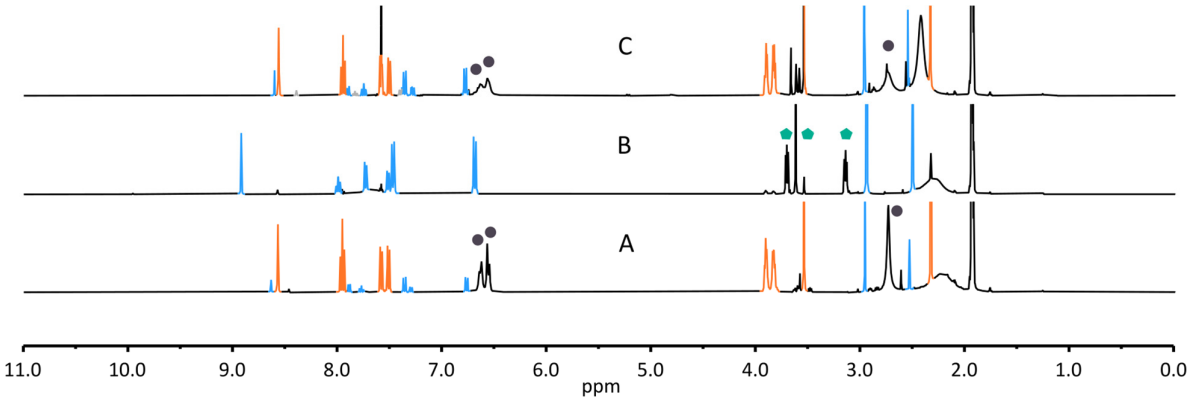

Figure S52. ^{1}H NMR spectra (400 MHz, 297 K, CD_3CN) of: (A) a mixture of [Ag(**3**$_2$,**2**)](SbF_6) and **1** in a 1:2 molar ratio, the evolution of this mixture 1.5 min (B) and 42 min (C) following the addition of 2.5 eq. CCl_3CO_2H. Diagnostic signals of [Ag(**3**$_2$,**2**)](SbF_6), and [Ag(**3**,**2**)$_n$](SbF_6) are highlighted respectively in orange and grey. Diagnostic signals of imine (**3**,**1**) and [Ag(**3**,**1**)$_2$](SbF_6) are highlighted in blue. Diagnostic signals of **1** and **2**+2H$^+$ are highlighted by grey circles and green pentagons, respectively.

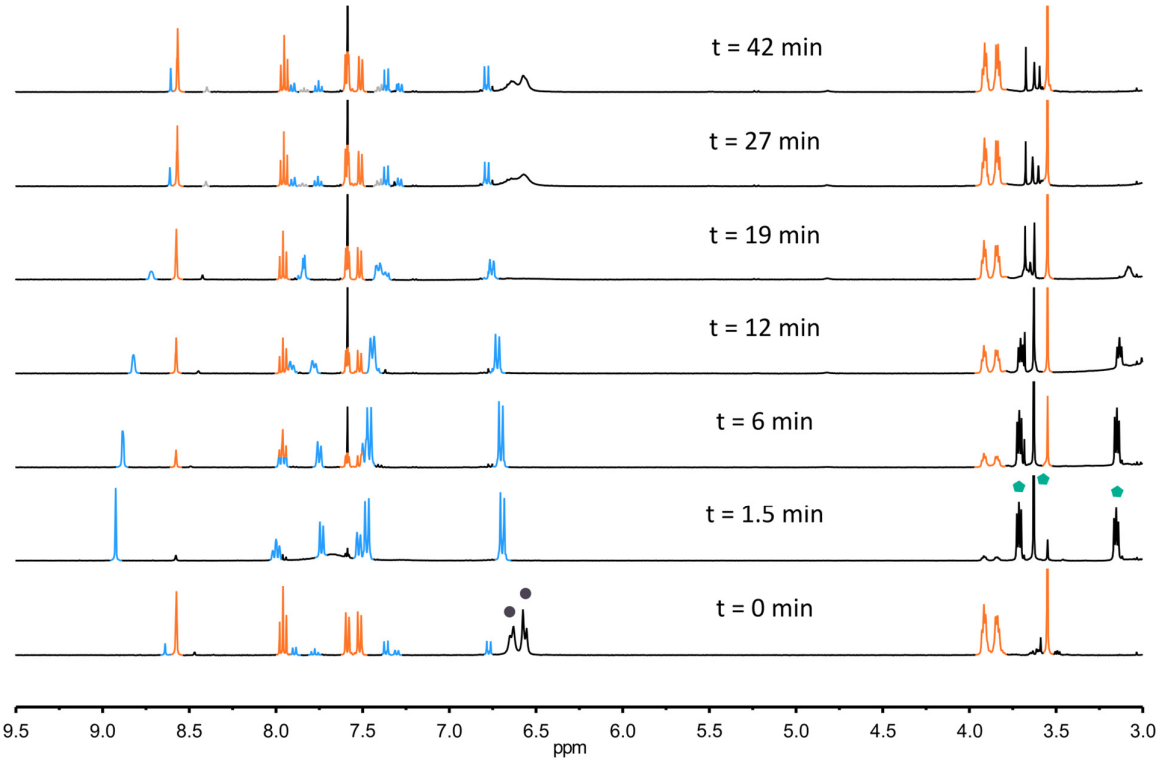

Figure S53. Monitoring by ^{1}H NMR spectroscopy (400 MHz, CD_3CN) of the transient self-assembly of [Ag(**3**,**1**)$_2$](SbF$_6$) from [Ag(**3**$_2$,**2**)](SbF$_6$) and **1** upon addition of an initial aliquot of trichloroacetic acid. Reagents and conditions: 2.5 eq. CCl_3CO_2H, CD_3CN, r.t. Spectra of the crude reaction mixture were recorded at increasing time increments (up to a final total time of 42 min), aromatic region and part of the aliphatic region of the spectra shown. Diagnostic signals of [Ag(**3**$_2$,**2**)](SbF$_6$), and [Ag(**3**,**2**)$_n$](SbF$_6$) are highlighted respectively in orange and grey. Diagnostic signals of imine (**3**,**1**) and [Ag(**3**,**1**)$_2$](SbF$_6$) are highlighted in blue. Diagnostic signals of **1** and **2**+2H$^+$ are highlighted by grey circles and green pentagons, respectively.

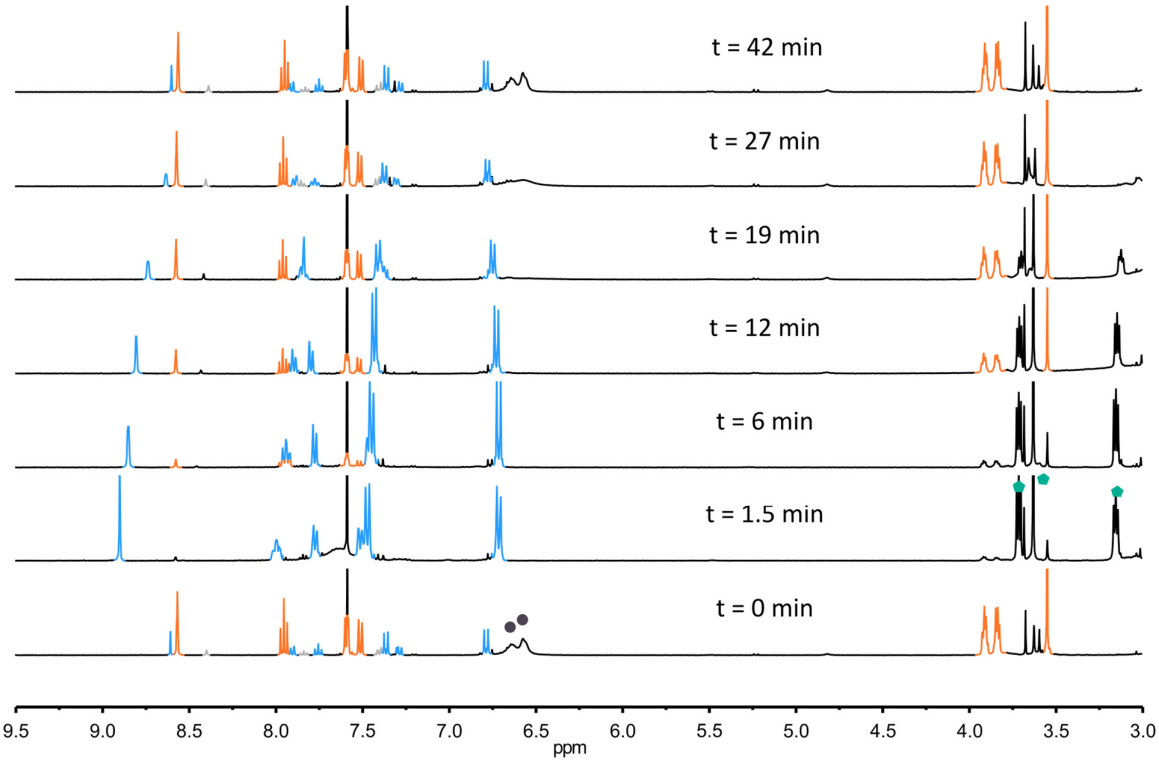

Figure S54. Monitoring by ^{1}H NMR spectroscopy (400 MHz, CD_3CN) of the transient self-assembly of [Ag(**3**,**1**)$_2$](SbF$_6$) from [Ag(**3**$_2$,**2**)](SbF$_6$) and **1** upon addition of a second aliquot of trichloroacetic acid. Reagents and conditions: 2.5 eq. CCl_3CO_2H, CD_3CN, r.t. Spectra of the crude reaction mixture were recorded at increasing time increments (up to a final total time of 42 min), aromatic region and part of the aliphatic region of the spectra shown. Diagnostic signals of [Ag(**3**$_2$,**2**)](SbF$_6$), and [Ag(**3**,**2**)$_n$](SbF$_6$) are highlighted respectively in orange and grey. Diagnostic signals of imine (**3**,**1**) and [Ag(**3**,**1**)$_2$](SbF$_6$) are highlighted in blue. Diagnostic signals of **1** and **2**+2H$^+$ are highlighted by grey circles and green pentagons, respectively.

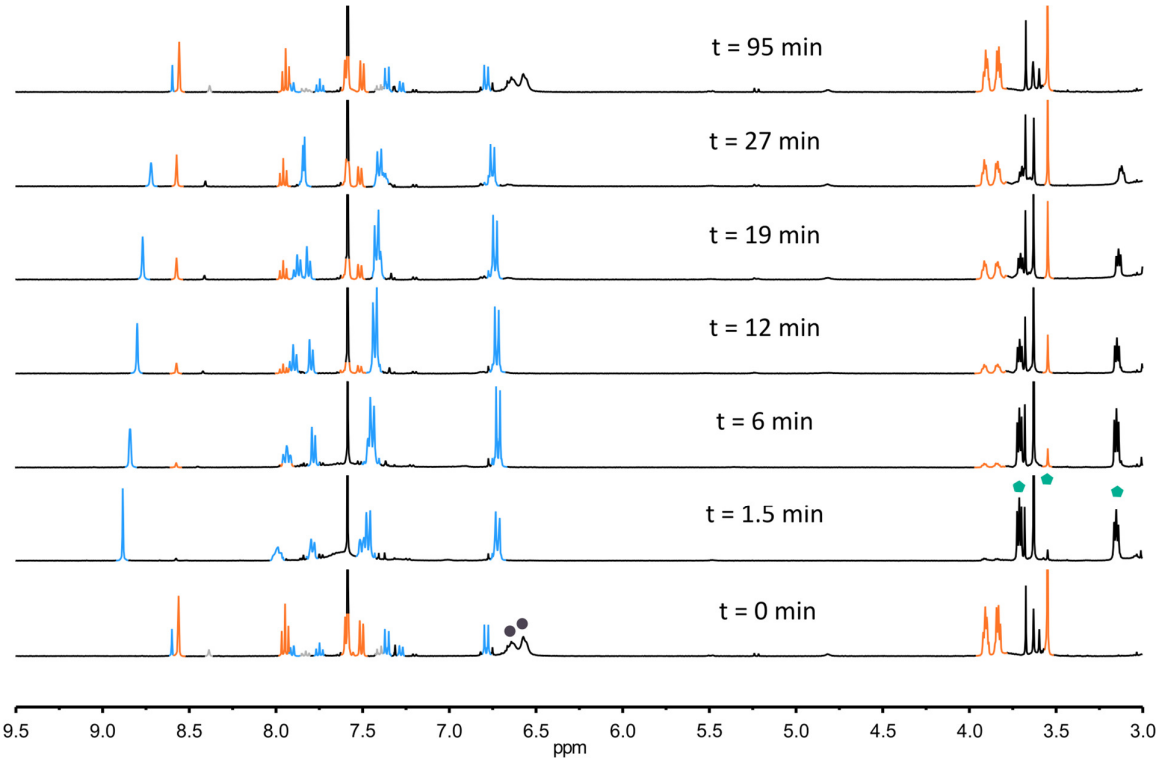

Figure S55. Monitoring by ^{1}H NMR spectroscopy (400 MHz, CD_3CN) of the transient self-assembly of [Ag(**3**,**1**)$_2$](SbF$_6$) from [Ag(**3**$_2$,**2**)](SbF$_6$) and **1** upon addition of a third aliquot of trichloroacetic acid. Reagents and conditions: 2.5 eq. CCl_3CO_2H, CD_3CN, r.t. Spectra of the crude reaction mixture were recorded at increasing time increments (up to a final total time of 42 min), aromatic region and part of the aliphatic region of the spectra shown. Diagnostic signals of [Ag(**3**$_2$,**2**)](SbF$_6$), and [Ag(**3**,**2**)$_n$](SbF$_6$) are highlighted respectively in orange and grey. Diagnostic signals of imine (**3**,**1**) and [Ag(**3**,**1**)$_2$](SbF$_6$) are highlighted in blue. Diagnostic signals of **1** and **2**+2H$^+$ are highlighted by grey circles and green pentagons, respectively.

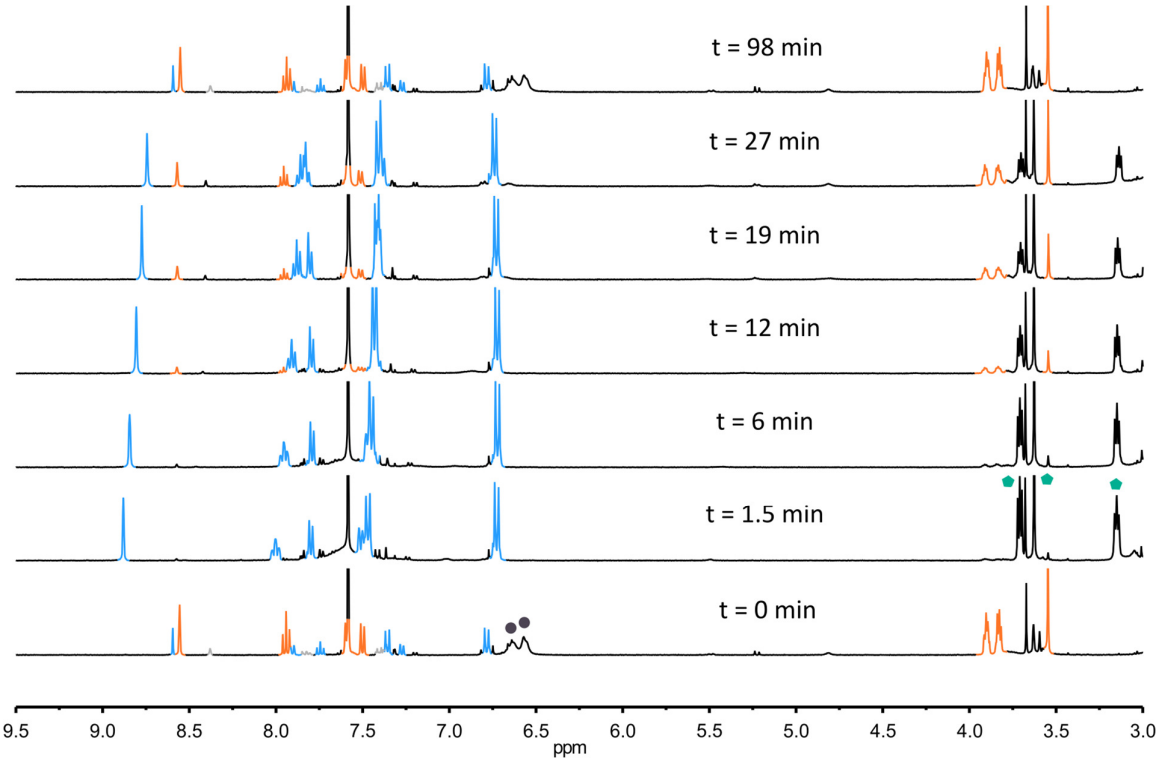

Figure S56. Monitoring by ^{1}H NMR spectroscopy (400 MHz, CD_3CN) of the transient self-assembly of [Ag(**3**,**1**)$_2$](SbF$_6$) from [Ag(**3**$_2$,**2**)](SbF$_6$) and **1** upon addition of a fourth aliquot of trichloroacetic acid. Reagents and conditions: 2.5 eq. CCl_3CO_2H, CD_3CN, r.t. Spectra of the crude reaction mixture were recorded at increasing time increments (up to a final total time of 42 min), aromatic region and part of the aliphatic region of the spectra shown. Diagnostic signals of [Ag(**3**$_2$,**2**)](SbF$_6$), and [Ag(**3**,**2**)$_n$](SbF$_6$) are highlighted respectively in orange and grey. Diagnostic signals of imine (**3**,**1**) and [Ag(**3**,**1**)$_2$](SbF$_6$) are highlighted in blue. Diagnostic signals of **1** and **2**+2H$^+$ are highlighted by grey circles and green pentagons, respectively.

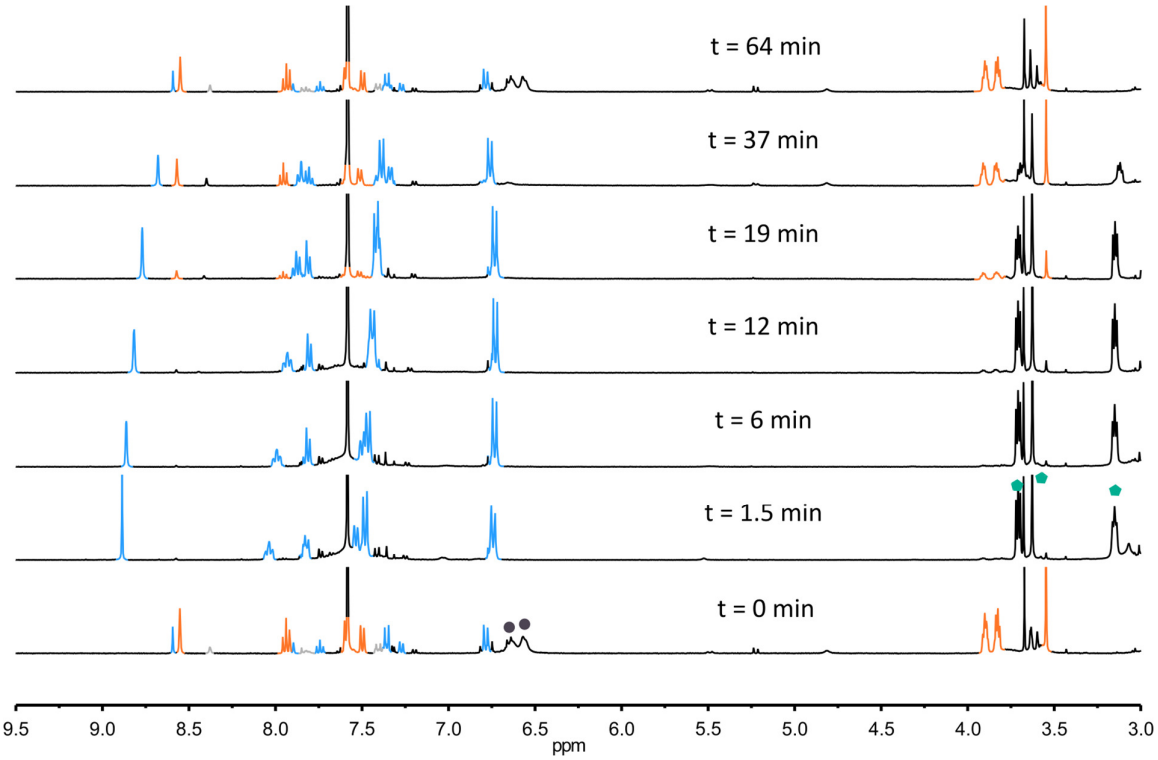

Figure S57. Monitoring by ^{1}H NMR spectroscopy (400 MHz, CD_3CN) of the transient self-assembly of [Ag(**3**,**1**)$_2$](SbF$_6$) from [Ag(**3**$_2$,**2**)](SbF$_6$) and **1** upon addition of a fifth aliquot of trichloroacetic acid. Reagents and conditions: 2.5 eq. CCl_3CO_2H, CD_3CN, r.t. Spectra of the crude reaction mixture were recorded at increasing time increments (up to a final total time of 42 min), aromatic region and part of the aliphatic region of the spectra shown. Diagnostic signals of [Ag(**3**$_2$,**2**)](SbF$_6$), and [Ag(**3**,**2**)$_n$](SbF$_6$) are highlighted respectively in orange and grey. Diagnostic signals of imine (**3**,**1**) and [Ag(**3**,**1**)$_2$](SbF$_6$) are highlighted in blue. Diagnostic signals of **1** and **2**+2H$^+$ are highlighted by grey circles and green pentagons, respectively.

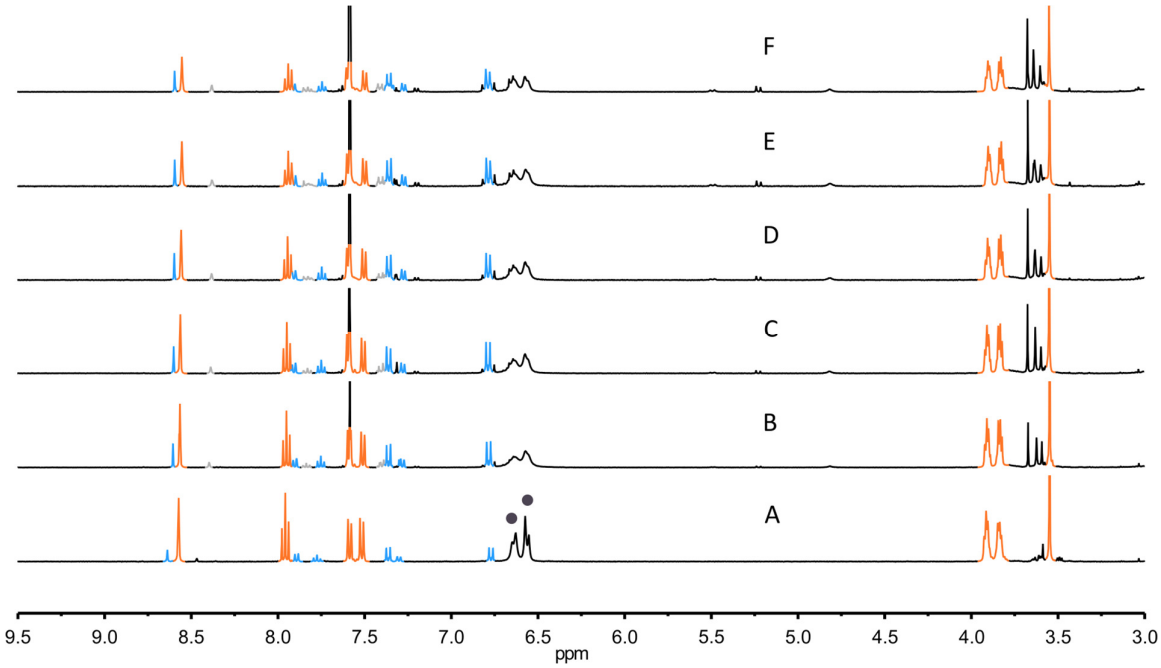

Figure S58. Evaluation of the stability of the system after several rearrangement cycles. Partial ^{1}H NMR spectra (400 MHz, CD_3CN) of: (A) a 1:2 mixture of [Ag(**3**$_2$,**2**)](SbF_6) and **1** before the addition of trichloroacetic acid, (B) this mixture following the re-assembly of [Ag(**3**$_2$,**2**)](SbF_6) upon consumption of the initial aliquot of trichloroacetic acid, (C) – (F) this mixture following two – five disassembly/re-assembly cycles. Reagents and conditions for each cycle: 2.5 eq. CCl_3CO_2H, CD_3CN, r.t. Diagnostic signals of [Ag(**3**$_2$,**2**)](SbF_6), and [Ag(**3**,**2**)$_n$](SbF_6) are highlighted respectively in orange and grey. Diagnostic signals of imine (**3**,**1**) and [Ag(**3**,**1**)$_2$](SbF_6) are highlighted in blue. Diagnostic signals of **1** are highlighted by grey circles.

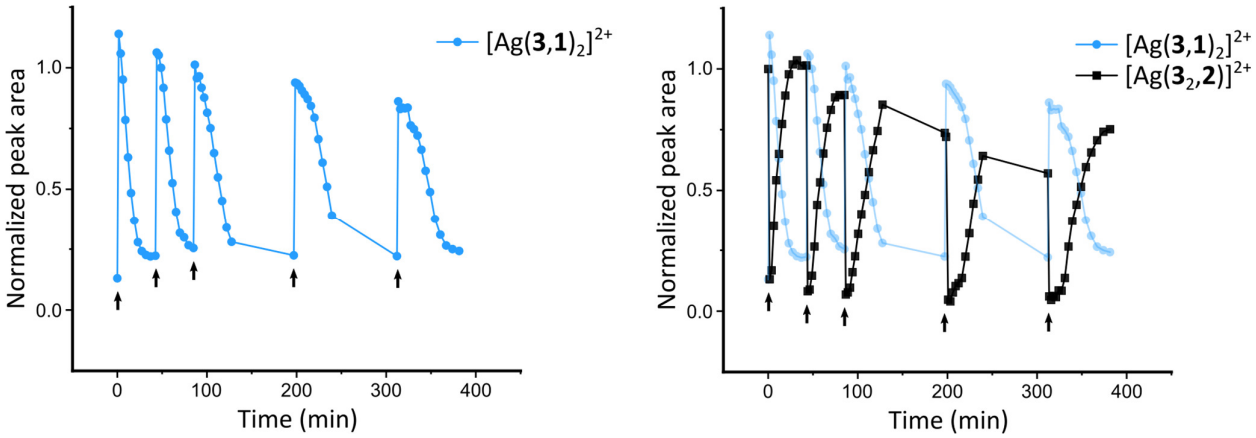

Figure S59. (Left) Assembly/disassembly as a function of time of [Ag(**3**,**1**)$_2$](SbF$_6$) upon addition of aliquots of trichloroacetic acid, monitored by ^{1}H NMR spectroscopy. (Right) Diassembly/assembly as a function of time of [Ag(**3**$_2$,**2**)](SbF$_6$) upon addition of aliquots of trichloroacetic acid, monitored by ^{1}H NMR. Graph plotting of the imine peak area for [Ag(**3**,**1**)$_2$](SbF$_6$) and [Ag(**3**$_2$,**2**)](SbF$_6$) both normalized to the imine peak area for [Ag(**3**$_2$,**2**)](SbF$_6$) prior to the first addition of trichloroacetic acid. Each arrow indicates the addition of an aliquot of trichloroacetic acid. Reagents and conditions for each cycle: 2.5 eq. CCl_3CO_2H, CD_3CN, r.t.

4.1.5 Transient self-assembly of [Cu(3,5)$_2$](BF$_4$) from [Cu(3$_2$,2)](BF$_4$) and 5

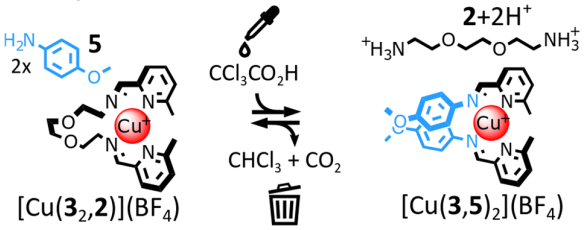

Scheme S15. Transient self-assembly of [Cu(**3**,**5**)$_2$](BF$_4$) from [Cu(**3**$_2$,**2**)](BF$_4$) and **5** in the presence of trichloroacetic acid. Reagents and conditions: 2.5 eq. CCl_3CO_2H, CD_3CN, r.t.

Complex [Cu(**3**$_2$,**2**)](BF$_4$) was prepared by heating at 60 °C for 12 h a mixture of CD_3CN solutions of 6-methyl-2-pyridinecarboxaldehyde **3** (100 µL of 64 mM, 6.4 µmol, 2 eq.), 1,2-bis(2-aminoethoxy)ethane **2** (100 µL of 33.6 mM, 3.36 µmol, 1.05 eq.) and [Cu(CH_3CN)$_4$](BF$_4$) (100 µL of 32 mM, 3.2 µmol, 1 eq.). After cooling to room temperature, the resulting CD_3CN solution of [Cu(**3**$_2$,**2**)](BF$_4$) was diluted with 100 µL of CD_3CN before being treated sequentially with CD_3CN solutions of p-anisidine **5** (100 µL of 64 mM, 6.4 µmol, 2 eq.) and trichloroacetic acid (10 µL of 0.8 M, 8.0 µmol, 2.5 eq.). The evolution of the reaction mixture was monitored over time by ^{1}H NMR spectroscopy. The complexes were never isolated, all the present experiments and analysis were performed on the crude reaction mixture.

4.1.5.1 Monitoring of the transient process by ^{1}H NMR spectroscopy

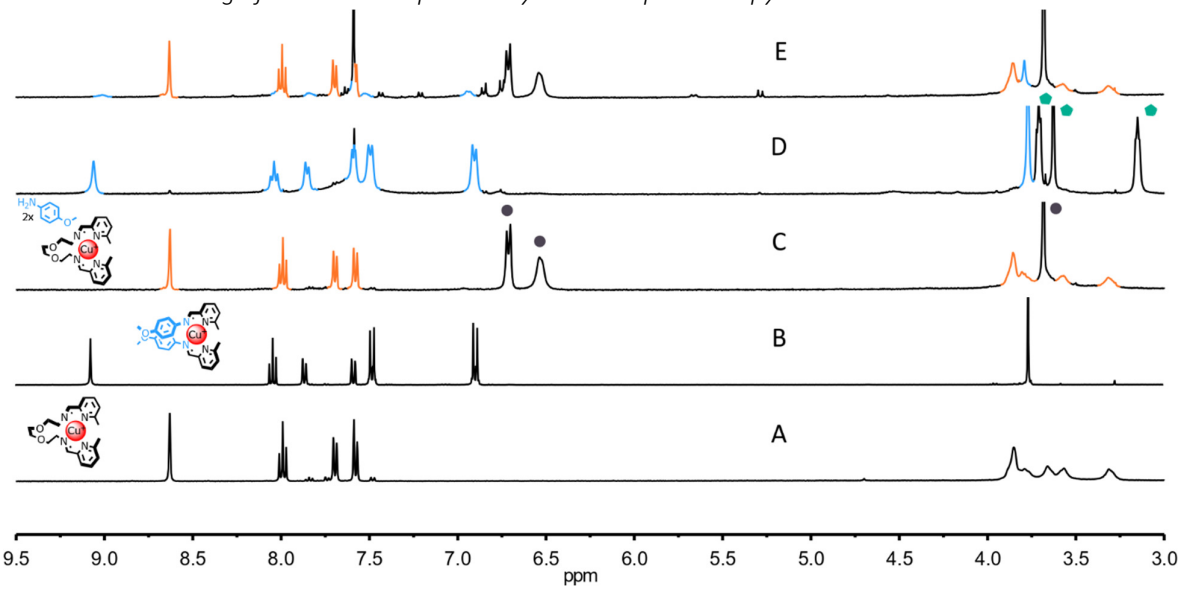

Figure S60. Partial ^{1}H NMR spectra (400 MHz, 297 K, CD_3CN) of: (A) complex [Cu(**3**$_2$,**2**)](BF_4), (B) complex [Cu(**3**,**5**)$_2$](BF_4), (C) a mixture of [Cu(**3**$_2$,**2**)](BF_4) and **5** in a 1:2 molar ratio, the evolution of this mixture 1.5 min (D) and 42 min (E) after the addition of 2.5 eq. CCl_3CO_2H. Diagnostic signals of [Cu(**3**$_2$,**2**)](BF_4) and [Cu(**3**,**5**)$_2$](BF_4) are highlighted respectively in orange and blue. Diagnostic signals of **5** and **2**+2H$^+$ are highlighted by grey circles and green pentagons, respectively.

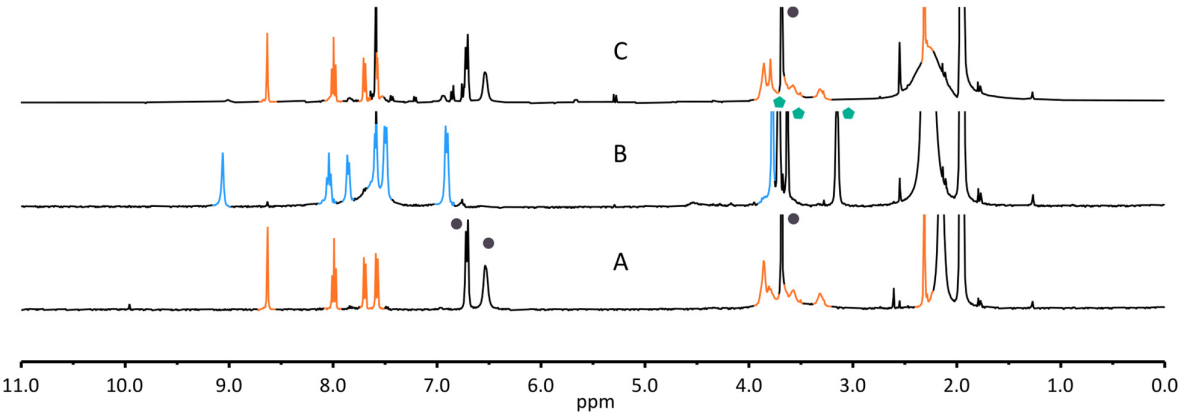

Figure S61. ^{1}H NMR spectra (400 MHz, 297 K, CD_3CN) of: (A) a mixture of [Cu(**3**$_2$,**2**)](BF_4) and **5** in a 1:2 molar ratio, the evolution of this mixture 1.5 min (B) and 42 min (C) after the addition of 2.5 eq. CCl_3CO_2H. Diagnostic signals of [Cu(**3**$_2$,**2**)](BF_4) and [Cu(**3**,**5**)$_2$](BF_4) are highlighted respectively in orange and blue. Diagnostic signals of **5** and **2**+2H$^+$ are highlighted by grey circles and green pentagons, respectively.

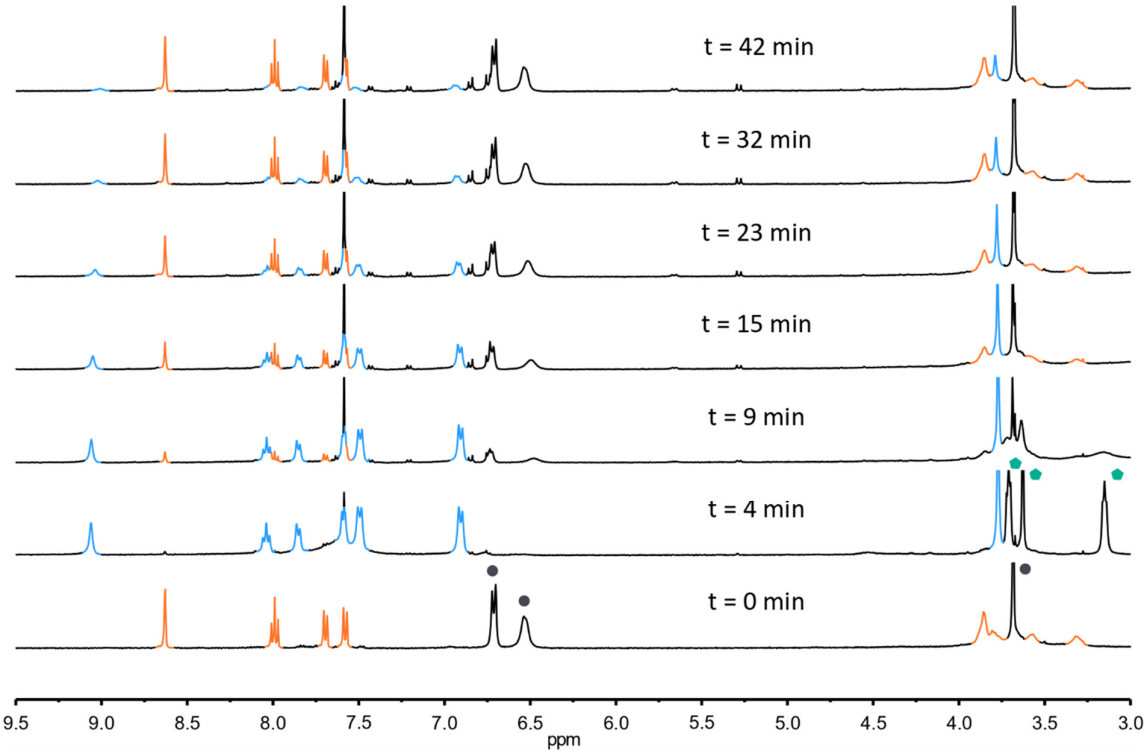

Figure S62. Monitoring by ^{1}H NMR spectroscopy (400 MHz, CD_3CN) of the transient self-assembly of [Cu(**3**,**5**)$_2$](BF$_4$) from [Cu(**3**$_2$,**2**)](BF$_4$) and **5** upon addition of an initial aliquot of trichloroacetic acid. Reagents and conditions: 2.5 eq. CCl_3CO_2H, CD_3CN, r.t. Spectra of the crude reaction mixture were recorded at increasing time increments (up to a final total time of 42 min), aromatic region and part of the aliphatic region of the spectra shown. Diagnostic signals of [Cu(**3**$_2$,**2**)](BF$_4$) and [Cu(**3**,**5**)$_2$](BF$_4$) are highlighted respectively in orange and blue. Diagnostic signals of **5** and **2**+2H$^+$ are highlighted by grey circles and green pentagons, respectively.

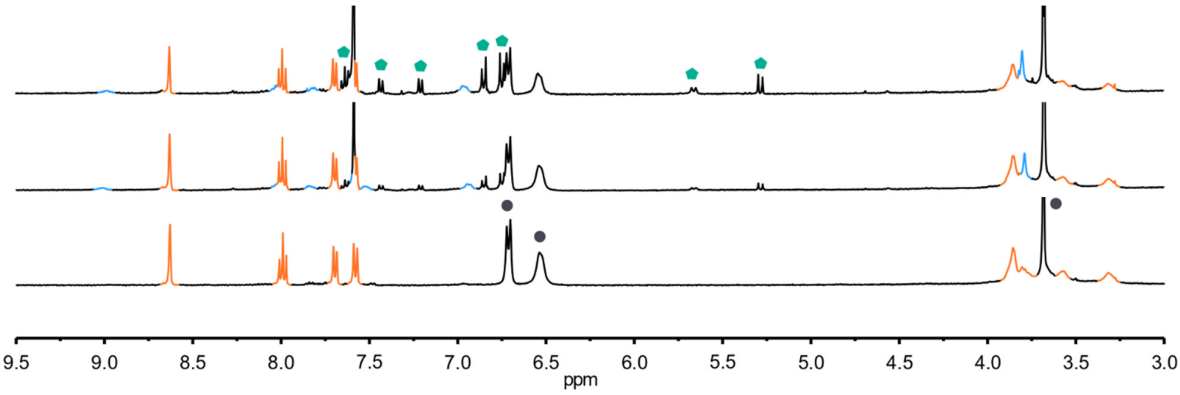

Figure S63. Evaluation of the stability of the system after several rearrangement cycles. Repetitive addition of CCl_3CO_2H resulted in the trichloromethylation of the imine (**3**,**5**). Partial ^1H NMR spectra (400 MHz, CD_3CN) of: (bottom) a 1:2 mixture of [Cu(**3**$_2$,**2**)$_2$](BF_4) and **5** before addition of acid, (middle) this mixture following the re-assembly of [Cu(**3**$_2$,**2**)](BF_4) upon consumption of the initial aliquot of trichloroacetic acid, (top) this mixture following a second disassembly/re-assembly cycle. Reagents and conditions for each cycle: 2.5 eq. CCl_3CO_2H, CD_3CN, r.t. Diagnostic signals of [Cu(**3**$_2$,**2**)](BF_4) and [Cu(**3**,**5**)$_2$](BF_4) are highlighted respectively in orange and blue. Diagnostic signals of **5** and of the α-trichloromethyl amine side product are highlighted by grey circles and green pentagons, respectively.

4.1.5.2 Monitoring of the transient process by ESI-MS

Complex [Cu(**3**$_2$,**2**)](BF_4) was prepared by heating at 60 °C for 12 h a mixture of CD_3CN solutions of 6-methyl-2-pyridinecarboxaldehyde **3** (100 µL of 64 mM, 6.4 µmol, 2 eq.), 1,2-bis(2-aminoethoxy)ethane **2** (100 µL of 33.6 mM, 3.36 µmol, 1.05 eq.) and [Cu(CH_3CN)$_4$](BF_4) (100 µL of 32 mM, 3.2 µmol, 1 eq.). The resulting CD_3CN solution of [Cu(**3**$_2$,**2**)](BF_4) was diluted with 100 µL of CD_3CN before being treated with a CD_3CN solution of p-anisidine **5** (100 µL of 64 mM, 6.4 µmol, 2 eq.) and left to react at 60 °C for 18 h. After cooling to room temperature, the resulting mixture was treated with trichloroacetic acid (10 µL of 0.8 M, 8.0 µmol, 2.5 eq.). The composition of the reaction mixture was monitored prior and after the addition of trichloroacetic acid via electrospray ionization mass spectrometry (ESI–MS). Samples for ESI–MS were prepared by diluting 5 µL of the reaction mixture into 1 mL of CH_3CN.

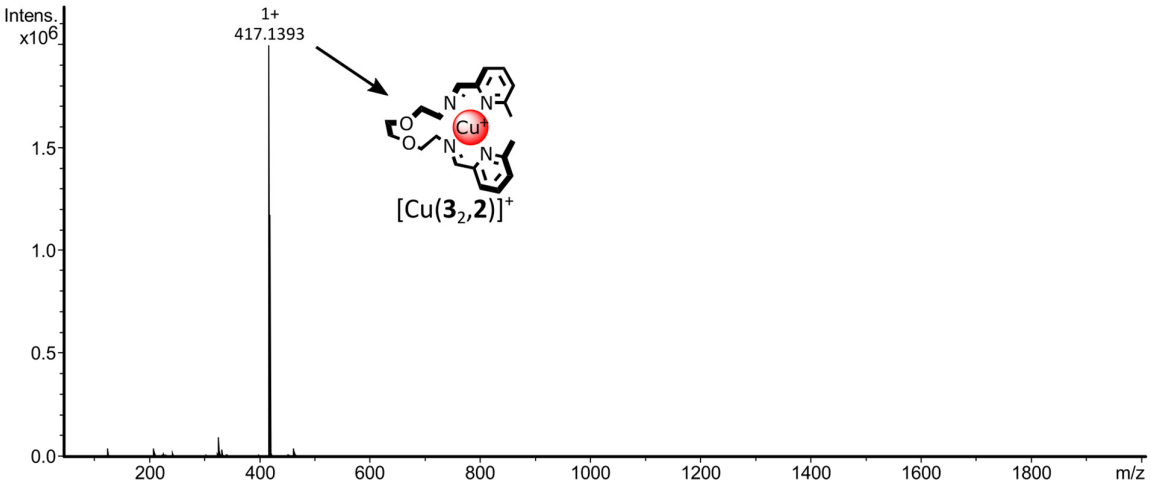

Figure S64. Electrospray ionization mass spectrometry (ESI–MS) analysis of a 1:2 mixture of [Cu(**3**$_2$,**2**)](BF$_4$) and **5** before the addition of trichloroacetic acid.

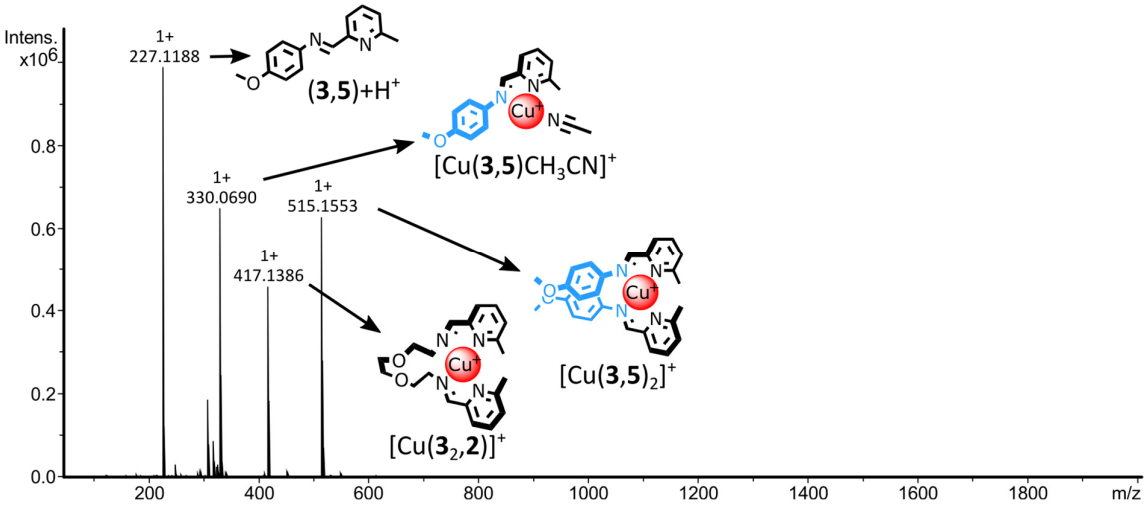

Figure S65. Electrospray ionization mass spectrometry (ESI–MS) analysis of a 1:2 mixture of [Cu(**3**$_2$,**2**)](BF$_4$) and **5** approximately 2 min following the addition of trichloroacetic acid.

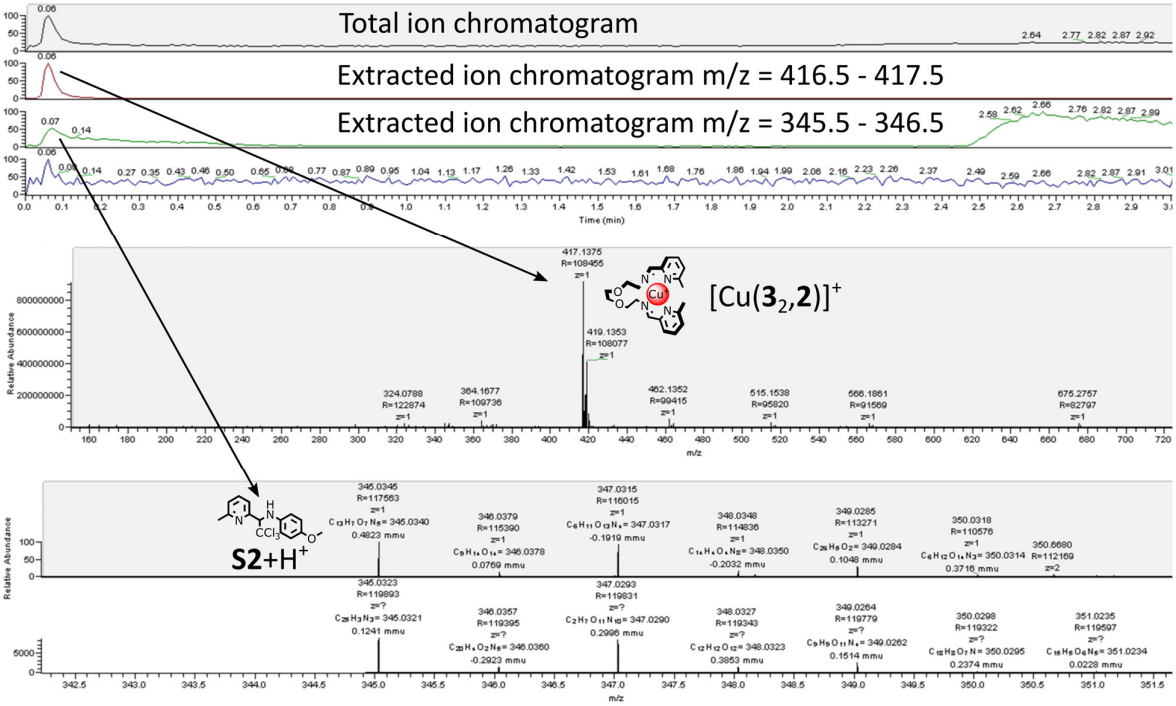

Figure S66. (Top) UPLC-ESI-HRMS profile of the crude reaction mixture obtained after a 1:2 mixture of [Cu(**3**$_2$,**2**)](BF$_4$) and **5** was subjected to two rearrangement cycles. Reagents and conditions for each cycle: 2.5 eq. CCl_3CO_2H, CD_3CN, r.t. (Middle) extracted-ion chromatogram at *m/z* 416.50 – 417.50 and observed isotope pattern corresponding to [Cu(**3**$_2$,**2**)]$^+$, (Bottom) extracted-ion chromatogram at *m/z* 345.52 – 346.52 and observed isotope pattern corresponding to [**S2**+H]$^+$.

4.2 Transient self-assembly of $[Ag_2(6,7_2)](SbF_6)_2$ from $[Ag_2(6_2,2_2)](SbF_6)_2$ and 7

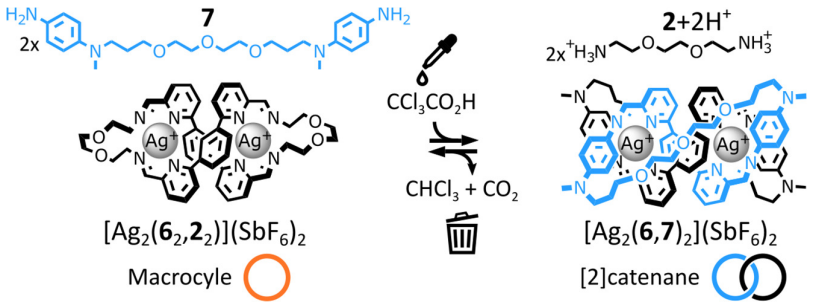

Scheme S16. Transient self-assembly of $[Ag_2(\mathbf{6},\mathbf{7})_2](SbF_6)_2$ from $[Ag_2(\mathbf{6}_2,\mathbf{2}_2)](SbF_6)_2$ and **7** in the presence of trichloroacetic acid. Reagents and conditions: 7.5 – 12 eq. CCl_3CO_2H, CD_3CN:$CDCl_3$ 3:1, r.t.

Complex $[Ag_2(\mathbf{6}_2,\mathbf{2}_2)](SbF_6)_2$ was prepared by heating at 60 °C for 12 h a mixture of a $CDCl_3$ solution of dialdehyde **6** (100 µL of 32 mM, 3.2 µmol, 1 eq.) and CD_3CN solutions of 1,2-bis(2-aminoethoxy)ethane **2** (100 µL of 35.2 mM, 3.52 µmol, 1.1 eq.) and $Ag(SbF_6)$ (100 µL of 32 mM, 12.8 µmol, 1 eq.). After cooling to room temperature, the resulting solution of $[Ag_2(\mathbf{6}_2,\mathbf{2}_2)](SbF_6)_2$ was diluted with 100 µL of CD_3CN:$CDCl_3$ 3:1 before being treated sequentially with CD_3CN solutions of diamine **7** (100 µL of 32 mM, 3.2 µmol, 1 eq.) and trichloroacetic acid (30 – 48 µL of 0.8 M, 24 – 38.4 µmol, 7.5 – 12 eq.). The evolution of the reaction mixture was monitored over time by ^{1}H NMR spectroscopy. The complexes were never isolated, all the present experiments and analysis were performed on the crude reaction mixture.

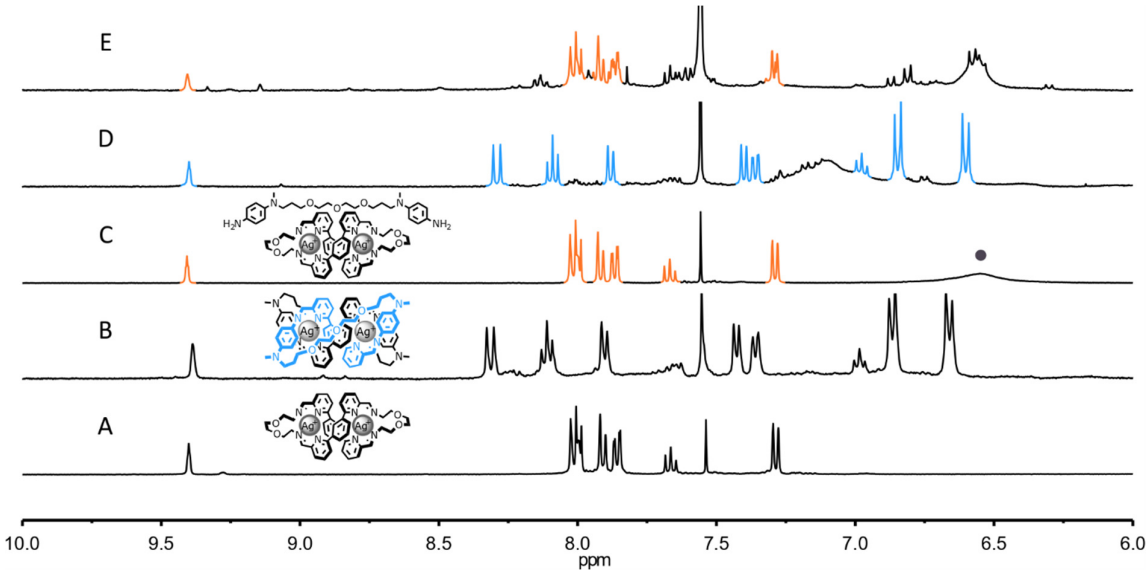

Figure S67. Partial ^{1}H NMR spectra (400 MHz, 297 K, CD_3CN:$CDCl_3$ 3:1) of: (A) complex $[Ag_2(\mathbf{6}_2,\mathbf{2}_2)](SbF_6)_2$, (B) complex $[Ag_2(\mathbf{6},\mathbf{7})_2](SbF_6)_2$ in the presence of 4 eq. CCl_3CO_2H, (C) a 1:2 mixture of $[Ag_2(\mathbf{6}_2,\mathbf{2}_2)](SbF_6)_2$ and **7**, the evolution of this mixture 4 h (D) and 18 h (E) following the addition of 10 eq. CCl_3CO_2H. Diagnostic signals of $[Ag_2(\mathbf{6}_2,\mathbf{2}_2)](SbF_6)_2$ and $[Ag_2(\mathbf{6},\mathbf{7})_2](SbF_6)_2$ are highlighted respectively in orange and blue. Diagnostic signals of **7** are highlighted by grey circles.

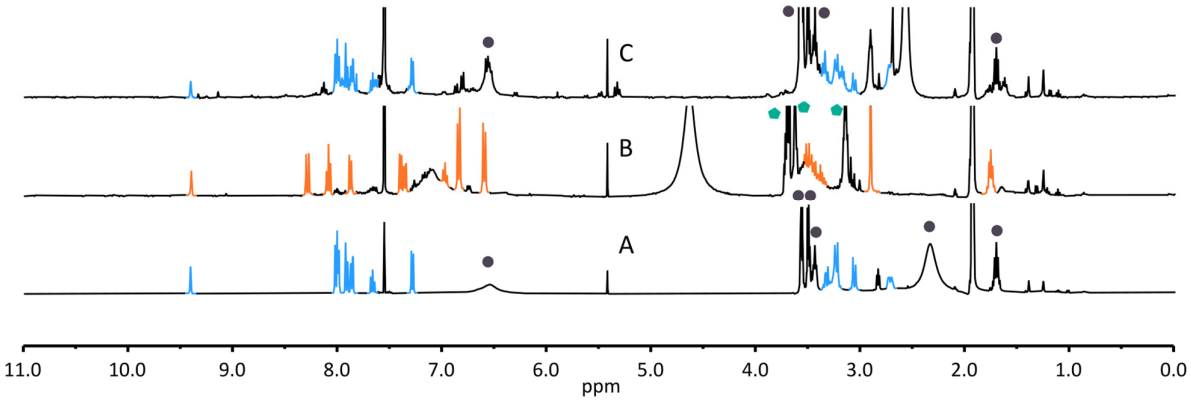

Figure S68. ^{1}H NMR spectra (400 MHz, 297 K, CD_3CN:$CDCl_3$ 3:1) of: (A) a 1:2 mixture of $[Ag_2(\mathbf{6}_2,\mathbf{2}_2)](SbF_6)_2$ and **7**, the evolution of this mixture 4 h (B) and 18 h (C) following the addition of 10 eq. CCl_3CO_2H. Diagnostic signals of $[Ag_2(\mathbf{6}_2,\mathbf{2}_2)](SbF_6)_2$ and $[Ag_2(\mathbf{6},\mathbf{7})_2](SbF_6)_2$ are highlighted respectively in orange and blue. Diagnostic signals of **7** are highlighted by grey circles.

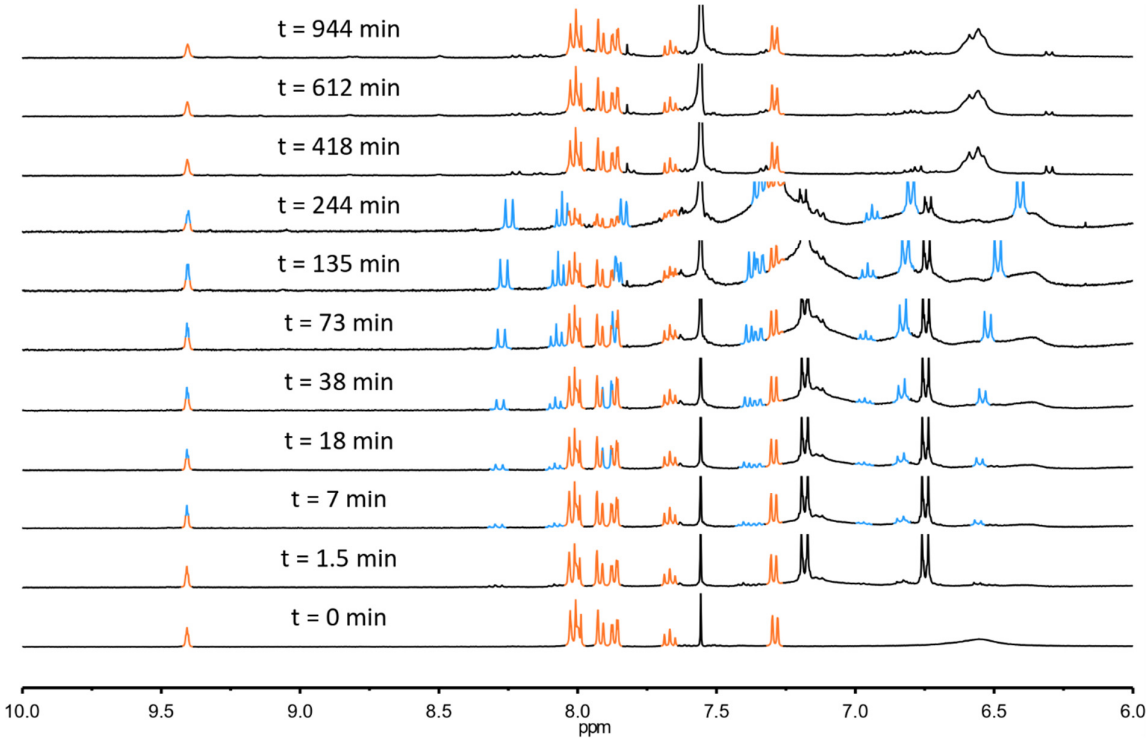

Figure S69. Monitoring by ^{1}H NMR spectroscopy (400 MHz, CD_3CN:$CDCl_3$ 3:1) of the transient self-assembly of $[Ag_2(\mathbf{6},\mathbf{7})_2](SbF_6)_2$ from $[Ag_2(\mathbf{6}_2,\mathbf{2}_2)](SbF_6)_2$ and **7** upon addition of 7.5 eq. of trichloroacetic acid. Reagents and conditions: 7.5 eq. CCl_3CO_2H, CD_3CN:$CDCl_3$ 3:1, r.t. Spectra of the crude reaction mixture were recorded at increasing time increments (up to a final total time of 944 min), aromatic region and part of the aliphatic region of the spectra shown. Diagnostic signals of $[Ag_2(\mathbf{6}_2,\mathbf{2}_2)](SbF_6)_2$ and $[Ag_2(\mathbf{6},\mathbf{7})_2](SbF_6)_2$ are highlighted respectively in orange and blue.

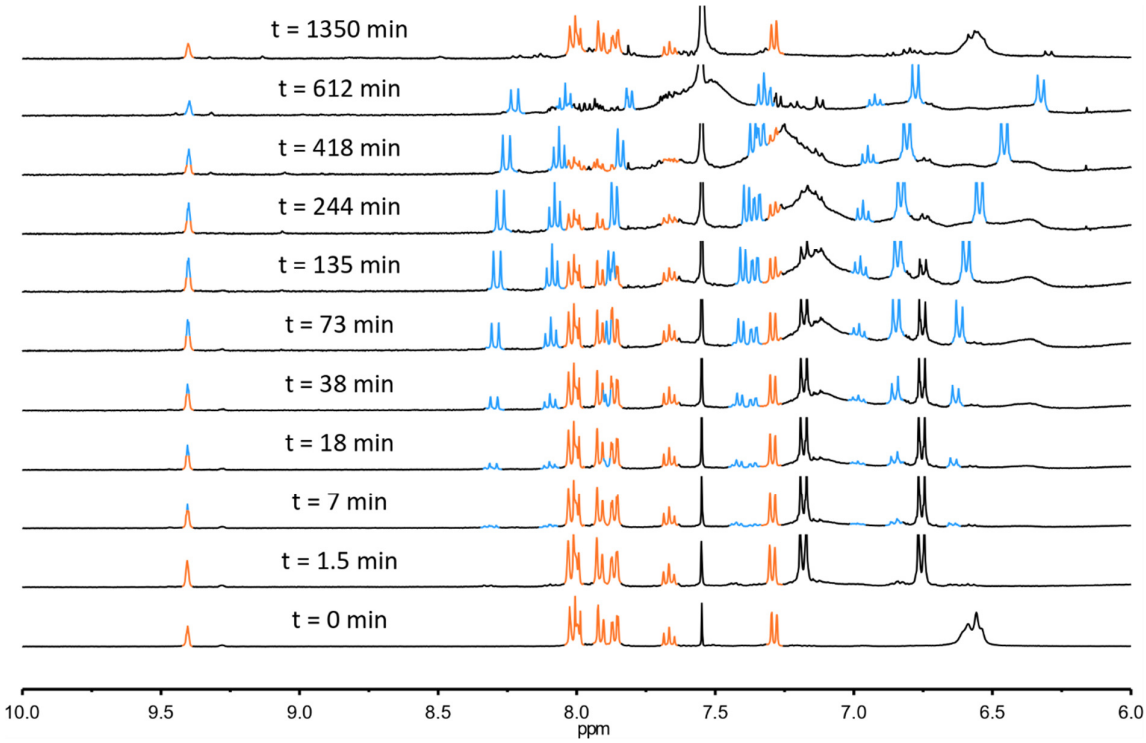

Figure S70. Monitoring by ^{1}H NMR spectroscopy (400 MHz, CD_3CN:$CDCl_3$ 3:1) of the transient self-assembly of $[Ag_2(\mathbf{6},\mathbf{7})_2](SbF_6)_2$ from $[Ag_2(\mathbf{6}_2,\mathbf{2}_2)](SbF_6)_2$ and **7** upon addition of 8.5 eq. of trichloroacetic acid. Reagents and conditions: 8.5 eq. CCl_3CO_2H, CD_3CN:$CDCl_3$ 3:1, r.t. Spectra of the crude reaction mixture were recorded at increasing time increments (up to a final total time of 1350 min), aromatic region and part of the aliphatic region of the spectra shown. Diagnostic signals of $[Ag_2(\mathbf{6}_2,\mathbf{2}_2)](SbF_6)_2$ and $[Ag_2(\mathbf{6},\mathbf{7})_2](SbF_6)_2$ are highlighted respectively in orange and blue.

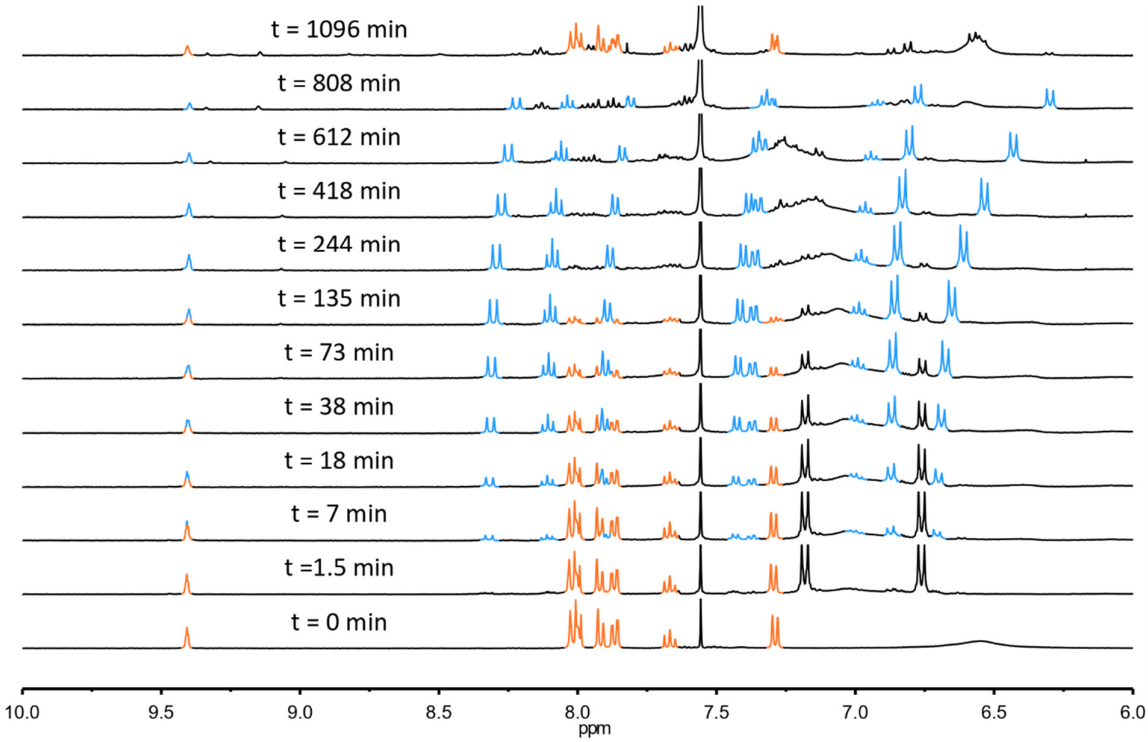

Figure S71. Monitoring by ^{1}H NMR spectroscopy (400 MHz, CD_3CN:$CDCl_3$ 3:1) of the transient self-assembly of $[Ag_2(\mathbf{6},\mathbf{7})_2](SbF_6)_2$ from $[Ag_2(\mathbf{6}_2,\mathbf{2}_2)](SbF_6)_2$ and **7** upon addition of 10 eq. of trichloroacetic acid. Reagents and conditions: 10 eq. CCl_3CO_2H, CD_3CN:$CDCl_3$ 3:1, r.t. Spectra of the crude reaction mixture were recorded at increasing time increments (up to a final total time of 1096 min), aromatic region and part of the aliphatic region of the spectra shown. Diagnostic signals of $[Ag_2(\mathbf{6}_2,\mathbf{2}_2)](SbF_6)_2$ and $[Ag_2(\mathbf{6},\mathbf{7})_2](SbF_6)_2$ are highlighted respectively in orange and blue.

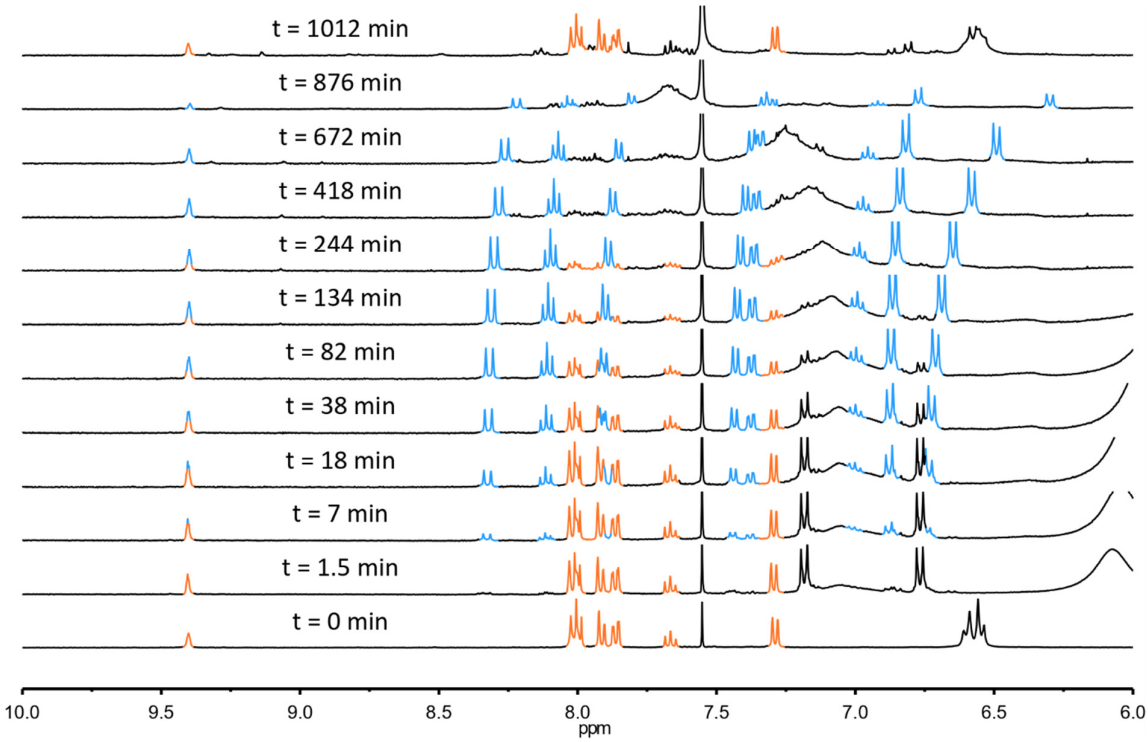

Figure S72. Monitoring by ^{1}H NMR spectroscopy (400 MHz, CD_3CN:$CDCl_3$ 3:1) of the transient self-assembly of $[Ag_2(\mathbf{6},\mathbf{7})_2](SbF_6)_2$ from $[Ag_2(\mathbf{6}_2,\mathbf{2}_2)](SbF_6)_2$ and **7** upon addition of 12 eq. of trichloroacetic acid. Reagents and conditions: 12 eq. CCl_3CO_2H, CD_3CN:$CDCl_3$ 3:1, r.t. Spectra of the crude reaction mixture were recorded at increasing time increments (up to a final total time of 1012 min), aromatic region and part of the aliphatic region of the spectra shown. Diagnostic signals of $[Ag_2(\mathbf{6}_2,\mathbf{2}_2)](SbF_6)_2$ and $[Ag_2(\mathbf{6},\mathbf{7})_2](SbF_6)_2$ are highlighted respectively in orange and blue.

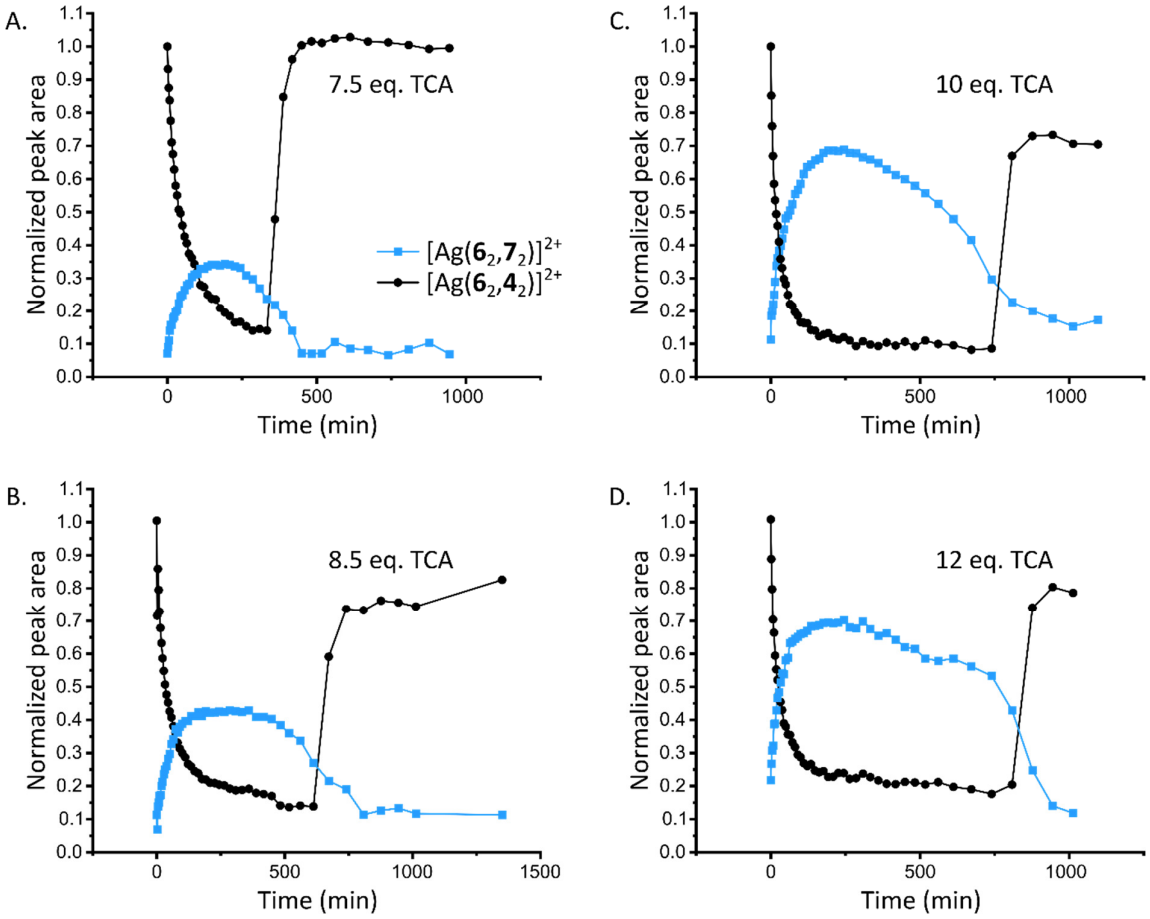

Figure S73. Transient self-assembly of $[Ag_2(\mathbf{6},\mathbf{7})_2](SbF_6)_2$ —blue squares—and disassembly/assembly of $[Ag_2(\mathbf{6}_2,\mathbf{2}_2)](SbF_6)_2$—black circles—as a function of time upon addition of : (A) 7.5 eq. of trichloroacetic acid, (B) 8.5 eq. of trichloroacetic acid, (C) 10 eq. of trichloroacetic acid or (D) 12 eq. of trichloroacetic acid. The evolution of the reaction mixture was monitored by ^{1}H NMR spectroscopy, graph plotting of the imine peak area for $[Ag_2(\mathbf{6}_2,\mathbf{2}_2)](SbF_6)_2$ and $[Ag_2(\mathbf{6},\mathbf{7})_2](SbF_6)_2$ normalized to the imine peak area for $[Ag_2(\mathbf{6}_2,\mathbf{2}_2)](SbF_6)_2$ prior to the first addition of acid. Reagents and conditions: 7.5 – 12 eq. CCl_3CO_2H, CD_3CN:$CDCl_3$ 3:1, r.t.

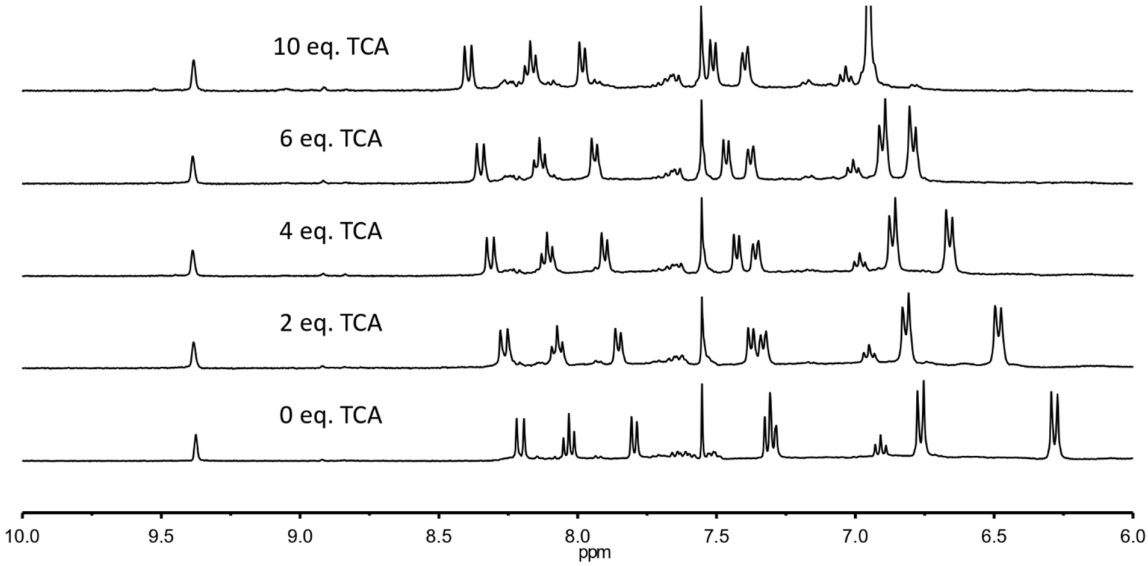

Figure S74. Partial ^{1}H NMR spectra (400 MHz, CD_3CN:$CDCl_3$ 3:1) of [2]catenane $[Ag_2(\mathbf{6},\mathbf{7})_2](SbF_6)_2$ in presence of 0–10 eq. of CCl_3CO_2H.

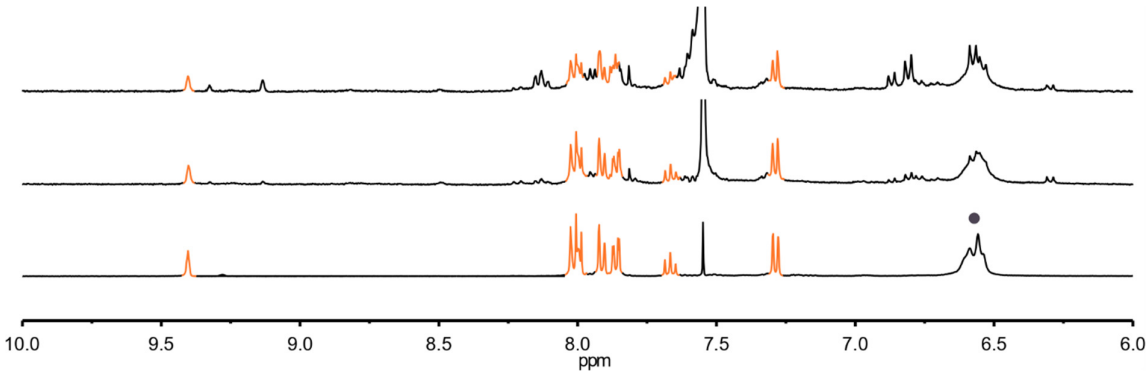

Figure S75. Evaluation of the stability of the system after several rearrangement cycles. Repetitive additions of CCl_3CO_2H resulted in the degradation of the system. Partial ^{1}H NMR spectra (400 MHz, CD_3CN:$CDCl_3$ 3:1) of: (A) a 1:2 mixture of $[Ag_2(\mathbf{6}_2,\mathbf{2}_2)](SbF_6)_2$ and **7** before addition of acid, (B) this mixture following the re-assembly of $[Ag_2(\mathbf{6}_2,\mathbf{2}_2)](SbF_6)_2$ upon consumption of the initial aliquot of trichloroacetic acid, (C) this mixture following a second disassembly/re-assembly cycle. Reagents and conditions for each cycle: 8.5 eq. CCl_3CO_2H, CD_3CN:$CDCl_3$ 3:1, r.t. Diagnostic signals of $[Ag_2(\mathbf{6}_2,\mathbf{2}_2)](SbF_6)_2$ are highlighted in orange. Diagnostic signals of **7** are highlighted by grey circles.

5. X-ray crystal structures

Single-crystal X-ray diffraction experiments were carried out by the service of the University of Strasbourg (Dr. Nathalie Kyritsakas and Dr. Lydia Karmazin). The crystals were placed in oil, and a single crystal was selected, mounted on a glass fiber and placed in a low-temperature N_2 stream.

CCDC-2162664 ($[Ag_2(\mathbf{6}_2,\mathbf{2}_2)](BPh_4)_2$) and CCDC-2162663 ($[Ag_2(\mathbf{6},\mathbf{7})_2](BPh_4)_2\cdot$xSolvent) contain the supplementary crystallographic data for this paper. These data can be obtained free of charge from The Cambridge Crystallographic Data Centre via www.ccdc.cam.ac.uk/data_request/cif.

5.1 X-ray crystal structure of $[Ag_2(\mathbf{6}_2,\mathbf{2}_2)](BPh_4)_2$

Single crystals of $[Ag_2(\mathbf{6}_2,\mathbf{2}_2)](BPh_4)_2$ were grown by solvent diffusion of diisopropyl ether into an acetonitrile solution of $[Ag_2(\mathbf{6}_2,\mathbf{2}_2)](OTf)_2$ containing excess $KBPh_4$.

A specimen of $C_{96}H_{88}Ag_2B_2N_8O_4$, approximate dimensions 0.080 mm x 0.090 mm x 0.100 mm, was used for the X-ray crystallographic analysis. The X-ray intensity data were measured (λ = 0.71073 Å). The integration of the data using a monoclinic unit cell yielded a total of 211120 reflections to a maximum θ angle of 28.07° (0.76 Å resolution), of which 9469 were independent (average redundancy 22.296, completeness = 98.9%, R_{int} = 7.55%, R_{sig} = 3.17%) and 6520 (68.86%) were greater than $2\sigma(F^2)$. The final cell constants of a = 17.5943(9) Å, b = 21.9079(9) Å, c = 21.0813(10) Å, β = 104.382(3)°, volume = 7871.2(6) $Å^3$, are based upon the refinement of the XYZ-centroids of reflections above 20 σ(I). The calculated minimum and maximum transmission coefficients (based on crystal size) are 0.7113 and 0.7437.

The structure was solved and refined using the Bruker SHELXTL Software Package, using the space group C 1 2/c 1, with Z = 4 for the formula unit, $C_{96}H_{88}Ag_2B_2N_8O_4$. The final anisotropic full-matrix least-squares refinement on $F^2$with 505 variables converged at R1 = 3.61%, for the observed data and wR2 = 9.82% for all data. The goodness-of-fit was 1.017. The largest peak in the final difference electron density synthesis was 0.823 $e^-/Å^3$ and the largest hole was -0.716 $e^-/Å^3$ with an RMS deviation of 0.065 $e^-/Å^3$. On the basis of the final model, the calculated density was 1.397 g/cm^3 and F(000), 3424 e^-.

5.2 X-ray crystal structure of $[Ag_2(6,7)_2](BPh_4)_2\cdot$xSolvent

Single crystals of $[Ag_2(\mathbf{6},\mathbf{7})_2](BPh_4)_2$ were grown by solvent diffusion of diisopropyl ether into an CH_2Cl_2 solution of $[Ag_2(\mathbf{6},\mathbf{7})_2](OTf)_2$ containing excess $KBPh_4$.

X-ray diffraction data collection was carried out on a Bruker PHOTON III DUO CPAD diffractometer equipped with an Oxford Cryosystem liquid N_2 device, using Mo-Kα radiation (λ = 0.71073 Å). The crystal-detector distance was 43mm. The cell parameters were determined (APEX3 software)[S6] from reflections taken from 1 set of 180 frames at 1s exposure. The structure was solved using the program SHELXT-2014[S7]. The refinement and all further calculations were carried out using SHELXL-2018[S8]. The H-atoms were included in calculated positions and treated as riding atoms using SHELXL default parameters. The non-H atoms were refined anisotropically, using weighted full-matrix least-squares on F^2. A semi-empirical absorption correction was applied using SADABS in APEX3[S5]; transmission factors: T_{min}/T_{max} = 0.7050/0.7456. The SQUEEZE instruction in PLATON[S9] was applied. The residual electron density was assigned to two molecules of the dichloromethane solvent

6. References

[S1] Ayme, J.-F.; Lehn, J.-M.; Bailly, C.; Karmazin, L. *J. Am. Chem. Soc.* **2020**, *142*, 5819–5824.

[S2] Men, G.; Lehn, J.-M. *J. Am. Chem. Soc.* **2017**, *142*, 2474–2483.

[S3] M. Hutin, M.; Schalley, C. A.; Bernardinelli, G.; Nitschke, J. R. *Chem. Eur. J.* **2006**, *12*, 4069–4076.

[S4] De, S.; Ghosh, S.; Bhunia, S.; Sheikh, J. A.; Bisai, A. *Org. Lett.* **2012**, *14*, 4466–4469.

[S5] Ayme, J.-F.; Lehn, J.-M. *Chem. Sci.* **2020**, *11*, 1114–1121.

[S6] "M86-EXX229V1 APEX3 User Manual", Bruker AXS Inc., Madison, USA, 2016.

[S7] G. M. Sheldrick, *Acta Cryst.* **2015***,* A71, 3–8.

[S8] G. M. Sheldrick, *Acta Cryst.* **2015**, C71, 3–8.

[S9] A.L. Spek, *J. Appl. Cryst.* **2003**, *36*, 7–13.